Fall November 2014

Asymptotic Analysis of Random Wireless Networks: Broadcasting, Secrecy, and Hybrid Networks

Cagatay Capar
University of Massachusetts - Amherst

ASYMPTOTIC ANALYSIS OF RANDOM WIRELESS NETWORKS: BROADCASTING, SECRECY, AND HYBRID NETWORKS

A Dissertation Presented

by

ÇAĞATAY ÇAPAR

Submitted to the Graduate School of the
University of Massachusetts Amherst in partial fulfillment
of the requirements for the degree of

DOCTOR OF PHILOSOPHY

September 2014

Electrical and Computer Engineering

ASYMPTOTIC ANALYSIS OF RANDOM WIRELESS NETWORKS: BROADCASTING, SECRECY, AND HYBRID NETWORKS

A Dissertation Presented

by

ÇAĞATAY ÇAPAR

Approved as to style and content by:

Dennis L. Goeckel, Chair

Patrick A. Kelly, Member

Hossein Pishro-Nik, Member

Don Towsley, Member

C. V. Hollot, Department Head
Electrical and Computer Engineering

To my parents Zeliha and Eyyup, and my sister Betül.

ACKNOWLEDGMENTS

It is the people I have met here who have made my time at UMass such a great experience. First and foremost, I would like to thank my advisor Prof. Dennis Goeckel, whom I owe so much. Throughout my many years here, I have always felt very lucky to have the privilege to be working with him. In addition to his excellent academic guidance through which I learned so much, he has always been also a source of great positive energy. It is thanks to his support and guidance that I am remembering such a positive experience as I reflect on my years here, and I leave here knowing that he is also a great friend I can always count on. I would also like to thank all my past and present professors, especially my committee members. In all my Ph.D. projects, I had the chance to work with Prof. Don Towsley – an experience I count myself so fortunate to have. Professors Patrick Kelly and Hossein Pishro-Nik have served also in my Master's committee and I am so grateful to have had the opportunity to learn from them for many years both as my committee members and teachers. I would also like to thank all members of the department who helped me along the way.

Throughout my years here, I have had the chance to make many great friendships that I enjoy knowing that I am carrying with me as I move on to a next chapter. First of all, I feel so grateful to have my current and former labmates who made my time here so much fun. Outside the lab, I would like to thank especially my roommates, whom I was fortunate to have not only as roommates but also as great friends. I would also like to thank all the people I had the chance to meet and work with at my internships, and our collaborators from all over the world. In addition, I would like to thank all the people I met at UMass, people I took classes with, people I met on and off campus. I am also so grateful to have

wonderful friends whom I met before I came to UMass but have been so close that they also made my time here so much better.

I would like to finish by thanking my family. My sister has always been such a great source of support. I shared with her many things that I felt comfortable sharing with her only. I don't know how I can ever thank my parents. I have the most supportive parents one can ever wish for. I guess I won't try and just say "Thank you so much!".

ABSTRACT

ASYMPTOTIC ANALYSIS OF RANDOM WIRELESS NETWORKS: BROADCASTING, SECRECY, AND HYBRID NETWORKS

SEPTEMBER 2014

ÇAĞATAY ÇAPAR, B.S., BOĞAZİÇİ UNIVERSITY

M.S., UNIVERSITY OF MASSACHUSETTS AMHERST

Ph.D., UNIVERSITY OF MASSACHUSETTS AMHERST

Directed by: Professor Dennis L. Goeckel

This thesis work is concerned with communication in large random wireless ad hoc networks. We mathematically model the wireless network as a collection of randomly located nodes, and explore how its performance scales as the network size increases. In particular, we study three important properties: broadcasting ability, rate of information exchange, and secret communication capability. In addition, we study connectivity properties of large random graphs in a more general context, where the graph does not necessarily represent a wireless communication network.

Broadcasting, i.e., delivering a message from a single node to the entire network in a wireless ad hoc network can be achieved by nodes acting as relays. However, due to the random placement of nodes, broadcasting gets more difficult as the network size increases. We study how a stronger form of cooperation where nodes coordinate and transmit at the same time to increase their collective transmit range can improve broadcast ability. We

show that, in this case, broadcast performance strongly depends on the type of wireless medium, in particular how fast the signal strength decays with distance. Specifically, we establish that, with increasing network size, broadcast probability goes to zero unless the attenuation in the medium is lower than a certain critical threshold.

We consider the case of a wireless ad hoc network that is supported by base stations to improve data rate, which is referred to as a hybrid network. Although the availability of base stations may improve the throughput between the wireless nodes by providing access to an overlaid high-speed wired network, this improvement does not necessarily bring a scaling advantage as the network gets larger. Motivated by work which suggests the capacity increase depends on at what rate the number of base stations scales in comparison to the number of wireless nodes, we study the ultimate constraints on the capacity of hybrid networks. In particular, we prove upper bounds on the capacity scaling benefit the base stations can provide and also show constructions that achieve these bounds in some cases.

We study secret communication capabilities of nodes in a large wireless ad hoc network that also includes eavesdropper nodes. Under an information-theoretic secrecy framework, we investigate whether nodes can exchange data while keeping bits secret from eavesdropper nodes without sacrificing on the data rate, and, most importantly, without location information about the eavesdroppers. We show that this is indeed possible by employing a combination of secret sharing, two-way communications and network coding, where nodes perform simple coding operations on messages instead of simply forwarding them.

Finally, motivated by the results in the theory of random graphs that facilitate the understanding of the behavior of large wireless networks, we study connectivity in general random graphs in more detail. In particular, we study the percolation phenomenon, which refers to the abrupt transition of connectivity in large random graphs from a combination of disconnected islands to a large cluster spanning the whole graph when a critical threshold on the randomness parameter is exceeded. We study the extension of this percolation behavior to the case of a multilayer graph, which is formed by merging different graphs on

the same vertex set, each representing a different type of connection between vertices. A multilayer graph, in general, is better connected than its individual layers, as vertices can be connected through paths traversing many layers. We numerically calculate the critical connectivity level on each layer such that the multilayer graph transitions to a well-connected state, i.e., percolates. Furthermore, we study the exact asymptotic behavior of this critical percolation threshold as the number of layers increases.

TABLE OF CONTENTS

APPENDICES

LIST OF TABLES

Table **Page**

LIST OF FIGURES

Figure **Page**

CHAPTER 1

INTRODUCTION

1.1 Motivation

Wireless ad hoc networks operate without centralized control and do not require access points or base stations. This makes their deployment easier and makes them an attractive choice for many networking applications. A common scenario for a wireless ad hoc network is where many wireless nodes, each with limited capabilities, are deployed over an area to achieve a specific goal, e.g., sensing. The nodes carry out common networking operations like routing, broadcasting, etc. as nodes in a traditional network would, but these operations are done in a distributed fashion. For example, messages may be delivered from one node to another by many nodes in between acting as relays, as opposed to an infrastructure network, e.g., a cellular network, where the source node sends its message to a base station which then delivers it to the destination node.

With practical wireless ad hoc networks becoming more common, a whole line of research has been dedicated to finding ways to make their operation more efficient, e.g., different routing algorithms are proposed that are specifically tailored to ad hoc networks with the unique characteristics of the wireless medium in mind. Apart from these practical studies and the subsequent advances achieved, another question of interest is of a more theoretical kind, where the ultimate capabilities of wireless ad hoc networks are explored. In this line of work, the network is mathematically modeled by making assumptions about the wireless nodes and the network, such as how nodes communicate, how messages are carried, what type of node deployment is done, what the wireless channel characteristics are, etc. Once the model is specified, a certain property of the network is investigated, for

example, how much information can be shared among the nodes per unit time, i.e., the throughput capability of the network. These studies serve as guidance to practical algorithms by showing what can be expected theoretically.

Many envisioned applications for wireless ad hoc networks involve very large networks and a fundamental question is what happens to a certain network property as the network gets larger; thus, one important characteristic these theoretical studies aim to extract is how the network properties *scale* with increasing network size. For example, one may investigate how the connectivity properties behave as a network with randomly located nodes, each with a given transmission range, has an increasing number of nodes. Under a given model, one can study, e.g., at what point connectivity breaks down, or how the transmission ranges should scale with increasing network size to sustain connectivity of the whole network.

This thesis work studies several scaling properties of wireless ad hoc networks where nodes are randomly distributed to a region. Mainly, we focus on three important properties: connectivity, information sharing capacity, and secret communication capabilities. In addition, we study the more general case of large random networks where the network is not necessarily a prototypical communication network. Our work is comprised of four projects summarized below.

1. We study the broadcast capabilities of nodes in a *cooperative* wireless ad hoc network. Here the distinguishing property is the type of cooperation the nodes are able to perform. In addition to simply relaying each other's messages, we assume the nodes are able to use a communication scheme where the same message is transmitted by many nodes at once to combine the received power at the receiver node to facilitate decoding. This cooperation improves the ability of nodes to broadcast their message to the entire network, where the message is distributed in waves of nodes transmitting together. We consider the extreme case of an infinite network, and explore whether by using this cooperation scheme, a message initiated at a node can

reach all nodes in the infinite network. Our work shows that the ability to broadcast strongly depends on the type of wireless medium, in particular how fast the received power decays with distance to the transmitting antenna. The probability of successful broadcast is shown to be zero above a certain critical threshold on the exponent that governs the relationship between the received power and the distance to the transmitter node.

2. We consider capacity scaling in *hybrid networks*. Hybrid networks include both ad hoc nodes and base stations. Here the wireless nodes have two options to deliver messages to their destination nodes. They can operate as a pure ad hoc network where other nodes are used as relays, or they can choose to switch to the wired network via base stations for at least some part of the route. Obviously, the availability of base stations may improve the communication capabilities of the wireless network by increasing the rate at which data can be shared by wireless nodes. However, it is of interest whether this improvement brings any scaling advantage as the network gets larger. Previous work showed achievable results on the throughput scaling of hybrid networks, hence showing a lower bound to the throughput benefit the base stations can provide. In our work, we study upper bounds to explore the ultimate advantage the base stations can realize. For a one-dimensional hybrid network where all nodes are located on a line, we prove upper bounds that match previous achievable results, hence completing the picture for the capacity of one-dimensional hybrid networks. For two-dimensional hybrid networks, we establish analogous upper bounds, but we have not shown these are achievable in all cases.

3. We consider scaling properties of *secret communication* in a wireless ad hoc network. Here, the network includes eavesdropper nodes in addition to the wireless nodes that share information. Starting with prior work that studies the fundamental communication capabilities, i.e., how many bits per second can be shared in a large wireless

network, we explore whether these limits can be achieved while also keeping the messages secret from eavesdropper nodes. We show that this is indeed possible. In particular, the throughput scaling shown in prior work can be achieved without revealing the information to the eavesdropper nodes. We make use of network coding tools to show this result, where nodes also perform simple coding operations instead of only forwarding messages. Most importantly, our results show that this scaling can be achieved without having to know where the eavesdroppers are located in the network, which had been the common assumption in prior work studying secret communication in wireless ad hoc networks.

4. We study connectivity properties of large random networks in general which do not necessarily represent communication networks. For example, the graph may represent a social network where vertices represent people, and edges represent the relationship between them. We focus on the case of "multilayer graphs", where different types of edges may exist between vertices, e.g., representing work or family relationships. For each type of edge, a separate graph corresponding to that layer can be formed, and the overall multilayer graph becomes the combination of these layers. In our work, we study the connectivity properties of the multilayer graph. Note that even when the layers are not well-connected individually, the multilayer graph can still be well-connected. In the social network example, although two people A and B may not be connected through a work-only chain, they may have a connection through a chain that includes a person C in the family layer. We try to answer the question *how connected should each layer be so that the overall multilayer graph just starts to be well-connected*? The transition of large random graphs to a well-connected state is studied in "percolation theory". For traditional (single-layer) graphs, connectivity behavior has been studied extensively in the literature. In our work, we extend these results to multilayer graphs, and study the critical connectivity behavior as a function

of the number of layers. In addition to numerical results, we also study analytically why the multilayer graph shows the observed behavior.

1.2 Background

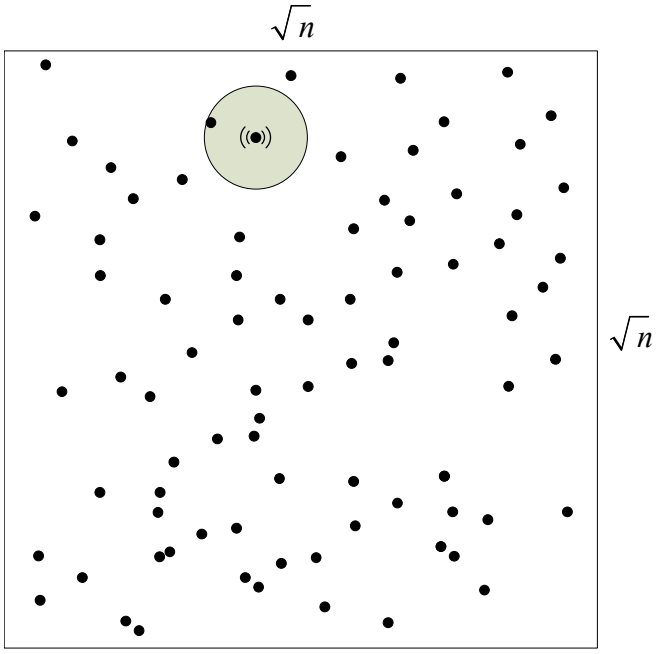

Figure 1.1: A typical model used for asymptotic analysis of wireless ad hoc networks is shown. The network is confined to a region of size n and contains n randomly placed nodes. Each node transmits with a power level that allows it to communicate to other nodes within a certain transmission range. In the asymptotic analysis, a network property is studied under this network model and it is investigated how this network property scales with growing n.

Here, we provide a brief background to set the context for our contributions presented in the following. More details are given in Chapter 2.

In this thesis work, in order to study large random networks, we use an infinite network model which is represented by a graph with an infinite number of vertices. In Chapters 3 and 6, our focus is on the connectivity properties of the infinite random network. For the infinite wireless ad hoc network, we assume nodes are distributed to the entire $\mathbb{R}^2$ plane according to a Poisson point process. Each node is represented by a vertex, and edges

are drawn between vertices that are within a certain transmission range. One fundamental property of interest is whether this infinite graph has full connectivity, i.e., whether there is a path between every pair of nodes. It can be shown that for this infinite graph, full connectivity never occurs for any finite node density and transmission range, because an isolated node can be found in the infinite network with probability one. In Chapter 3, we study how this situation can be improved by cooperation between nodes.

An infinite graph which is not fully connected can still be "well-connected", meaning that although there are small isolated islands, there is a cluster spanning an infinite number of nodes. In that case, this graph is said to "percolate". Percolation theory studies the connectivity properties of the infinite random graph. Central to percolation theory is the phase transition phenomenon, in which as a local parameter is varied, the graph abruptly transitions from a state of many small clusters to one giant cluster. The value at which this transition happens is called the critical percolation threshold. Percolation is observed for a wide range of infinite random graphs which do not necessarily represent communication networks. An example is the infinite square lattice, where each vertex has four neighbors. Consider a random process on this infinite graph, where each edge is independently deleted with some probability. Clearly, as this deletion probability is varied from zero to one, the resulting infinite network becomes less and less connected. What is less obvious is that, there is a critical value at which the resulting graph suddenly transitions from one big connected cluster to many small connected islands. This phase transition observed in the infinite random graph is used to explain and model many real-life phenomena in a wide range of fields. In Chapter 6, we study critical percolation thresholds for a special family of graphs called multilayer graphs.

In order to study the asymptotic behavior of networks, we use an infinite network model. However, sometimes it is also of interest to consider how the network converges to its asymptotic behavior. In other words, the *scaling* properties of the network may be of interest. This is the case in Chapters 4 and 5. In that case, we use a finite network model, and

study how a certain property of the network scales as the networks get larger. Figure 1.1 shows a typical model used for the asymptotic analysis of wireless ad hoc networks. Nodes are randomly distributed to a two-dimensional box of size $\sqrt{n} \times \sqrt{n}$ with unit density, so the region contains n wireless nodes on average. These n nodes form the wireless network. For the traffic pattern, it is usually assumed that the nodes are randomly matched into source-destination pairs, so that we have n pairs with their respective information flows. Because nodes share the same medium, a fundamental property of wireless communication is *interference*. Whenever a node transmits, it creates interference to nearby nodes and degrades the quality of the signal they receive. This puts a constraint on simultaneous transmissions, which creates the fundamental limitation on the communication capacity of the network as a whole.

In order to create as little interference as possible, one could limit the transmission power of the wireless nodes so that nodes with enough separation between them can transmit at the same time to improve the capacity of the network. However, with smaller transmit power, it becomes harder for a source node to reach its destination directly, and therefore it needs to use neighboring nodes as relays to forward its message. Hence, a message needs to be transmitted many times before arriving at the destination, which decreases the capacity. In other words, there is a trade-off between the *spatial reuse* of the band which helps the capacity and the *relaying burden* caused by multihop transmission.

In their seminal paper [29], Gupta and Kumar study this trade-off and explore the fundamental limits on the rate data can be shared in multihop wireless networks. They show that in to order to maximize capacity, it is optimal to reduce the transmit power as much as possible. However, if the transmit power is too small, the connectivity of the network itself breaks down. They establish that if the network is operated at the critical power threshold for connectivity, the total throughput realized by the network scales proportional to $\sqrt{n/\log n}$ bits per second as n grows. This means the throughput available to each pair goes down to zero with $1/\sqrt{n \log n}$, showing that wireless ad hoc networks in fact *do not*

scale well in terms of capacity. This result initiated a surge of research activity on the problem. Later works that explore improvements to this scaling include [16], where it is shown that the per-node throughput can be slightly improved to achieve order of $1/\sqrt{n}$ bits per second by allowing the nodes to pick different transmit power levels. Other works study whether the capacity can be improved by enabling different communication mechanisms not included in the original model such as a more sophisticated form of node cooperation [58]. Yet another line of work looks at whether other factors such as node mobility can help improve capacity [26].

One natural way to improve capacity scaling in wireless networks is to provide users access to an overlaid wired network. This is done by including base stations in the network that are connected to each other through a separate, high capacity wired network so that messages can be carried on the wired network for at least a part of the route. This way wireless nodes can choose to connect to a base station in addition to the option of pure wireless communication. These types of networks are called *hybrid networks*, and the capacity scaling of hybrid networks has been studied in a number of works [1, 45]. These works show constructions where nodes access the base stations in addition to multihop communication and achieve a certain throughput. Under these constructions, depending on how the number of available base stations scales relative to the number of wireless nodes, the achieved throughput scaling may or may not be better than pure ad hoc. Note that these are achievability results, and hence, they provide lower bounds on the scaling benefit the base stations can provide. In Chapter 4, we consider upper bounds for this scaling.

Another implication of the capacity scaling of wireless networks is on the security aspect on communication; in particular on *secrecy*. In secret communication, the goal is to be able to convey a message to the intended receiver successfully while also preventing any eavesdropping adversary from doing the same, which is harder to achieve over the wireless medium. In the secrecy extension of the original capacity scaling problem, one considers the same network shown in Fig. 1.1, but this time also including eavesdropper

nodes. Here, the fundamental question becomes whether achieving secret communication is possible, and if it is, whether it will require compromise on the throughput scaling. The secrecy notion adapted here is information-theoretic secrecy as originally studied for the single-sender-single-receiver case in the framework of the wiretap channel [75]. In this domain of research, [39] shows that the same construction used in [16] can be modified and the same per-node throughput scaling of $1/\sqrt{n}$ bps can be achieved while keeping all the information secret from eavesdroppers. In the proposed construction in [39], messages are routed away from eavesdroppers to force them to have low received signal quality. This requires the knowledge of eavesdropper locations, which is an undesired assumption. In [73], it is shown that by using friendly jamming it is possible to achieve the same secrecy scaling; however, the number of eavesdroppers that can be tolerated is limited to $\log n$. We consider in Chapter 5 whether this latter scaling result can be improved.

1.3 Contributions

1. We establish asymptotic results on the broadcast capabilities of nodes in a cooperative wireless network. In particular, we consider a type of cooperation where a cooperating set of nodes transmit the same message simultaneously to a single node where the received power is summed to achieve better decoding ability. We show that, even under this cooperative scheme, for a wide range of cases, the probability of successful broadcast to all nodes in a random network goes to zero as the network grows. Specifically, if the path loss exponent of the medium is greater than one in a one-dimensional network, and greater than two in a two-dimensional network, the broadcast probability goes to zero. In other cases, the broadcast probability is strictly larger than zero even for an infinite network. This relates to prior work in the area as follows:

    - Our results complement previous work on cooperative networks by studying a weaker type of cooperation. In particular, [19] studies a similar problem where

a set of *receiver* nodes also cooperate to decode a message simultaneously sent by a set of sender nodes. Similar results to our case are obtained in [19], showing that even under a stronger form of cooperation than assumed in our work, the asymptotic broadcast capability of the network and its dependence of the type of medium largely remains the same.

- The problem of broadcasting in cooperative networks was studied in prior work in [69] for the same type of cooperative scheme but under a different type of network model. Our results reveal that the broadcast capability of the network can be quite different based on the assumed network model. In particular, [69] studies a network confined to a finite size region with a growing number of nodes. Under this model, [69] points to a much more positive result, implying that broadcast is possible regardless of the speed of power decay in the wireless medium. On the other hand, our results prove that this is only true if the network gets infinitely denser, not necessarily as the number of nodes grows.

  Our work on broadcast in cooperative wireless networks is presented in detail in Chapter 3.

2. In our work on hybrid networks, we establish upper bounds on per-node throughput scaling. This relates to prior work in the area as follows:

   - Previous results have provided lower bounds on the capacity of hybrid networks for a wide range of number of base stations; however, upper bounds have not been established. We adapt cutset bound techniques used for the study of pure ad hoc network throughput to the hybrid case and establish upper bounds. In one-dimensional hybrid networks, these upper bounds match the achievability results for any number of base stations, hence completely characterizing the capacity scaling. In two-dimensional networks, the upper bounds are tight in some cases.

- Previous work shows that the per-node throughput increases linearly in the number of base stations for the case where the number of base stations grows faster than the square root of the number of wireless nodes. This implies that in the case where the number of base stations grows proportional to the number of wireless nodes, it could potentially be possible to provide constant throughput to nodes. By establishing a new result on the maxima of a sequence of Poisson random variables, we show that this is not possible for some subset of nodes in the network and their throughput goes to zero as the network grows. Furthermore, we provide a matching lower bound on per-node throughput, therefore completing the capacity result in the case where the number of base stations is proportional to the number of wireless nodes.

Our work on hybrid networks is given in Chapter 4.

3. In our work on secrecy, we show that secret communication in large wireless networks is possible without having to know the locations of the eavesdroppers. This is a significant improvement to previous work, where knowledge of eavesdropper locations has been the common assumption. Further, we show that secrecy can be achieved without having to compromise on the throughput scaling. This relates to prior work in the area as follows:

   - Our results in secrecy reveal how coding techniques can be immensely useful for secret communication in wireless ad hoc networks, which had previously not been considered in the case of large wireless networks. Coding techniques allow important problems to be tackled easily without resorting to expensive physical-layer solutions such as the friendly jamming used in prior work. Furthermore, for two-dimensional networks, we show that coding can also enable secrecy in a more general case than typically considered in prior work by pro-

viding secrecy where an arbitrary number of eavesdroppers can be arbitrarily located.

- We also study the case of secrecy in one-dimensional large networks, a problem not considered in previous work. Secrecy is especially challenging in this case, as it is not possible to route around eavesdroppers, and a single eavesdropper can practically disable secret communication between two sides of a point on the line. We show that by using coding in addition to friendly jamming, secret communication is possible, again without having to know eavesdropper locations and without compromising on throughput scaling.

Details of our work on secrecy in wireless networks can be found in Chapter 5.

4. We study site percolation properties of the random multilayer graph. In site percolation, vertices (sites) of a given graph are randomly labeled occupied or unoccupied, and the edges incident on the unoccupied vertices are removed. Suppose each site is occupied with probability q. Then there exists a critical value of q, q_c, at which the graph transitions from many small clusters to one giant cluster. This value is called the site percolation threshold. The value of q_c for many types of graphs has been studied extensively in the literature. In our case, we generate several site percolation instances of the same graph with some probability q, calling each of them a layer. We call the union of these layers the multilayer graph, and we are interested in the critical q value that makes the multilayer graph percolate. Obviously, this value is smaller than the single-layer case, and decreases as the number of layers increase. In our work, we show by simulations that the critical threshold value follows an inverse square root behavior. In particular, if the graph is formed by combining M layers, the critical threshold scales with $1/\sqrt{M}$. Moreover, we study analytically the exact function that governs this behavior, and conjecture an asymptotic relation that matches numerical results very closely.

CHAPTER 2

BACKGROUND

This chapter presents models for wireless communication networks, and discusses important previous results in the area of asymptotic analysis of wireless networks that serve as a background for the following chapters.

2.1 Introduction

Wireless communication networks have been rapidly replacing their wired counterparts in many applications. However, most current wireless networks are, in fact, a relatively small appendage to a large traditional wired network. For example, in cellular networks, cell phones communicate directly with base stations which are part of the traditional telephone network. Similarly, in WiFi networks, wireless devices such as laptops and tablets are just a single wireless connection away from the wired internet infrastructure.

The advances in wireless communications now also make it possible to form what are called "wireless ad hoc networks". In wireless ad hoc networks, wireless devices communicate with each other, possibly through multiple "hops", without the need for centralized control, e.g., a base station. An example is a collection of laptops in the same building that form a wireless network to exchange messages without the need for an access point. Wireless ad hoc networks bring greater flexibility and quick deployment of networks where infrastructure may not be available or may be costly to deploy. This makes them an attractive choice for many applications including future generation wireless technologies [52].

The following chapters are concerned with modeling and performance analysis of large wireless ad hoc networks, i.e., wireless ad hoc networks with many nodes. Although each

chapter is focused on a different property of wireless ad hoc networks, the underlying communication and network models are very similar. In this chapter, we present these models in detail.

2.2 Communication and Network Model

2.2.1 Communication Model

When wireless node A transmits with a certain transmit power $P_A > 0$, we assume the received power at another wireless node B due to A is

$$P^{A\to B} = \frac{P_A}{d_{AB}^{\alpha}}, \tag{2.1}$$

where d_{AB} is the distance between nodes A and B, and $\alpha > 0$ is the *path loss exponent* which is a characteristic of the specific wireless environment. In other words, we assume the path loss imposed by the environment is uniform in all directions. It is important to note that this model does not include the random and time-varying effects of multipath fading or shadowing. A wideband communication scheme which averages out these random effects is an example where this model is appropriate.

At the receiver side we assume additive white gaussian noise (AWGN) with power $N_0 > 0$. Due to the broadcast nature of the wireless medium, the receiver also suffers from signals coming from other active transmissions in the network, which is referred to as "interference" (see Figure 2.1). Let $\mathcal{T}$ be the set of active nodes transmitting at the same time on the same frequency band as wireless node A, and consider the case where wireless node B wants to decode the message sent by A. Then an important quantity of interest is the "signal-to-interference-and-noise ratio" (SINR) at the node B, defined as

$$\text{SINR}_B = \frac{P^{A\to B}}{N_0 + \sum\limits_{i\in\mathcal{T}\setminus\mathcal{A}} P^{i\to B}}. \tag{2.2}$$

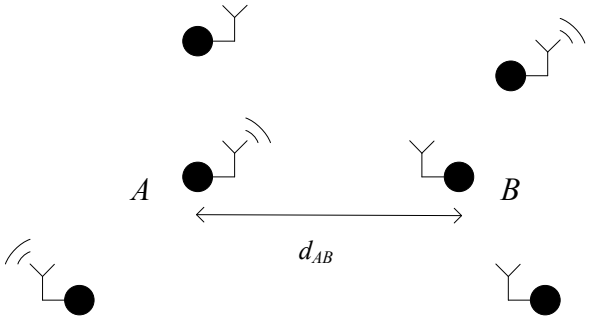

Figure 2.1: In the communication model, wireless nodes are assumed to be point sources. The signal power received at a wireless node B due to another node A decays with the distance d_{AB} between nodes. When trying to decode A's message, B suffers interference from signals coming from other active nodes.

We assume the interference power that reaches a wireless node B from node i, $P^{i\to B}$, follows the same path loss rule in (2.1) [1]. The only exception to the above formulation is in Chapter 3, where all active nodes transmit the *same* message and the received power from other nodes (second term in the denominator in (2.2)) is not treated as interference. Details are given in Section 3.2.

For modeling the successful decoding of a message transmitted by A at node B, we assume an *SINR threshold rule*: For some threshold $\gamma > 0$, we assume B can decode the message perfectly (with zero probability of error) if and only if

$$\text{SINR}_B \geq \gamma. \tag{2.3}$$

If $\text{SINR}_B < \gamma$, transmission fails, meaning B cannot decode the message. We assume partial decoding is not possible, i.e., when $\text{SINR}_B < \gamma$, B has zero information about the message. The threshold γ is a value that is dictated by the details of the underlying

[1] Note that this model of communication and interference is sometimes called the "Physical Model" in the literature. A simpler, high-level model is the "Protocol Model", where it is assumed that there is an interference range around every active node outside of which the node causes no interference [29].

communication system. For the problems in this thesis, it is assumed γ is given, and the system parameters for the respective problem are designed around this value.

2.2.2 Network Model

In this work, we are interested in the *asymptotic* performance of wireless ad hoc networks. This means the network contains infinitely many nodes. We assume nodes are at fixed, random locations. We study both one-dimensional and two-dimensional networks. In the one-dimensional case, the nodes are placed on the real line $\mathbb{R}$, and in the two-dimensional case, on the plane $\mathbb{R}^2$ (see Figure 2.2). Nodes are assumed to be placed according to a homogeneous Poisson point process with node intensity $\lambda > 0$. Notice that we model wireless nodes as point sources and enforce no minimum distance between nodes. Under this model, we study how this infinite network performs. For example, in Chapter 3 we study whether a node can broadcast its messages to the entire infinite region.

When we study asymptotic limits, we are sometimes also interested in how the quantity of interest goes to that limit, i.e., the convergence rate may also be of concern. In that case, we need to define a finite network model and study explicitly how this network performs as it contains more and more nodes and gets closer to the infinite network defined above. This is the case in Chapters 4 and 5, where we are interested in the performance *scaling* of the network. In these works, we consider a certain region inside $\mathbb{R}$ or $\mathbb{R}^2$, and define the finite network as the set of nodes that fall inside this region. In particular, for the variable $n > 0$, we consider the interval $[-n/2, n/2]$ and the box $[-\sqrt{n}/2, \sqrt{n}/2] \times [-\sqrt{n}/2, \sqrt{n}/2]$, for the one-dimensional and the two-dimensional cases, respectively (see Figure 2.3). Assuming a node density of $\lambda = 1$, we study how the performance of the network scales as $n \to \infty$.

Note that another way to do asymptotic analysis is to study a network with infinitely many nodes in a finite size region. This model is often referred to as a "dense network", whereas our model described above is called an "extended network".

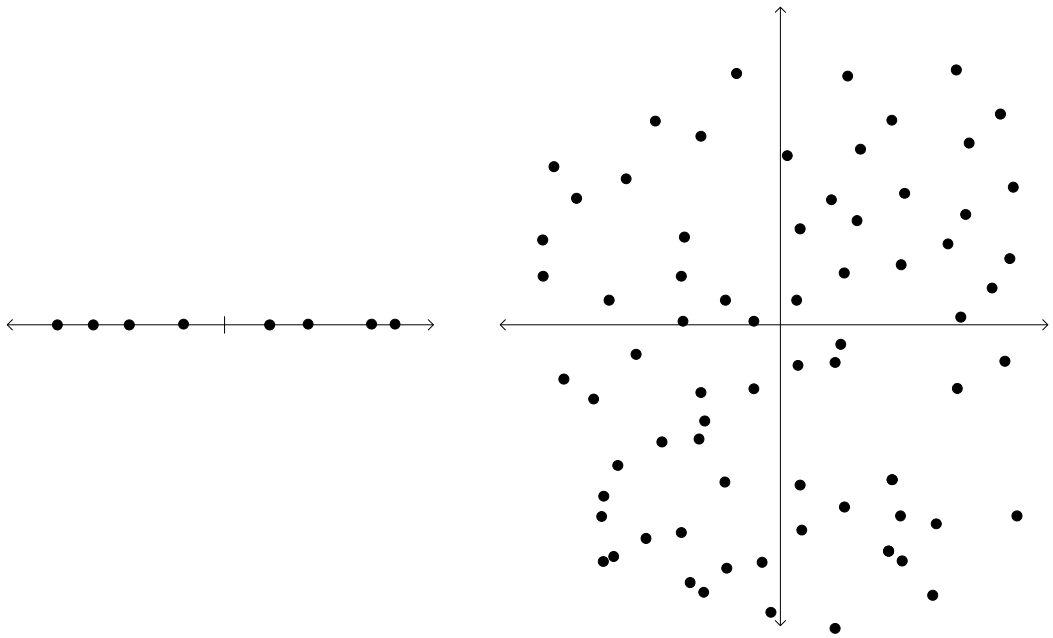

Figure 2.2: In the network model, we assume nodes to be placed randomly according to a Poisson point process in an infinite region. In the one-dimensional case, nodes are on the real line $\mathbb{R}$ (left figure). In the two-dimensional case, nodes are on the infinite plane $\mathbb{R}^2$ (right figure).

2.3 Connectivity of Wireless Ad Hoc Networks

One basic property of interest for any communication network is its "connectivity". Connectivity determines the network's ability to carry information between its members. In order to study connectivity, it is convenient to model the network as a graph with a set of vertices and edges, where vertices represent the members of the network and an edge exists between two vertices whenever the nodes representing them have a direct connection. For wired networks, there is a natural mapping from the network to a graph as every edge corresponds to a physical link.

Mapping a wireless ad hoc network to a graph to study its connectivity is not as obvious as in the wired case. A direct link between two wireless nodes may be introduced depending on the wireless signal quality. One basic way to do this is to assume a "transmit range" for each node. Here, it is assumed that every node has a certain region around it and it has a

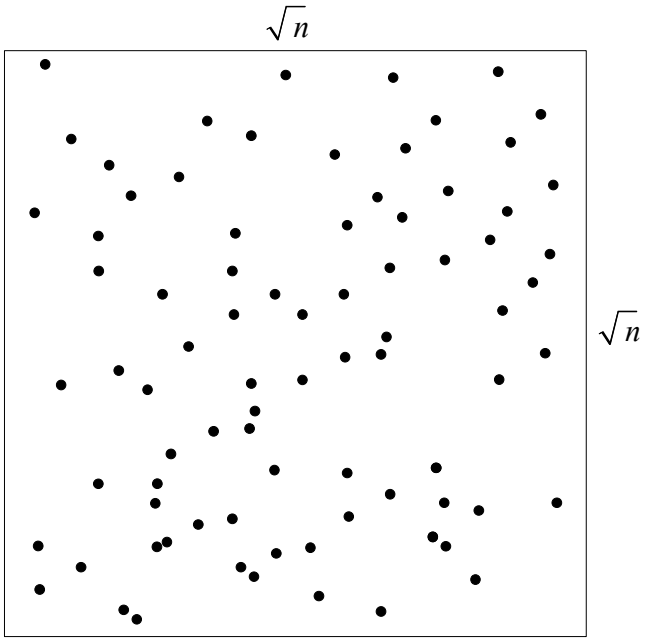

Figure 2.3: In order to study performance scaling of a wireless ad hoc network as the network gets larger, we construct a finite network model. The finite network is defined by the nodes that are placed according to a Poisson point process with node density $\lambda = 1$ and fall within a certain finite region. In the one-dimensional case, the finite network is the collection of nodes that fall within an interval of size n (not shown). In the two-dimensional case (shown here), the finite network is comprised of nodes within a square region of size n. Under this model, we study how the quantity of interest scales as n grows.

directed edge to any node within that region. This transmit range is determined based on the transmit power, the communication system employed, and the medium characteristics. One simple model is where a circle of certain "transmit radius" is assumed for each node's transmit range. Assuming further that the transmit radius, r, is the same for every node, undirected edges can be drawn between nodes that are separated by a distance less than r. An example can be found in Figure 2.4. Notice that for the sake of exploring the necessary connectivity conditions, this model ignores interference that may be caused by other active nodes. In other words, to study whether two nodes can ever be connected, we consider the "best case" where all other nodes are silent.

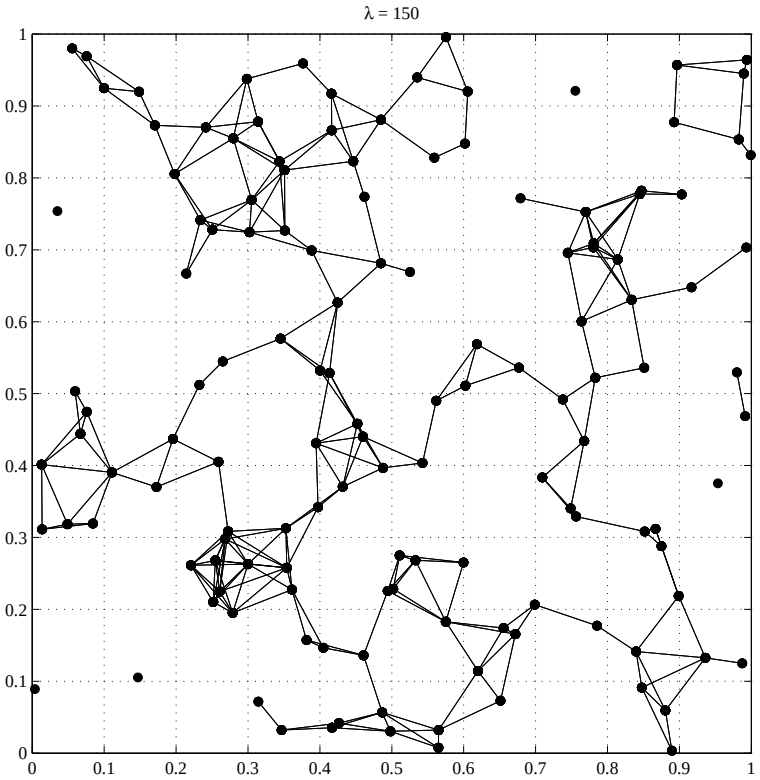

Figure 2.4: A random geometric graph mapped from a wireless network. Nodes are randomly placed inside the region $[0, 1] \times [0, 1]$ with node intensity $\lambda = 150$. The transmit radius is $r = 0.1$. Vertices within r are connected by an edge.

Under this rule, the wireless ad hoc network with given node locations and transmit radius is mapped to a graph. Under the random network model described above, the corresponding graph is a *random geometric graph* (more specifically, a graph generated by a *Poisson Boolean Model* [51]). One can then study the (statistical) properties of this graph, e.g., whether the graph is connected or not (with a certain probability), cluster sizes, cluster distributions, etc. In this section, our focus is on the graph's connectedness in relation with the transmit radius. Under the network model described above, we study two cases: i) the connectivity of the infinite network under a *constant* transmit radius, and ii) the scaling of connectivity of the finite network under a transmit radius that *grows* with network size.

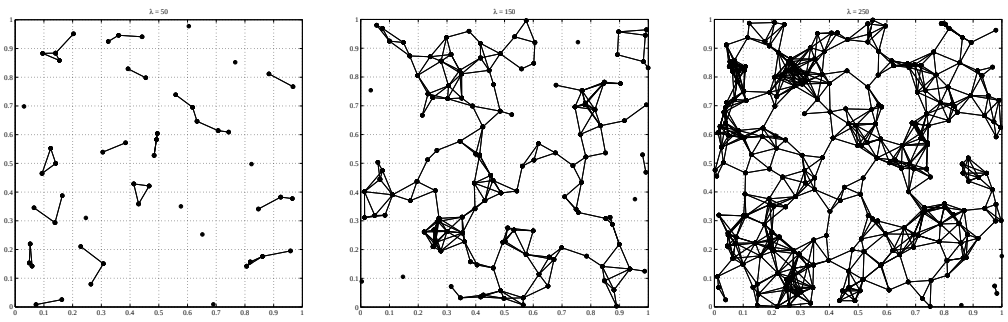

(a) (b) (c)

Figure 2.5: Instances of a random graph generated by transmit radius $r = 0.1$ and three node density values, $\lambda = 50, 150, 250$, are shown in (a), (b), (c), respectively. As λ increases, the graph transitions from many small clusters to one giant cluster.

First, consider the infinite network formed with fixed parameters λ and r. One can study the "full connectivity" of the network, which translates to having a path between every pair of nodes in the corresponding infinite graph. However, due to the fact that the network is infinite, it can be easily shown that there is an isolated node, i.e., a node with no other nodes within r, with probability one for any finite value of λ. In other words, under the above model with constant r, full connectivity never occurs for an infinite network in both the one-dimensional and the two-dimensional cases [14]. In Chapter 3, we study how this situation can be improved by enabling cooperation among nodes.

Although full connectivity cannot occur, the infinite network in the two-dimensional case can still be "well-connected" with only a small fraction of the nodes being disconnected from the rest of the network. More specifically, it can be shown that for a given transmit radius r, there exists a critical node density λ_c above which the network contains a giant cluster with an infinite number of nodes along with finite-size isolated islands. In that case, the graph is said to "percolate". However, whenever $\lambda < \lambda^*$, the network consists of many finite-size isolated clusters (see Figures 2.5 and 2.6). This sudden transition in long-range connectivity in infinite graphs is studied in *percolation theory* [51] and it has been an important part of the study of wireless ad hoc networks [17]. One-dimensional infinite

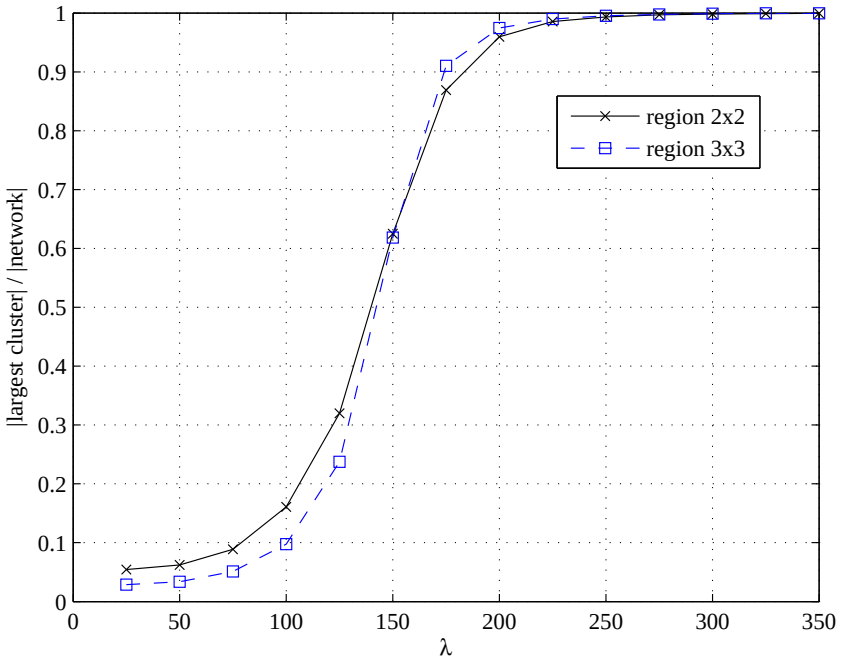

Figure 2.6: The number of nodes in the largest cluster divided by the size of the network averaged over 1000 runs for different values of λ. As λ gets larger, the value approaches 1 showing the network goes from many small clusters to one single big cluster. Simulations are done for networks confined in a region of size 2×2 and 3×3, both with transmit radius $r = 0.1$. As the simulated network region gets larger, the plots get steeper. For the infinite network, this transition is sharp around a critical λ value numerically estimated to be around $\lambda_c = 144$ (see [62] and note the threshold is given for the value $\lambda\pi(r/2)^2$).

networks, in addition to never being fully connected, also do not percolate for any finite parameters, λ, r [14]. The studies in [20] and our work in Chapter 3 shows that, thanks to cooperative schemes, percolation can be achieved in one-dimensional networks for certain types of wireless channels. Furthermore, by enabling cooperation, the critical percolation threshold, λ_c, can be reduced for two-dimensional networks.

Second, consider the scaling of connectivity of the finite network (Figure 2.3) for the case of growing transmit radius. The results on the infinite network already imply that, with constant transmit radius r, full connectivity of a finite network of size n breaks down at some point as $n \to \infty$. The problem of how the transmit radius should scale with n to

keep the network fully connected is studied in [28] and it has been shown that the transmit radius needs to grow at a rate of at least $\sqrt{\log n}$ for the two-dimensional network to be fully connected (with probability approaching one as n grows). Similarly, in one-dimensional networks, $r(n)$ needs to grow with $\log n$. (Note that [28] studies the dense network model but its results can be mapped to the extended model. For the extended model case and more detailed results see [17, Section 3.3.2].) This important result is at the center of the multihop communication scheme introduced in the next section, and is the basis of our designs in Chapters 4 and 5.

Finally, note that the above-mentioned percolation phenomenon is not restricted to random geometric graphs. In fact, percolation can be observed in many types of random infinite graphs which do not necessarily represent communication networks [25]. In Chapter 6, we study percolation in general random graphs. Our focus is on the case where there are different "types" of connections available and a pair of nodes may have more than one edge connecting them each belonging to a certain type. For a communication network, this may represent, e.g., different communication technologies. This network can be seen as a combination of different "layers" each representing one connection type . We study the percolation properties of the corresponding *multilayer graph*.

2.4 Capacity of Wireless Ad Hoc Networks

In addition to connectivity, a very important property of a wireless ad hoc network is its *capacity*. Connectivity properties determine if nodes can exchange data between them. In the capacity problem, the question is *at what rate* data can be shared. In this section, under the communication and network model described above, we explore the capacity problem in detail. In particular, we study how capacity *scales*, i.e., how many bits per second can be shared by nodes in the finite network (see Figure 2.3) as the size of the network gets larger. Note that the term "capacity" here is not used in the strict information theoretic sense, and we use the terms throughput and capacity interchangeably. For the rest of the section, we

confine ourselves mostly to two-dimensional networks and then finish by briefly presenting the one-dimensional case.

2.4.1 Traffic Model

The nodes in the two-dimensional finite network are matched into source-destination pairs uniformly at random. Hence, each node is the source for an information flow, and also the destination for another (see Figure 2.7). This kind of traffic pattern is also called multiple unicast. The network needs to carry roughly n information flows, and the question of interest is at what rate these flows can be carried. There is a frequency band of fixed bandwidth allocated for this traffic. Over this band, nodes can transmit at W bits per second (bps) and this value is a constant (does not grow with n). In order to carry the traffic load, a certain routing and multiple-access algorithm (which together we call a "construction") needs to be designed, and the selected construction determines the achieved throughput.

2.4.2 Multihop Routing

In order to get a sense of the capacity problem, consider the simple multiple-access algorithm for carrying the n information flows where nodes simply take turns to deliver their messages. Assuming that each node transmits with enough power to reach its destination, i.e., with a single-hop routing algorithm, it takes on the order of n time slots to finish carrying the total load (see Figure 2.7). In other words, with this construction, a throughput value that scales as $1/n$ bps is achieved per source-destination pair. Hence, as the network gets larger, the number of bits that can be shared by each pair under this construction goes down to zero at a rate reciprocal of the number of nodes.

The problem with the above construction is that the active node creates too much interference, and hence, the rest of the network needs to stay idle. In order to increase efficiency, the transmit power of the nodes can be turned down to decrease interference so that nodes with enough distance between them can be active simultaneously, i.e., the nodes can benefit from the spatial reuse of the available band. However, this in turn makes the source

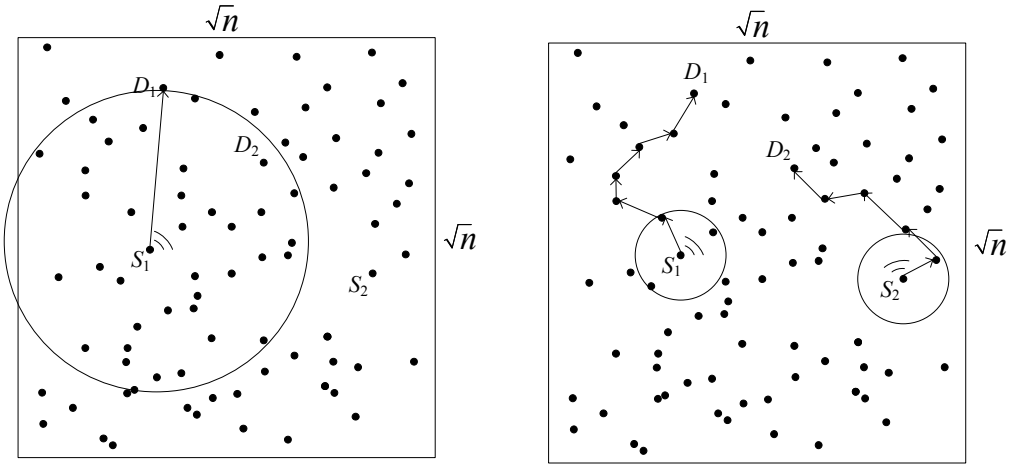

Figure 2.7: The nodes in the network are mapped into source-destination pairs uniformly at random. Each node is the source for one flow and the destination for another. The network needs to carry roughly n flows by a certain routing and multiple-access method, which in turn corresponds to a certain throughput. One way to carry this load is to let nodes take turns. While the source node for the first flow S_1 transmits to its destination node D_1 with enough transmit power, the rest of the nodes stay silent (left figure) and this is repeated for every flow. This method achieves a per-node throughput that scales with $1/n$ bps. By turning down the transmit power and hence causing less interference, multiple flows can be active at once. However, this time sources cannot reach their destinations in one hop and instead need to deliver messages to nearby nodes that act as relays. In that case, the messages are carried in a multihop fashion (right figure).

nodes unable to reach their destination in one hop, which means messages need be carried over multiple hops until they reach the destination (see Figure 2.7). Hence, nodes need to act as relays to carry each other's messages, and this has a decreasing effect on capacity. Therefore, the trade-off here is "interference vs. relaying load". One needs to choose the optimal transmit range, i.e., the optimal transmit power, to operate the network at the point that maximizes capacity. This optimization problem is addressed in the seminal paper [29].

2.4.3 Optimal Capacity under Multihop Routing

The fundamental result in [29] is that for the multihop routing algorithm described above, it *always helps capacity* to decrease the transmit power. In other words, the loss of capacity due to increased number of hops is always exceeded by the gain obtained by

reduced interference. The basic idea is that decreasing the transmit range $r(n)$ increases the number of hops linearly, however, it also frees up space for spatial reuse that increases quadratically [29]. Although capacity increases with decreasing transmit radius, the transmit radius cannot be decreased indefinitely. As discussed in the previous section, connectivity breaks down for too small $r(n)$. Hence, the optimal operating point for multihop routing is exactly the critical transmit power required for connectivity. Assuming the same transmit power for each node, this means a transmit range $r(n)$ that scales as $\sqrt{\log n}$ maximizes capacity.

In order to see what capacity scaling is achieved under multihop routing with $r(n)$ that scales with $\sqrt{\log n}$, we present a construction, i.e., a routing and multiple-access algorithm, that uses this transmit power. We divide the finite network into "squarelets" of size $\sqrt{\log n} \times \sqrt{\log n}$ as shown in Figure 2.8. It can be easily shown that each squarelet contains at least one node with high probability (w.h.p.), i.e., with probability going to one as n increases. Inside each squarelet, we designate one node to be the relay of that squarelet. For each information flow, we define a path between the source and the destination node that consists of squarelets on straight lines (see Figure 2.8). Each message is carried on this path by the corresponding relays until it reaches its destination. Because the transmit radius is selected to grow with $\sqrt{\log n}$, relays are able to reach the next node on the path.

The multiple-access algorithm is defined such that squarelets with a certain minimum distance between them can be active at the same time. This minimum distance can be determined by measuring the total interference at a receiving relay arriving from all active squarelets. The important detail here is that for path loss exponents $\alpha \geqslant 2$, this minimum distance can be selected to be a constant value that is independent of n. Time is divided into periods and the squarelets take turns. At the end of a constant number of periods, each squarelet gets to be active once (see Figure 2.8).

The throughput achieved under this construction can be found by focusing on the relaying load of a single relay in a given squarelet. Due to the way paths are defined, this relay

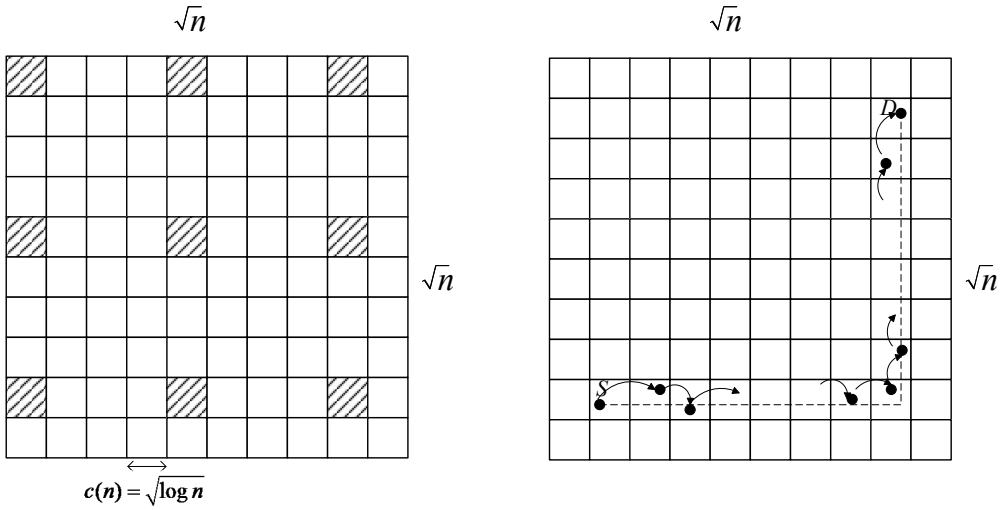

Figure 2.8: A construction that carries the information flows between source-destination pairs is shown. The finite network is divided into squarelets of size $\sqrt{\log n} \times \sqrt{\log n}$. Time is divided into periods where in each period, squarelets with a certain minimum distance are active (active squares are shown shaded in the left figure). For the network shown, it takes 16 periods for every squarelet to be active at least once. Paths between sources and destinations are defined such that they consist of at most two straight lines (right figure). A node in each squarelet is designated to be the relay of that squarelet. Messages are carried by relays inside the squarelets that belong to the corresponding path. Transmit power is chosen to make sure receiving relays in the neighboring squarelet can decode the message. This construction can be shown to achieve a per-node throughput that scales with $1/\sqrt{n \log n}$.

needs to carry messages that belong to source nodes that are located inside squarelets on the same row or the column. The number of nodes inside that region can be easily shown to scale as $\sqrt{n \log n}$ w.h.p. Hence, the total traffic load of this relay can be finished in a constant factor of $\sqrt{n \log n}$ periods. Further, it can be shown that no relay has to deliver more than a constant factor of $\sqrt{n \log n}$ messages. This means under the multihop routing case with optimal transmit radius, the throughput achieved per source-destination pair scales as $1/\sqrt{n \log n}$ bps.

In Chapter 5, we study scaling of the *secrecy capacity* in a wireless ad hoc network. The only difference in the problem formulation is that now the network also includes eavesdropping nodes from which the bits need to be kept secret. We explore how many *secret* bits per

second the source-destination pairs can share. We show how a construction that is based on the one described here (Figure 2.8) can achieve the throughput scaling of $1/\sqrt{n \log n}$ bps while keeping the bits secret from eavesdroppers.

We see that even under optimal transmit power, nodes can share data at $1/\sqrt{n \log n}$ bps, which shows the capacity of wireless ad hoc networks does not scale well. This result, presented in [29], had a very important impact on the research activity in wireless ad hoc networks as explained in the following section.

2.4.4 Improved Capacity

The finding that the capacity of wireless ad hoc networks does not scale well [29] initiated a surge of research activity, especially in order to explore to what degree this result is tied to the specific model in [29]. It is important to note that being a highly theoretical study, there are many underlying assumptions to the capacity problem definition which may each potentially change the answer. These include the modeling of the wireless nodes, the network, the wireless environment, how interference is assumed to affect nodes, what the underlying point-to-point communication method is, what the transmit power contraints are, etc. A tabulated summary of some major results categorized according to these assumptions can be found in [49] and [79, page 152].

The focus of many of the works following [29] has been on whether it is possible to improve capacity scaling under a different set of assumptions, which could serve as an important guideline to practical implementations of large wireless ad hoc networks. In this section, we review a number of the important results that show how the capacity can be improved. It should be noted, however, that the results of [29] have been shown to generalize to a much broader set of assumptions and communication techniques [79].

The construction described above (see Figure 2.8) achieves a capacity scaling on the order of $1/\sqrt{n \log n}$. It is further shown in [29] that, under their communication and network model, no other construction employing multihop routing can achieve a better scaling than

$1/\sqrt{n}$. This small difference between the lower and upper bounds on capacity was closed by the work in [16], which showed a construction that achieves $1/\sqrt{n}$ capacity scaling. The main reason behind the loss of a factor of $\sqrt{\log n}$ is the transmit radius employed. As discussed in the previous section, under a smaller transmit radius, the network is no longer fully connected. However, the network can still be "well-connected" under a constant transmit radius with only a relatively small number of nodes disconnected. The majority of the nodes form a big connected cluster, and can serve as a traffic-carrying backbone, called "percolation highways" in [16]. The construction in [16] employs *power control*, providing a transmit radius of $\sqrt{\log n}$ to only the nodes that need it, and giving a constant radius to the rest of the nodes. A construction that uses only the constant-radius nodes for relaying is shown to achieve $1/\sqrt{n}$ scaling in [16], demonstrating that the capacity upper bound given in [29] can be reached by employing power control.

Under our communication model, the throughput between a single source-destination pair under ideal conditions is W bits per second. We have seen that due to the presence of other active nodes, this throughput goes down with increasing network size n. An important study which shows that a constant throughput can still be achieved in a large network is [26]. The network model in [26] assumes *mobile* nodes as opposed to static nodes as in our model. The fact that nodes are mobile dramatically changes how routing can be done, as it is now possible that the source and destination nodes get closer in time. We have seen that a constant factor of n simultaneous transmissions is indeed possible (see Figure 2.8). However, these transmissions are between nearby nodes who are not necessarily source-destination pairs. When nodes are mobile, from time to time, the nearby nodes can indeed be source-destination pairs. In other words, even with a small transmit radius, it is possible to use single-hop routing in a wireless ad hoc network if the nodes are mobile. The work in [26] considers this possibility. It is shown that, at a given time there may not be enough number of nearby source-destination pairs to make full utilization of transmissions. However, by using *two-hop routing*, i.e., by giving messages to nearby nodes which wait

until they get close to the destination, it is shown that constant throughput is possible. This drastic capacity improvement, however, comes at the price of increased delay.

In addition to the network model, another important consideration is the communication model. Here, the question is whether capacity scaling can be improved by more advanced physical layer communication techniques than the simple point-to-point decoding with fixed rate based on the SINR threshold rule. Hence, the ultimate throughput capacity, regardless of the underlying physical layer communication scheme, is of interest. This requires a more information-theoretic approach, and the first work that took this approach is [77]. Here, it is shown that, for high-attenuation channels, the upper bound of $1/\sqrt{n}$ actually holds for any communication scheme. More specifically, for path loss exponents $\alpha > 6$, the scaling achieved by the construction shown above with multihop decoding-and-forwarding routing is indeed optimal in the order sense. This threshold was later improved in [78] to $\alpha > 4$. The question of whether any capacity scaling improvement is possible in low-attenuation regime was answered in [58]. It is shown in [58] that for path loss exponents $2 \leq \alpha \leq 3$, improvement is indeed possible using a distributed multiple-input-multiple-output (MIMO) scheme referred to as "hierarchical cooperation". In particular, they showed that this construction achieves a per-node scaling of $n^{1-\alpha/2}$, which is better than the simple multihop routing construction for $2 \leq \alpha \leq 3$. Further, they showed that no improvement was possible for $\alpha > 3$. Note that, in the special case $\alpha = 2$, this translates to having *constant per-node throughput*. In other words, nodes do not suffer any capacity loss in the scaling sense. This is an example of how the specific type of wireless medium can significantly effect the capacity results [59].

Finally, another way to improve capacity scaling is by supporting the wireless ad hoc network with an overlaid wired network, which together is called a *hybrid network*. This is done by placing base stations in the network, so that wireless nodes have the option of carrying the messages on the wired network for some part of the path. The wired network does not have its own traffic, so it can only improve wireless network's capacity. Whether

this improvement brings any scaling advantage is studied in works such as [45, 46]. These works present constructions that improve capacity scaling, but only if the number of base stations scale faster than $\sqrt{n}$. In Chapter 4, we prove upper bounds on the capacity scaling of hybrid networks.

2.4.5 One-dimensional networks

Two-dimensional models are a good approximation to many real networks. However, for some special configurations such as a collection of nodes in a narrow valley or a network of cars on a road, the network is better modeled as one-dimensional. In addition to modeling these networks, studying the one-dimensional case also has the added benefit of providing a starting point to get insight into the two-dimensional case. Also, the one-dimensional properties often carry over to the two-dimensional "strip" case, where the region is significantly longer in one of the dimensions [15].

The infinite one-dimensional network model is shown in Figure 2.2. The nodes are assumed to be point sources placed according to a homogeneous Poisson point process on the real line. As stated in the connectivity discussion, one-dimensional networks are much more restrictive compared to the two-dimensional case. In this section, we briefly cover the *capacity scaling* of the one-dimensional network.

The finite one-dimensional network model is shown in Figure 2.9. The network is comprised of nodes that fall within an interval of size n. Under the same traffic model described above, we present a construction to carry the n information flows between source-destination pairs. We divide the interval into "segments" of size $\log n$. It can be shown that each segment contains at least one node w.h.p. In each segment, one node is designated to be the relay. Messages are carried from the source to the destination via relays inside the segments that fall between the source and the destination. Similar to the two-dimensional case, time is divided into periods and the segments take turns in being active (see Figure 2.9).

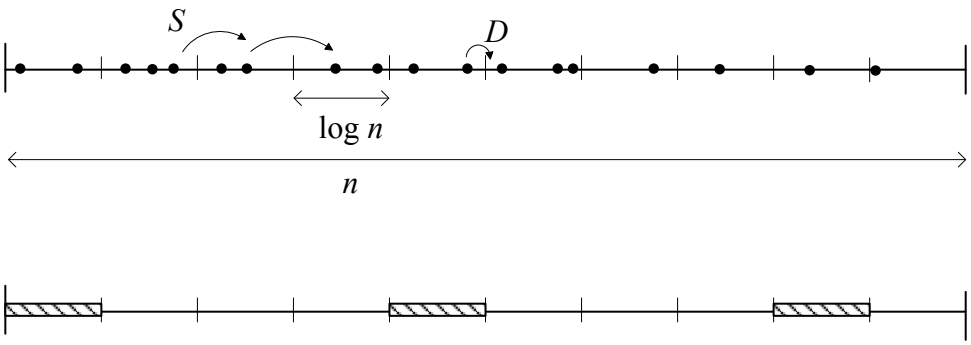

Figure 2.9: The finite one-dimensional network consists of nodes inside an interval of size n. A construction that carries the information flows between source-destination pairs is shown. The interval is divided into segments of size $\log n$ (top figure). Time is divided into periods where, in each period, segments with a certain minimum distance are active (active segments are shown shaded in the bottom figure). For the network shown, it takes 4 periods for every segment to be active at least once. A node in each segment is designated to be the relay of that segment. Messages are carried by relays inside the segments that belong to the corresponding path. Transmit power is chosen to make sure receiving relays in the neighboring segment can decode the message. This construction can be shown to achieve a per-node throughput that scales with $1/n$.

The capacity achieved by this construction can be found by calculating the workload on the relays. Consider a relay located close to the middle point of the interval. This relay needs to forward messages for roughly $n/4$ source-destination pairs w.h.p. It can be shown that no other relay has more workload w.h.p. Hence, it takes a constant factor of n periods to carry the traffic load. Therefore, the per-node throughput achieved by this multihop construction scales as $1/n$ bps.

Note that the one-dimensional network has worse capacity compared to the two-dimensional case. In fact, we achieve the same capacity scaling with the simpler one-hop (i.e., no relaying) construction. The fundamental reason for this constrained scaling is due to the fact that basically all information flows have to go through the same point, hence creating a bottleneck.

2.5 Summary

This chapter has introduced the models and some of the important previous results in the area of wireless ad hoc networks. These serve as a background for the following chapters. In Chapter 3, we study broadcast connectivity in cooperative wireless ad hoc networks. In Section 2.3, we argued that full connectivity never occurs for infinite networks with nodes with constant transmit radius. This means broadcast to the entire infinite network is not possible. In Chapter 3, we explore whether node cooperation can improve this situation. In the broadcast case, nodes transmit the same message, hence they can cooperate by combining their transmit power to reach further distances. We show that although this helps reaching a larger region, broadcast to the infinite network is still not possible except for low-attenuation cases. Chapter 4 studies the capacity scaling of hybrid networks. The addition of base stations helps improve the capacity of wireless ad hoc networks, and in Chapter 4, we show limitations on this throughput benefit. Chapter 5 uses the capacity results shown here, especially the construction in Figure 2.8, and extends them to the case of secrecy capacity. We show how network coding techniques in addition to a construction based on the one presented in Figure 2.8 can achieve secret communication from eavesdroppers of unknown location in the network without any compromise on the throughput. Finally, in Chapter 6, our focus is on the percolation phenomenon introduced here in Section 2.3. The sudden transition from disconnected clusters to a well-connected network occurs in many types of infinite graphs in addition to the random geometric graphs discussed above (see Figure 2.5). We study percolation in other types of infinite graphs for the case where edges between nodes can be of different types. For each type of connection, we can form a separate graph and the overall network can be seen as the combination of these different "layers". A node can have a path to another node that passes through multiple layers. We study percolation of the overall multilayer graph. In particular, we explore the minimum connectivity required for each layer in order to just start seeing a well-connected multilayer graph.

CHAPTER 3

BROADCAST IN COOPERATIVE WIRELESS NETWORKS

3.1 Introduction

Cooperation among nodes is a powerful tool to improve the performance of wireless networks. A simple example of cooperation is multihop forwarding, where intermediate nodes transmit a source node's message along a path to a receiver which is not within the source's direct reach. More powerful forms of cooperation have emerged in recent years. For example, there has been interest in cooperative diversity, where nodes place a signal simultaneously in the same frequency band to provide spatial diversity from the source to a next-hop destination [41, 65]. Such cooperation improves link-level performance such as reducing the probability of error, outage probability, etc. [65], [57], and has been considered for improving connectivity [65] and capacity [58] in large wireless networks.

Broadcast is a common operation in wireless networks. Examples include the periodic broadcast of routing updates and other control messages, and emergency signaling. It is important that a network successfully deliver these messages to the entire network, as failure to do so may block other operations and can severely impact network functionality. The important operation of broadcasting is especially challenging in a mobile ad hoc network (MANET) in which each node typically has a very limited communication range and broadcast messages have to be carried by nodes in a multihop fashion [55, 74]. A simple approach to broadcast in a MANET is to require each node to retransmit the message once it receives the message. However, flooding the network in this manner leads to frequent collisions and wastes network resources.

As with other network functions, and, perhaps more so, broadcast operation can be potentially enhanced by enabling a form of cooperative diversity. In particular, if the set of nodes that has decoded the message transmits using a distributed space-time code, this results in enhanced diversity against multipath fading and improved link performance rather than collisions. In addition, by combining their resources (e.g., power), cooperating nodes may be able to reach more distant nodes than would be possible without cooperation. In accordance with these ideas, several studies report improvements in broadcast performance in harsh environments [4,5]. It is therefore important to understand the theoretical limits of broadcast performance gain that can be realized by cooperation. In this chapter, we study the asymptotic limits of broadcast capabilities for large cooperative networks.

We investigate the ability of a source to transmit a message to the whole network when nodes are randomly distributed according to a Poisson point process. The source transmits the message with a given transmit power. The set of nodes that receive this signal with sufficiently large signal-to-noise ratio (SNR) *cooperatively* transmit the message to reach the next set of nodes, which again cooperate to reach further nodes and so forth. In this manner, the broadcast message propagates through the network, and, if this wave of message transmissions reaches the entire network, broadcast is said to be successful. In a random network, for a given source node, the probability of successful broadcast is strictly less than one, as there is always a nonzero probability that the source lacks any one-hop neighbors with which to initiate broadcast in the first place. Clearly, the probability of successful broadcast monotonically decreases as the size of the network grows. In our analysis, we explore whether the broadcast probability is zero or strictly between zero and one, in a network over an infinite-size region. The results, summarized in Table 3.1, show that the broadcast capability of the network strongly depends on the path loss exponent. For example, in an infinite 1-D network, the broadcast probability is zero for path loss exponents larger than 1, and nonzero for path loss exponents less than 1, regardless of the node density. Note that path loss exponents $\alpha < 1$ in 1-D and $\alpha < 2$ in 2-D might seem to be of

Table 3.1: Broadcast probabilities of cooperative wireless networks (α: path loss exponent, λ: node density, B: event of broadcast, r: transmission radius)

Probability of Broadcast for Extended Cooperative Networks			
1-D		2-D	
$\alpha < 1$	$0 < P(B) < 1$, $\forall \lambda > 0, r > 0$	$\alpha < 2$	$0 < P(B) < 1$, $\forall \lambda > 0, r > 0$
$\alpha = 1$	$0 < P(B) < 1$, $\lambda r > 1$	$\alpha = 2$	$0 < P(B) < 1$, $\lambda r^2 > 4/\pi$
$\alpha > 1$	$P(B) = 0$ $\forall \lambda > 0, r > 0$	$\alpha > 2$	$P(B) = 0$ $\forall \lambda > 0, r > 0$

only theoretical interest, but such exponents are sometimes observed in practice [70]. The broadcast capability of cooperative networks has previously been considered in [69] under a quite different model: a finite size network where the density of nodes goes to infinity, which motivates a deterministic approach. Under our same infinite network model, *connectivity* in a cooperative wireless network is analyzed in [19], where a stronger form of cooperation than assumed here is used, which results in a symmetric connectivity property between nodes. Therefore, in [19], a set of nodes being connected implies any member of the connected set can send a broadcast message to the entire set successfully.

The rest of the chapter is organized as follows: Section II describes the network assumptions and introduces the cooperative communication model. In Section III, we establish results on broadcast performance of cooperative wireless networks summarized in Table 3.1. Section IV is the conclusion. The results in this chapter is reported in [10].

3.2 Cooperative Network Model

We assume an extended wireless network, where nodes are randomly distributed in an infinite region according to a Poisson point process with node density $\lambda < \infty$. Each node is assumed to transmit with peak power P_t, which allows it to communicate, without cooperation, to nodes within transmission radius r. A node's transmission radius is defined to be the range within which other nodes can receive its signal with a power above a specified

decoding threshold, τ, which allows a receiver to satisfy a minimum signal-to-noise ratio (SNR) for physical layer functionality so that the two nodes are *connected*. With these definitions, r is given by:

$$P_t r^{-\alpha} = \tau, \tag{3.1}$$

where α is the path loss coefficient which determines the rate at which the received power decays with distance.

When two or more nodes cooperate, they simultaneously transmit the same message such that they can reach a greater distance than they would otherwise reach without cooperation. In this work, we assume cooperation provides *power summing* at the receiver. More formally, the condition for a cooperating set of nodes Ω to reach a node k is

$$P_t \sum_{j \in \Omega} (d_{j,k})^{-\alpha} \geqslant \tau, \tag{3.2}$$

where $d_{j,k}$ is the distance between nodes j and k.

We assume that the source initiates cooperative broadcast by transmitting the message, which is heard by nodes within the source's transmit range. In the second step, those nodes that have just received the message transmit cooperatively and reach a further set of nodes. In successive steps, the set of nodes that have received the message from the previous step cooperatively transmit. As in the maximum multihop diversity case in [69], we assume that a receiving node accumulates power from all previous steps. Hence, a node k can successfully decode the broadcast message, if this accumulated power satisfies (3.2), with Ω being the set of nodes that have previously decoded the message. If a message transmitted from a given node reaches all of the nodes in the network, then broadcast is said to be achieved. Without loss of generality, we consider a source node at the origin. We formally define the broadcast event B to be the event that the message sent from the

origin can be received by a node at any point in the entire infinite region, and $P(B)$ as the probability of successful broadcast.

3.3 Broadcast Analysis

With our assumptions on the network given in Section 3.2, there is always a nonzero probability that there are no nodes in the transmission range of the source, which means the broadcast cannot even be initiated. Hence, our analysis focuses on determining whether or not the broadcast probability is strictly larger than zero.

The problem considered is closely related to *percolation*, which has been extensively studied for (non-cooperative) wireless networks [51]. For an infinite network, percolation is said to occur if there exists a connected cluster with an infinite number of nodes. More formally, for a random graph, if the probability that a vertex (e.g., a node at the origin) connects to an infinite number of vertices is strictly larger than zero, this graph is said to percolate. In order to study the properties such as percolation, full connectivity, capacity, etc., an asymptotic analysis of wireless networks is usually done in one of two ways [17]: one can fix the size of the region and let the number of nodes go to infinity (dense network), or one can let the size of the region grow for some fixed node density (extended network). Here, we study the broadcast capability of cooperative wireless networks in an extended network setting. In particular, we assume a network where nodes are placed over an infinite region with a finite node density.

In the following analysis, without loss of generality, we assume that $\tau = P_t$, which makes the transmission radius $r = 1$ in (3.1). Some of the results (Theorems 3.1 (first part), 3.2, 3.3 (first part)) are for all node densities; therefore, those results are valid for any $r > 0$. The results in Theorems 3.1 (second part) and 3.3 (second part) are valid for $\lambda r > 1$ and $\lambda r^2 > 4/\pi$.

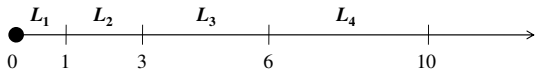

Figure 3.1: Division of the line used in the proof of Theorem 3.1. The positive real line is divided into intervals $\{L_k, k = 1, 2, \cdots\}$. Note that the length of the kth interval is $|L_k| = k$.

3.3.1 1-D Networks

Theorem 3.1. *In a 1-D extended cooperative wireless network, a node can broadcast its message to the entire network with nonzero probability (i) for any node density $\lambda > 0$ and any path loss exponent $\alpha < 1$, (ii) for any node density $\lambda > 1$ and path loss exponent $\alpha = 1$.*

Proof. Assume there is a node at the origin, and consider broadcast in the positive direction on the real line. Showing a nonzero probability of broadcast in the positive direction implies a nonzero broadcast probability for the entire network. Divide the line into intervals $\{L_k, k = 1, 2, \cdots\}$ as given in Figure3.1. Notice that the length of interval L_k equals k. In the following, we describe an event corresponding to a sufficient number of nodes in each interval for broadcast, and then show that this event occurs with positive probability.

Define the following events:

B_1: the event that interval $L_1 = (0, 1]$ contains at least $\lceil 2^\alpha \rceil$ nodes. B_2: the event that interval $L_2 = (1, 3]$ contains at least $\lceil 3^\alpha \rceil$ nodes, $\cdots$, B_k: the event that interval L_k contains at least $\lceil (k+1)^\alpha \rceil$ nodes. Let the random variable n_k be the number of nodes in interval L_k. With this definition,

$$P(B_k) = P(n_k \geq \lceil (k+1)^\alpha \rceil), \quad \forall k \in \{1, 2, \cdots\}.$$

The node at the origin can reach nodes within L_1 without cooperation. B_1 guarantees that the message can be broadcast to nodes within $L_1 \cup L_2$. Similarly, for any positive

integer q, if $\bigcap_{k=1}^{q} B_k$ occurs, this guarantees broadcast in $\bigcup_{k=1}^{q+1} L_k$. This can be seen by lower bounding the power received at the rightmost end of $\bigcup_{k=1}^{q+1} L_k$ by assuming all nodes in $\bigcup_{k=1}^{q} L_k$ are located at the origin and recalling $\alpha \leqslant 1$. With all nodes assumed to be located at the origin, the received power is:

$$\frac{P_t\big(1+\sum_{k=1}^{q}\lceil (k+1)^{\alpha}\rceil\big)}{|\bigcup_{k=1}^{q+1} L_k|^{\alpha}} \geq \frac{P_t\big(\sum_{k=1}^{q+1} k^{\alpha}\big)}{\big(\sum_{k=1}^{q+1} k\big)^{\alpha}} \geq \tau. \tag{3.3}$$

Note the simplifying assumption that $P_t = \tau$. The next step is to show that the event $\bigcap_{k=1}^{\infty} B_k$, which enables broadcast, has nonzero probability.

Consider $\lambda > 0$ for $\alpha < 1$, and $\lambda > 1$ for $\alpha = 1$. The number of nodes n_k in the interval L_k has expected value $k\lambda$. Let N be the smallest integer such that this expected value is greater than the number of nodes required for B_N to occur; that is $N\lambda > \lceil (N+1)^{\alpha}\rceil$. It is always possible to find such an N because as $k \to \infty$, $\lceil (k+1)^{\alpha}\rceil / k \to 0$ for $\alpha < 1$, and $\lceil (k+1)^{\alpha}\rceil / k \to 1$ for $\alpha = 1$. Now write

$$P(B^*) \geq P(\bigcap_{k=1}^{\infty} B_k) = \prod_{i=1}^{N-1} P(B_i) \prod_{k=N}^{\infty} P(B_k), \tag{3.4}$$

where B^* denotes the event that broadcast in the positive direction on the line happens. Clearly $\prod_{i=1}^{N-1} P(B_i) > 0$. Next consider $\prod_{k=N}^{\infty} P(B_k)$. Let $\delta \in (0,1)$ be defined as:

$$(1-\delta)E(n_N) = (1-\delta)\lambda N = \lceil (N+1)^{\alpha}\rceil \tag{3.5}$$

Using a Chernoff bound, we find a lower bound for $P(B_N)$.

$$\begin{aligned} P(B_N) &= P(n_N \geq \lceil (N+1)^{\alpha}\rceil) \\ &= P(n_N \geq (1-\delta)\lambda N) \\ &\geq 1 - \exp(-\lambda N \delta^2/2). \end{aligned} \tag{3.6}$$

The final step is to find lower bounds for $P(B_k)$ for $k > N$. As k increases, the ratio of the required number of nodes in interval L_k to the expected number $k\lambda$ gets smaller. Thus, using the same δ, which is constant given N as above,

$$\begin{aligned} P(B_k) &= P(n_k \geq \lceil (k+1)^\alpha \rceil) \\ &\geq 1 - \exp(-\lambda k \delta^2/2) \quad \text{for } k \geq N. \end{aligned} \tag{3.7}$$

Then,

$$\prod_{k=N}^{\infty} P(B_k) \geq \prod_{k=N}^{\infty} (1 - \exp(-\lambda k \delta^2/2)) > 0. \tag{3.8}$$

The last inequality above can be seen by noting that $\sum_{k=N}^{\infty} \exp(-\lambda k \delta^2/2)$ is a convergent series and hence, the infinite product is convergent [32]. Finally,

$$P(B^*) \geq \prod_{i=1}^{N-1} P(B_i) \prod_{k=N}^{\infty} P(B_k) > 0, \tag{3.9}$$

and $P(B) > 0$, where B is the event of broadcast to the entire line. □

Remark 3.1. *Theorem 3.1 states that a randomly selected node can broadcast to the entire network with nonzero probability. It may also be of interest to consider the existence of a node that can broadcast its message to the entire line with probability one. In fact, Theorem 3.1 indeed implies that, with probability one, there exists a node on the line which can broadcast to the entire network. This argument can be shown by considering the network as a disjoint union of finite size regions. For any given $\varepsilon > 0$, the length of the regions can be selected large enough, so that if a node can broadcast to an entire region, it can broadcast to the rest of the network with probability $(1 - \varepsilon)$. The result follows by noticing that, with arbitrarily high probability, there exists a node inside a finite union of these regions which can broadcast to its entire region.*

Theorem 3.2. *In a 1-D extended cooperative wireless network, the probability that a node can broadcast its message to the entire network is zero for any node density $\lambda > 0$ for path loss exponent $\alpha > 1$.*

Proof. Without loss of generality, assume that $P_t = \tau = 1$. For some $t \in \mathbb{R}$, consider nodes distributed in $(-\infty, t)$ according to a Poisson point process. Let x represent a realization of this random process, and let $\mathcal{X}$ be the set of all realizations. For some $l > 0$, a node to the left of t can send a broadcast message to point $(t + l)$ on the line only if, at some time in the execution of the broadcast, it belongs to a connected cluster Ω such that

$$\sum_{k \in \Omega} \frac{1}{(t + l - x_k)^\alpha} \geq 1, \tag{3.10}$$

where x_k is the location of node k in Ω. Let $A \subset \mathcal{X}$ denote the set of all such realizations.

Next, let $B \subset \mathcal{X}$ be the set of realizations such that if all the nodes in $(-\infty, t)$ transmit simultaneously, the received power at $(t + l)$ is larger than the threshold; i.e.,

$$B = \{x \in \mathcal{X} | \sum_{k} \frac{1}{(t + l - x_k)^\alpha} \geq 1\} \tag{3.11}$$

where, x_k is the location of node k for the realization $x \in \mathcal{X}$. For any $x \in A$, clearly $x \in B$, and hence $A \subset B$. So, $I_A(x) \leq I_B(x), \forall x \in \mathcal{X}$, where $I_A(\cdot), I_B(\cdot)$ denote the indicator functions of the sets A, B, respectively. The probability that a node to the left of t can broadcast to a node at $(t + l)$ is $E[I_A]$, which, by the monotonicity of integration, is upper bounded by $E[I_B]$. Therefore, for any $l > 0$ and $t \in \mathbb{R}$, the broadcast probability at $(t + l)$ by nodes in $(-\infty, t)$ is upper bounded by the probability that combined power from $(-\infty, t)$ can reach $(t + l)$.

Now, consider a node j at x_j, and assume nodes are distributed according to a Poisson point process to the left of x_j in $(-\infty, x_j)$. For some $l > 0$, consider the power received at j when all the nodes to the left of $(x_j - l)$ transmit simultaneously:

$$Y = \sum_{x_k \in (-\infty, x_j - l)} \frac{1}{(d_{k,j})^\alpha},$$

where $d_{k,j}$ is the distance between nodes j and k.

When $\alpha > 1$, the random variable Y has a finite mean, $\mu = E(Y) < \infty$. Next, define $Y(d)$ for an *integer* $d > l$ as

$$Y(d) = \sum_{x_k \in [x_j - d, x_j - l)} \frac{1}{(d_{k,j})^\alpha}. \tag{3.12}$$

For any sample point for which Y converges, $Y(d)$ is non-negative and non-decreasing with d, and, hence

$$E(Y(d)) \to E(Y), \quad d \to \infty \tag{3.13}$$

by the monotone convergence theorem. Then for arbitrarily small $\varepsilon/2 > 0$, there exists a d^* such that for $d \geqslant d^*$, $E(Y) - E(Y(d)) < \varepsilon/2$. Define:

$$Z(d) = Y - Y(d) = \sum_{x_k \in (-\infty, x_j - d)} \frac{1}{(d_{k,j})^\alpha}.$$

By the Markov inequality,

$$P(Z(d^*) > 1) \leq E(Z(d^*)) < \frac{\varepsilon}{2}. \tag{3.14}$$

Hence, with probability larger than $1 - \varepsilon/2$, a node with no neighbors within d^* to its left cannot be reached by combined power from all the nodes to its left. Then, as shown above, the probability that such a node can receive a broadcast message by cooperation of nodes to its left is less than $\varepsilon/2$.

Next, consider a 1-D network where nodes are distributed in $(-\infty, \infty)$ according to a Poisson point process with density $\lambda > 0$. Starting from the origin and moving to the left,

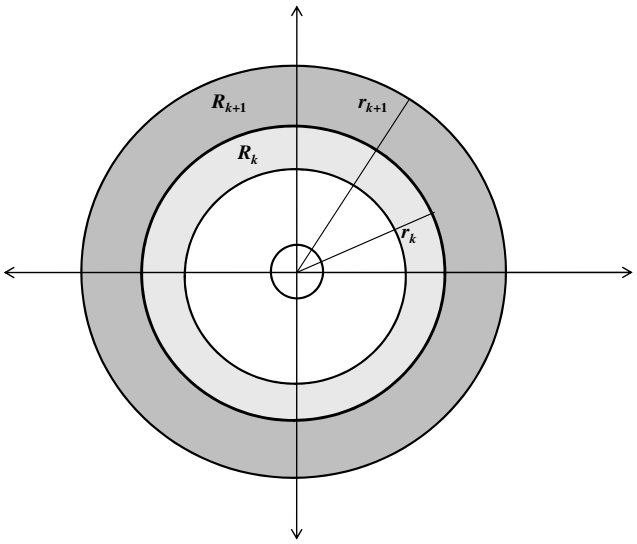

Figure 3.2: Division of $\mathbb{R}^2$ into rings $\{R_k, k = 1, 2, \cdots\}$ as used in proof of Theorem 3.3. R_k is the ring which corresponds to the region outside the circle of radius r_{k-1} and inside the circle of radius r_k, where $r_k = \sqrt{1 + 2 + \cdots + k}$

consider the first gap which is larger than d^*. For any $\varepsilon > 0$, such a gap exists within the first N gaps with probability

$$1 - (1 - \exp(-\lambda d^*))^N > 1 - \varepsilon/2$$

for some integer N. Consider the node at the right end of this gap. By (3.14), the probability that a broadcast message can be delivered to this node by nodes to its left is less than $\varepsilon/2$. Hence, probability of broadcast to the whole network can be upper bounded by an arbitrarily small number $\varepsilon > 0$. □

3.3.2 2-D Networks

Theorem 3.3. *In a 2-D extended cooperative wireless network, a node can broadcast its message to the entire network with nonzero probability (i) for any node density $\lambda > 0$ and*

any path loss exponent $\alpha < 2$, (ii) for any node density $\lambda > \frac{4}{\pi}$ and path loss exponent $\alpha = 2$.

Proof. Consider a division of $\mathbb{R}^2$ into rings $\{R_k, k = 1, 2, \cdots\}$ as given in Figure3.2. We are interested in the probability that a node at the origin can broadcast its message to the entire network. Similar to the 1-D case, we describe an event corresponding to a sufficient number of nodes in each ring for broadcast, and then show that this event occurs with positive probability.

Let R_k denote the kth ring and $r_k = \sqrt{1 + 2 + \cdots + k}$ be the radius of the circular area including the first k rings. Notice that the kth ring has area πk. Let the random variable n_k denote the number of nodes in the kth ring. We define the following events: B_1 is the event that R_1 contains at least $\lceil 2^\alpha(1 + 2^{\alpha/2})\rceil$ nodes, and for $k \geq 2$, B_k is the event that R_k contains at least $\lceil 2^\alpha(k + 1)^{\alpha/2}\rceil$ nodes.

The node at the origin can reach any node within the first ring (which is in fact a disk of radius 1) without cooperation. For any positive integer q, the event $\bigcap_{k=1}^{q} B_k$ guarantees broadcast in $\bigcup_{k=1}^{q+1} R_k$. This can be seen by lower bounding the power coming from the first q rings received at a point located at distance r_{q+1} from the origin. If all nodes in the first q rings are assumed to be located at the maximum possible distance from this point (i.e., at distance $r_q + r_{q+1}$ each), the power received would be

$$P_t \frac{\big(1 + n_1 + n_2 + \cdots + n_q\big)}{(r_q + r_{q+1})^\alpha} \tag{3.15}$$

$$\geq \quad P_t \frac{2^\alpha(1 + 2^{\alpha/2} + \cdots + (q + 1)^{\alpha/2})}{(2r_{q+1})^\alpha} \tag{3.16}$$

$$= \quad P_t \frac{2^\alpha \sum_{k=1}^{q+1} i^{\alpha/2}}{2^\alpha(\sum_{k=1}^{q+1} i)^{\alpha/2}} \geq \tau, \qquad \text{for } \alpha \leq 2. \tag{3.17}$$

Therefore, the transmission power from the first q rings suffices to reach the $(q + 1)$th ring.

We next show that $P(\cap_{k=1}^{\infty} B_k) > 0$. Note that the number of nodes in the kth ring has expected value $E[n_k] = \pi\lambda k$. At each step for $k \geq 2$, we require $\lceil 2^\alpha(k + 1)^{\alpha/2}\rceil$

nodes in R_k. Let N be the smallest integer such that $\pi\lambda N > \lceil 2^\alpha (N+1)^{\alpha/2} \rceil$. It is always possible to find such an N because as $k \to \infty$, $\lceil 2^\alpha (k+1)^{\alpha/2} \rceil / \pi k \to 0$ for $\alpha < 2$, and $\lceil 2^\alpha (k+1)^{\alpha/2} \rceil / \pi k \to 4/\pi$ for $\alpha = 2$. Let B be the event that broadcast happens. Then

$$P(B) \geq P(\bigcap_{k=1}^{\infty} B_k) = \prod_{i=1}^{N-1} P(B_i) \prod_{k=N}^{\infty} P(B_k). \tag{3.18}$$

Clearly $\prod_{i=1}^{N-1} P(B_i) > 0$. Next consider $\prod_{k=N}^{\infty} P(B_k)$. Let $\delta \in (0,1)$ be defined as:

$$(1-\delta)E(n_N) = (1-\delta)\pi\lambda N = \lceil 2^\alpha (N+1)^{\alpha/2} \rceil \tag{3.19}$$

Using a Chernoff bound, we find a lower bound for $P(B_N)$.

$$\begin{aligned} P(B_N) &= P(n_N \geq \lceil (N+1)^{\alpha/2} \rceil) \\ &= P(n_N \geq (1-\delta)\pi\lambda N) \\ &\geq 1 - \exp(-\pi\lambda N \delta^2/2) \end{aligned} \tag{3.20}$$

The final step is to lower bound $P(B_k)$ for $k > N$. As k increases, the ratio of the required number of nodes in the ring R_k to the expected number $\pi\lambda k$ gets smaller. Thus, using the same δ, which is constant given N as above,

$$\begin{aligned} P(B_k) &= P(n_k \geq \lceil 2^\alpha (k+1)^{\alpha/2} \rceil) \\ &\geq 1 - \exp(-\pi\lambda k \delta^2/2) \quad \text{for } k \geq N. \end{aligned} \tag{3.21}$$

Then,

$$\prod_{k=N}^{\infty} P(B_k) \geq \prod_{k=N}^{\infty} (1 - \exp(-\pi\lambda k \delta^2/2)) > 0, \tag{3.22}$$

which implies

$$P(B) \geq \prod_{i=1}^{N-1} P(B_i) \prod_{k=N}^{\infty} P(B_k) > 0.$$

□

Theorem 3.4. *In a 2-D extended cooperative wireless network, the probability that a node can broadcast its message to the entire network is zero for any node density $\lambda > 0$ for path loss exponent $\alpha > 2$.*

Proof. The proof is very similar to the proof of Theorem 3.2. It is based on the idea that there exists a critical distance $r^* < \infty$ such that, with high probability, the network cannot deliver a broadcast message to a node that has no neighbors within a radius of r^*. As the size of the network grows, it includes such an isolated node with high probability . □

Thus, in a 2-D extended network with $\alpha > 2$, broadcast to the entire network is not possible. However, in contrast to a 1-D network with $\alpha > 1$, it is possible (with nonzero probability) for a node to broadcast its message to an *infinite* number of nodes in a 2-D extended network with $\alpha > 2$. This result follows from Theorem 4.3 of [19].

3.3.3 Comparison with Continuum Analysis

A theoretical analysis with the same goal of considering broadcast performance in cooperative wireless networks has previously been considered in [69] for a dense network. The key element of the analysis in [69] (and similarly in [34, 35, 68]) is that the random network is approximated by a deterministic *continuum model*, where it is assumed that the transmit power is distributed to the entire network as a continuum as opposed to separate randomly placed nodes in discrete locations with some nonzero transmit power. For a 2-D dense network where the transmit power coming from the cooperating nodes is assumed to be summed at the receiver, [69] shows that broadcast performance depends on what scale *multihop diversity* is exploited. In multihop diversity, power is accumulated from

$m \geqslant 1$ previous levels. If, as assumed here, power is accumulated from all previous levels ($m = \infty$), it is shown (for path loss exponent $\alpha = 2$) that the message is broadcast to the whole network [69]. This result can be easily extended to arbitrary path loss exponents in a 1-D network by observing that in the continuum limit, if nodes in a region of size 1 can reach nodes within a region of size $(1+\varepsilon_1), \varepsilon_1 > 0$, in the next level, broadcast will reach a region of size $(1 + \varepsilon_1 + \varepsilon_2)$ with $\varepsilon_2 > \varepsilon_1$. Hence, the broadcast region grows to infinity for all path loss exponents and power densities. The same result follows analogously in 2-D.

Thus, the results of [69] appear to be quite at odds with the results derived here. However, the dichotomy can be explained by carefully considering the assumptions in our work and in [69]. In the continuum analysis of [69], one models the random network in the limit of high node densities, where the distribution of nodes becomes deterministic, and then checks whether broadcast is possible or not. As noted above, under the $m = \infty$ assumption, this results in broadcast with probability one to the entire network, even in the limit of very large networks, because of the deterministic uniformity of the node distribution. Here, in contrast, we consider fixed node densities $\lambda < \infty$, with the associated randomness of node distributions, for infinitely large networks. Because of the randomness in the node locations, for $\alpha > 1$ (1-D) or $\alpha > 2$ (2-D) it is very likely that one will find an isolated node if the network is large enough, as formally described in the proofs of Theorems 3.2 and 3.4. Hence, the probability of broadcast is zero regardless of the node density λ. Hence, it is clear that one must be careful in choosing the appropriate model for a given application. The model of [69] has been successfully employed in numerous works [11, 33, 35], but our results would suggest caution in its application to very large random networks which require many hops for broadcast to reach the entire network.

3.4 Conclusion

We analyze the theoretical limits of node broadcast in a cooperative wireless network. For a network where nodes are distributed randomly to an infinite region, we calculate the

probability that a node can broadcast its message to the whole network. Using an exact discrete model, we show that broadcast performance of the cooperative network strongly depends on the path loss exponent, and that there is zero probability of broadcast for a large range of path loss exponents regardless of the node density.

3.5 Acknowledgment

The work in this chapter was supported in part by the National Science Foundation under grants CNS-0721861 and CNS-1018464, and in part by the U.S. Army Research Laboratory and the U.K. Ministry of Defence, and was accomplished under Agreement Number W911NF-06-3-0001.

CHAPTER 4

CAPACITY OF HYBRID NETWORKS

4.1 Introduction

Consider a wireless ad hoc network where n nodes are placed in a two-dimensional region, and are randomly matched into n source-destination pairs. As reviewed in Chapter 2, Gupta and Kumar showed in [29] that the rate of information that can be shared by each pair scales at most with $1/\sqrt{n}$, which shows that the capacity of wireless networks does not scale well. Successive works to [29] improved this scaling by considering cases not assumed in the original network or communication model, such as node mobility [26], a sophisticated physical layer scheme [58], etc.

One straightforward way to increase the capacity of an ad hoc network is to add infrastructure, i.e., an overlaid wired network connecting b base stations which help carry information between the wireless nodes. This type of a network is commonly referred to as a "hybrid network" [15, 45], and the capacity that can be achieved by ad hoc nodes in a hybrid network is the problem of interest in this chapter.

The scaling of capacity in hybrid networks has been studied in a number of works under different network and communication models starting with [40, 45]. Some of these works observe that whether or not infrastructure improves capacity scaling depends on how the number of base stations b scales as compared to n. In particular, the works of [45, 72, 80] show that the per-node throughput scaling of $1/\sqrt{n}$ remains the same if b grows at most with $\sqrt{n}$. Only after that point does the capacity start to increase. On the other hand, [1, 40] study the special case where $b = \Theta(n)$, and explore the possibility of providing each pair $\Theta(1)$ throughput. In particular, [1] shows that this is indeed possible for a fraction of node

pairs arbitrarily close to one. The cases of mobile nodes [50], multicast communication [12], and base stations with multiple antennas [67] in hybrid networks are studied in other related work.

The work of most interest to us is that of [46]. Under the Physical Model [29], [46] considers both one-dimensional and two-dimensional hybrid networks. A simple construction where each node gives their message to the closest base station via multihop is shown in [46] to provide a per-node throughput scaling of b/n bits per second. Note that, for 1-D networks, this is a significant improvement to pure ad hoc capacity of $1/n$. However, in 2-D networks, only when b grows faster than $\sqrt{n}$, does b/n provide a better throughput than pure ad hoc scaling of $1/\sqrt{n}$, which is consistent with previous results. The throughput scaling of b/n is shown to hold for values of b that satisfy $b \log b \leqslant n$. When b scales faster, e.g., when $b = \Theta(n)$, the construction is shown to achieve $1/\log b$ bits per second, i.e., a value less than b/n. The reason for this change is the fact that the workload on base stations is no longer uniformly bounded by their expected value. However, this result is an achievability result and it is of interest whether the throughput can be further improved.

In this chapter, we study lower and upper bounds on per-node throughput in 1-D and 2-D hybrid networks under the Physical Model. We show that the construction proposed in [46] in fact achieves better throughput than previously thought in the case where $b \log b$ grows faster than n. In addition to improving the achievability results, we show upper bounds on per-node throughput. Central to our work is a new result we establish on the maxima of a sequence of Poisson random variables. The phase transition that happens on the maxima of a sequence of Poisson random variables, namely that the maxima diverges from a constant factor of the mean for sequences with slowly growing mean values, had been shown in the literature [3]. However, the exact value (or the distribution) that the maxima takes was not identified, except for the special case of constant-mean Poisson sequences [37]. We establish how the maxima scales for the entire divergent range. This result helps characterize more accurately the throughput achieved by the construction

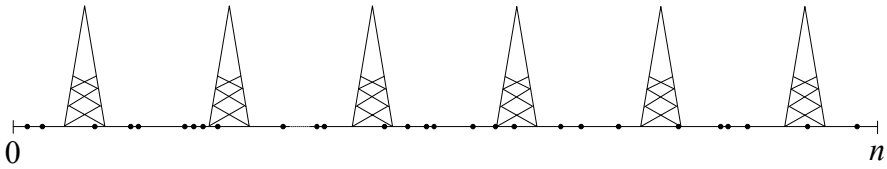

Figure 4.1: The one-dimensional hybrid network consists of randomly placed ad hoc nodes (represented by dots) and regularly placed base stations in the interval $[0, n]$. The base stations are connected through an infinite-capacity wired network.

in [46]. Further, using this result in addition to extending cutset methods that have been previously used for ad hoc networks under the Protocol Model [47], we prove upper bounds on throughput. These upper bounds match the lower bounds in the 1-D case, hence completely characterizing the capacity of 1-D hybrid networks. In 2-D, the bounds are tight for a range of values of b.

4.2 Model and The Main Results

4.2.1 Network Model

The hybrid network consists of static ad hoc nodes and base stations. The 1-D hybrid network is inside the interval $[0, n]$, and the 2-D hybrid network is inside the square $[0, \sqrt{n}] \times [0, \sqrt{n}]$ (see Figures 4.1, 4.2). Ad hoc nodes are distributed randomly according to a homogeneous Poisson point process with density 1, so there are n nodes in the network on average. Base stations are placed regularly in the network with a total of $b(n) \leqslant n$ base stations, where $b(n) \to \infty$, as n grows. Base stations are connected through a high-capacity wired network, which we assume to be infinite-capacity for our analysis. Ad hoc nodes are matched into source-destination pairs uniformly at random such that each node is the destination for exactly one source node, and is the source for exactly one destination node. Base stations are neither the source nor the destination of any flow of information, and simply help carry the traffic between ad hoc node pairs.

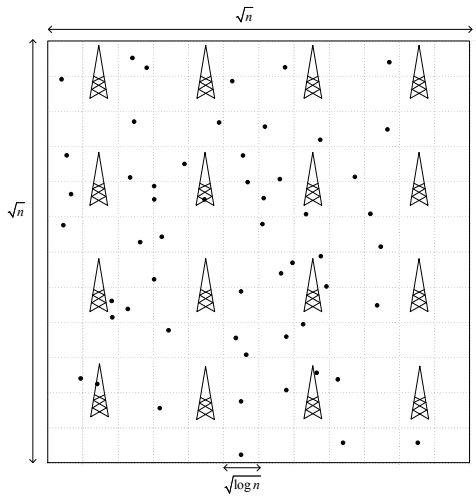

Figure 4.2: The two-dimensional hybrid network consists of randomly placed ad hoc nodes (represented by dots) and base stations regularly placed as a square grid inside the region $[0, \sqrt{n}] \times [0, \sqrt{n}]$. The base stations are connected through an infinite-capacity wired network.

4.2.2 Channel and Interference Model

The communication over the wireless channel is modeled such that, when node A transmits, the received power at node B due to A is

$$P^{A \to B} = P / d_{AB}^{\alpha},$$

where P is the transmit power, d_{AB} is the distance between nodes A, B, and $\alpha > 1$ in 1-D, $\alpha > 2$ in 2-D, is the path loss exponent. The received signal-to-interference-plus-noise ratio (SINR) at B is then

$$\text{SINR}_B = \frac{P^{A \to B}}{N_0 + \sum_{i \in \mathcal{T} \setminus \{A\}} P^{i \to B}}, \tag{4.1}$$

where N_0 is the power in the additive white Gaussian noise (AWGN) at the receiver, and $\mathcal{T}$ is the set of all transmitting nodes. The same model is used for all wireless communications including communications between a node and a base station. Nodes use a common transmit power P, but note that P can be a function of n. We assume that A can send data

to B at a fixed rate of W bits per second only if $\text{SINR}_B \geqslant \gamma$ for some threshold $\gamma > 0$. Thus the rate between a sender and a receiver is either W or 0 bps. Note that this channel and interference model is introduced in [29] as the "Physical Model".

4.2.3 Main Results

Based on the above network and channel models, our main results in this chapter are given in the following two theorems for the 1-D and 2-D hybrid networks, respectively. [1]

Theorem 4.1. *Consider a one-dimensional hybrid network as defined in Section 4.2.1. The per-node throughput shared by ad hoc nodes $T(n)$ in this network is upper-bounded as*

$$T(n) = \begin{cases} O(\frac{b}{n}), & b \log b = O(n), \\ O\left(\dfrac{\log(\frac{\log b}{n/b})}{\log b}\right), & \textit{otherwise,} \end{cases}$$

with high probability (w.h.p.). Furthermore, these upper bounds are tight, i.e., the above throughput values are achievable w.h.p.

Theorem 4.2. *Consider a two-dimensional hybrid network as defined in Section 4.2.1. The per-node throughput $T(n)$ in this network is upper-bounded as*

$$T(n) = \begin{cases} O(\frac{1}{\sqrt{n}}), & b = O(\sqrt{n}), \\ O(\frac{b}{n}), & b = w(\sqrt{n}) \text{ and } b \log b = O(n), \\ O\left(\sqrt{n/b}\dfrac{\log(\frac{\log b}{n/b})}{\log b}\right), & b \log b = w(n), \end{cases}$$

[1] The following order notation is used. $f(n) = O(g(n))$ if there exists a constant k such that $f(n) \leqslant kg(n)$ for n sufficiently large (for all $n > n_0$ for some n_0). $f(n) = \Omega(g(n))$ if $g(n) = O(f(n))$. $f(n) = \Theta(g(n))$ if $f(n) = O(g(n))$, and $g(n) = O(f(n))$. $f(n) \sim g(n)$ if $f/g \to 1$, $f = o(g)$ if $f/g \to 0$, which is equivalent to $g = w(f)$. Finally, we say $f(n) = O(g(n))$ w.h.p. if $P(f(n) \leqslant kg(n)) \to 1$ for some k.

w.h.p. For $b \log b = O(n)$, these upper bounds are tight, i.e., the above throughput values are achievable w.h.p. For $b \log b = w(n)$, $T(n) = \Omega\left(\log(\frac{\log b}{n/b})/\log b\right)$.

Note that, in the two-dimensional case, a per-node throughput on the order of $1/\sqrt{n \log n}$ bps is already achievable via pure ad hoc communication as shown in Section 2.4.3, i.e., $T(n) = \Omega(1/\sqrt{n \log n})$ for all cases. Overall, we have the following achievability results in the 2-D case:

$$T(n) = \begin{cases} \Omega(\frac{1}{\sqrt{n \log n}}), & b = O(\sqrt{n/\log n}), \\ \Omega(\frac{b}{n}), & b = w(\sqrt{n/\log n}) \text{ and } b \log b = O(n), \\ \Omega\left(\dfrac{\log(\frac{\log b}{n/b})}{\log b}\right), & b \log b = w(n). \end{cases}$$

4.3 Cutset Bounds

In this section, we prove two cutset results for upper bounding the total rate of information that can be achieved from a set of nodes inside a given region to nodes outside. Similar cutset bounds under the Protocol Model were shown in [47]. Here, we extend these results to the Physical Model. These results are used in proving the upper bounds in Theorems 4.1 and 4.2.

The following result establishes the fact that under the Physical Model, when nodes are located on a line, at most a constant rate of information can be delivered across a given point regardless of the number or the locations of the nodes.

***Lemma* 4.1.** *Consider an interval $[t_1, t_2]$ on the real line (see Figure 4.3). Under the Physical Model, when nodes are located on the real line, the rate of information that can be delivered from inside the interval to outside is upper bounded by $2W(1/\gamma + 1)$ bps.*

Proof. For convenience, first consider only the source-destination pairs where the destination nodes are placed to the right of the cut. Suppose there are m such active source-destination pairs. Let the set of source nodes be $\{S_1, S_2, \cdots, S_m\}$, where the numbering

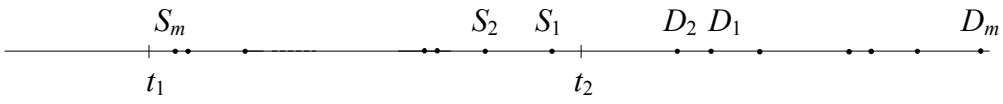

Figure 4.3: The cutset bound on the total rate of information that can be delivered from nodes inside an interval $[t_1, t_2]$ to outside is calculated. Message transmission from the interval can happen in either direction – left or right. There are m active source-destination pairs that communicate across t_2. The source nodes $S_1, S_2, \cdots, S_m$ are labeled in increasing distance from t_2.

is done in increasing order of distance from the point b (see Figure 4.3). Let D_i be the destination node of the source node S_i, $i = 1, 2, \cdots, m$. Hence, the SINR condition is satisfied for each pair S_i, D_i, and each pair shares W bits per second with a total of mW bits per second crossing the cut through point t_2.

Let $P^{S_i \to D_j}$ be the power received at D_j due to node S_i. The SINR condition at D_m requires

$$\frac{P^{S_m \to D_m}}{N_0 + \sum_{i=1}^{m-1} P^{S_i \to D_m}} \geq \gamma.$$

Note that, $P^{S_i \to D_m} \geqslant P^{S_m \to D_j}$, as nodes use common transmit power and the received power monotonically decreases with distance. Hence,

$$P^{S_m \to D_m} > \gamma \sum_{i=1}^{m-1} P^{S_m \to D_m} \geq \gamma(m-1) P^{S_m \to D_m},$$

which implies

$$m < \frac{1}{\gamma} + 1.$$

Therefore, there can be at most $\frac{1}{\gamma} + 1$ simultaneous transmissions crossing the cut through point t_2. A similar argument can be shown for transmissions through point t_1. Hence, the cutset capacity is upper-bounded by $2W(1/\gamma + 1)$ bps. □

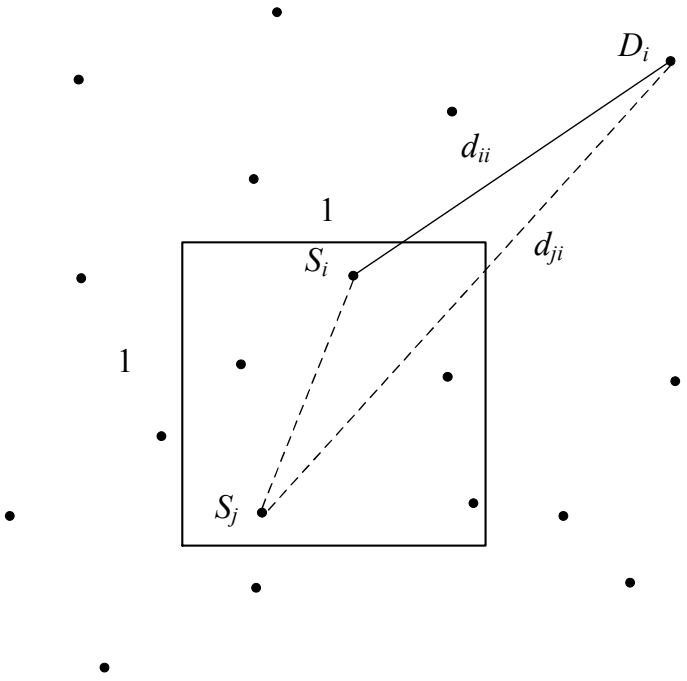

Figure 4.4: The first cut used in the proof of Lemma 4.2. A square region of size 1×1 is chosen as the cut. The source nodes are located inside the cut, and the destination nodes are located outside. Lemma 4.2 states that the number of simultaneous transmissions that can take place between such source-destination pairs is upper bounded by $3^\alpha/\gamma + 1$.

The following result shows that, in the two-dimensional case, under the Physical Model, the total rate of information that can be delivered from inside a given region to outside is proportional to the "edge length" of the region regardless of the number or the locations of nodes.

***Lemma* 4.2.** *Consider a box of size $\ell \times \ell$ on the two-dimensional plane. Under the Physical Model, and with the constraint that the received power cannot exceed the transmit power, the rate of information that can be delivered from inside the box to outside is upper bounded by $4W\ell(2 + \frac{2^\alpha+3^\alpha}{\gamma})$ bps.*

Proof. We first show that the number of simultaneous transmissions outside a box of size 1×1 is upper bounded a constant. Again, we consider one-hop transmissions between

node pairs where the source node is inside the box and the destination node is outside. Let $\mathbb{S} = \{S_1, S_2, \cdots, S_m\}$ be the set of sources (see Figure 4.4). Let D_i be the destination node for source node $S_i, i \in \{1, 2, \cdots, m\}$. The SINR at node D_i can be bounded as in the following.

$$\begin{aligned}
\text{SINR}_{D_i} &= \frac{P^{S_i \to D_i}}{N_0 + \sum_{j=1, j\neq i}^{m} P^{S_j \to D_i}} \\
&= \frac{P \min\{1, 1/d_{ii}^{\alpha}\}}{N_0 + \sum_{j=1, j\neq i}^{m} P \min\{1, 1/d_{ji}^{\alpha}\}} \\
&< \frac{P \min\{1, 1/d_{ii}^{\alpha}\}}{\sum_{j=1, j\neq i}^{m} P \min\{1, 1/(d_{ii}+2)^{\alpha}\}} \\
&= \frac{1}{m-1}(d_{ii}+2)^{\alpha} \min\{1, 1/d_{ii}^{\alpha}\} \\
&\leq \frac{3^{\alpha}}{m-1}
\end{aligned}$$

Since D_i needs to satisfy the SINR threshold, [2]

$$m \leq \frac{3^{\alpha}}{\gamma} + 1.$$

Now, consider a "strip" of size $1 \times \ell$ as shown in Figure 4.5. Similar to the 1-D case, we consider transmissions across the cut line. We now show that the number of simultaneous transmissions is upper bounded by a constant independent of the length of the strip as in the 1-D case. We divide the strip into a 1×1 box and a $1 \times \ell - 1$ strip as shown in Figure 4.6. We already know that there can be at most $\frac{3^{\alpha}}{\gamma} + 1$ transmissions from inside the box

[2]Note that, in order to avoid the singularity at vanishing distance between nodes, we impose the condition that the received power cannot be larger than the transmit power P. This is only necessary for the cutset bound proofs, as the nodes are assumed to be arbitrarily located. Although the path loss formulation here suggests $d = 1$ is the distance outside which the received power is assumed to decrease, in reality, there is a certain reference distance d_0 calculated for the specific conditions, and the received power is assumed to decay with $1/(d/d_0)^{\alpha}$ (see e.g., [23, page 46]).

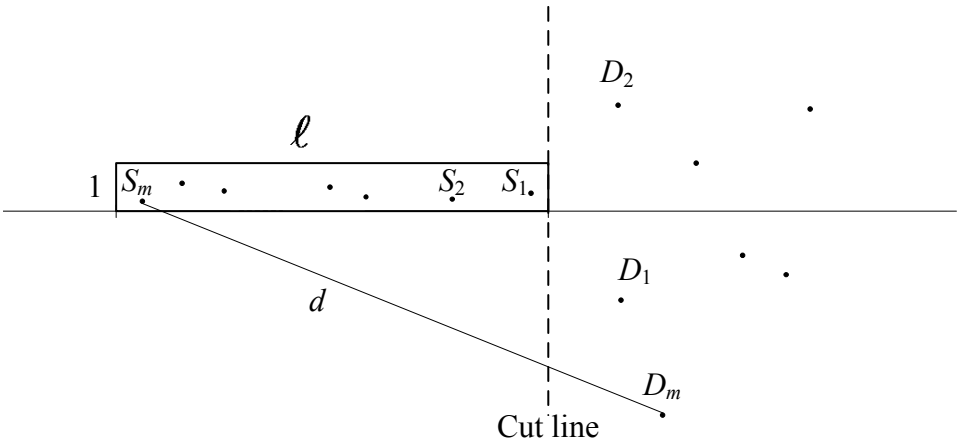

Figure 4.5: The strip used in the proof of Lemma 4.2. The number of simultaneous transmissions that can take place from sources inside the strip to destinations to the right of the cut line is upper bounded by a constant. To prove the argument the division of the strip as in Figure 4.6 is used.

of size 1×1 to outside. Suppose the strip of size $1 \times \ell - 1$ contains m' active sources. We label them in increasing order of their "horizontal distance" to the cut. Let d be the distance between $S_{m'}$ and $D_{m'}$. Consider the SINR value at $D_{m'}$.

$$\begin{aligned}
\text{SINR}_{D_{m'}} &= \frac{P^{S_{m'} \to D_{m'}}}{N_0 + \sum_{j=1}^{m'-1} P^{S_j \to D_{m'}}} \\
&= \frac{P/d^\alpha}{N_0 + \sum_{j=1}^{m'-1} P/|S_j - D_{m'}|} \\
&< \frac{P/d^\alpha}{\sum_{j=1}^{m'-1} P/(2d)^\alpha} \\
&= \frac{1}{m'-1} 2^\alpha
\end{aligned}$$

Since $D_{m'}$ needs to satisfy the SINR threshold

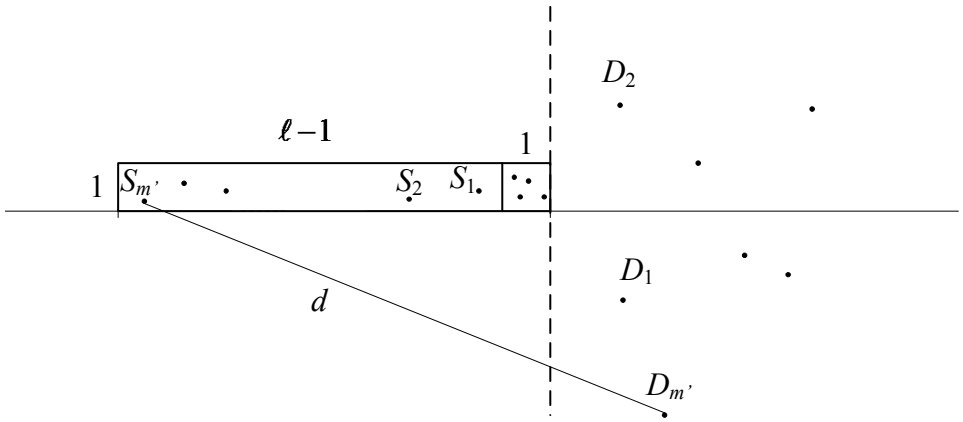

Figure 4.6: The strip is considered as the union of a square of size 1×1 and a strip of size $1 \times \ell - 1$. The proof is obtained by upper bounding the number of transmissions that can take place from source nodes within each region.

$$m' \leq \frac{2^\alpha}{\gamma} + 1$$

Hence, the total number of transmissions from the $1 \times \ell$ strip is upper bounded by $\frac{2^\alpha + 3^\alpha}{\gamma} + 2$.

Finally consider the $\ell \times \ell$ box shown in Figure 4.7. Any destination node outside the box has to be on the other side of one of the four cut lines shown. Hence, the number of transmissions are upper bounded by the sum of the number of transmissions crossing these four lines. For any cut line, the $\ell \times \ell$ box can be divided into ℓ strips of size $1 \times \ell$. We have shown above that there can be at most $\frac{2^\alpha + 3^\alpha}{\gamma} + 2$ transmissions from a strip, so the total number of transmissions from the $\ell \times \ell$ box crossing one cut line is upper bounded by $\ell(\frac{2^\alpha + 3^\alpha}{\gamma} + 2)$. Considering all four cut lines, the total number of transmissions is upper bounded by $4\ell(\frac{2^\alpha + 3^\alpha}{\gamma} + 2)$.

□

4.4 Maxima of a sequence of Poisson random variables

The regularly-placed b base stations can be thought of as dividing the network into b equal size "cells". In 1-D, each cell is a subinterval of length n/b, $[0, n/b]$ being the first

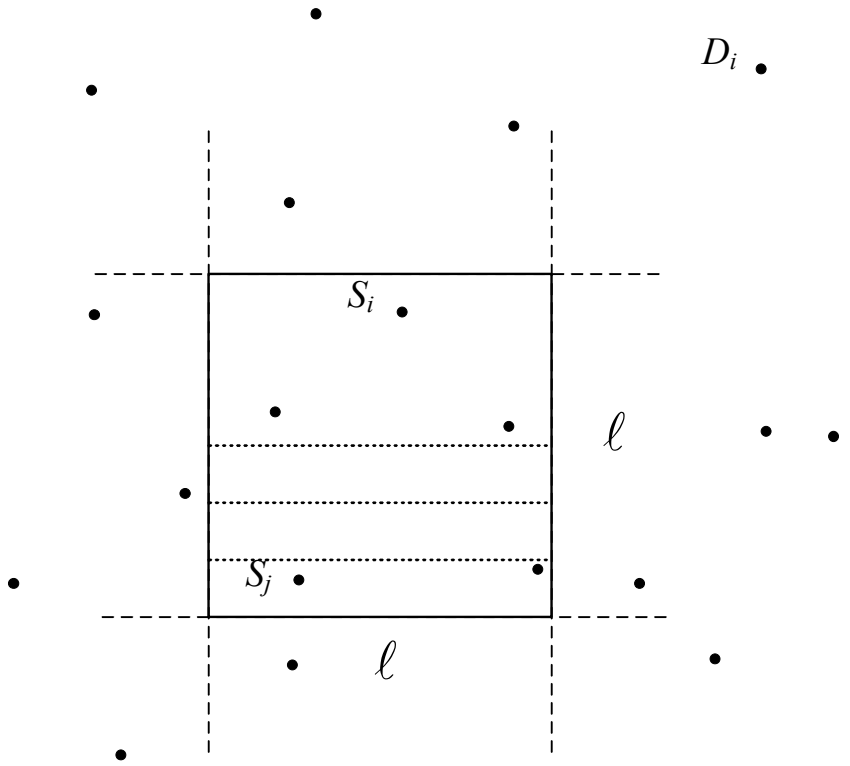

Figure 4.7: The box of size $\ell \times \ell$ is considered as a union of four $1 \times \ell$ strips for each cut line. Hence, the number of transmissions through each cut line is upper bounded by a number proportional to ℓ. Considering all four cut lines that the transmissions can cross, the total rate of information that can be transmitted to the outside of the box is upper bounded by a value proportional to the edge length ℓ.

cell (see Figure 4.8). In 2-D, each cell is a square of size $\sqrt{n/b} \times \sqrt{n/b}$. Consider each base station as serving the nodes inside its corresponding cell. Let X_i be the number of nodes in the ith cell, $i = 1, \cdots, b$. Note that X_i is a Poisson random variable with mean $\lambda_b = n/b$. As will be clear in the following, the overall achievable per-node throughput depends on the maximum number of nodes in any cell, i.e., the number of nodes in the busiest cell, which we denote by M_b, defined as $M_b = \max\{X_1, X_2, \cdots, X_b\}$. We are interested in the behavior of M_b as $b \to \infty$. Here it is very important to note that the distribution of the random variables X_i depend on b, i.e., the sequence of random variables $\{X_i, i = 1, 2, \cdots, b\}$ is an i.i.d. sequence, but with distributions that change at every value of b as b increases (we do not make this dependence explicit in the notation here for

simplicity). This type of a sequence is called a "triangular array of random variables" [3]. As will be seen in the following, the behavior of M_b as a function of b depends on how the distribution of X_i changes with b. In particular, M_b exhibits two different behaviors depending on how the mean of X_i grows with b (column-wise) [3]. The exact behavior of M_b is shown in the following lemma. This key result is what enables us to improve the previous achievable results in [46] for the case $b \log b = w(n)$ and also to help prove upper bounds for any value of b.

***Lemma* 4.3.** *Let $\{X_{b,1}, X_{b,2}, \cdots, X_{b,b}\}$ for $b = 1, 2, \cdots$ be a triangular array of Poisson random variables that are independent and row-wise identically distributed with mean λ_b, where λ_b is some non-decreasing function of b. Let M_b be defined as $M_b = \max_{1 \leqslant i \leqslant b} X_{b,i}$, so $\{M_b, b = 1, 2, \cdots\}$ is the sequence of the row-wise maxima. Then,*

1. *If $\lambda_b = \Omega(\log b)$, then for some $c < \infty$ independent of n, $P(M_b \leq c\lambda_b) \to 1$.*

2. *Define*

$$h(b) = \frac{\log b}{\log\left(\frac{\log b}{\lambda_b}\right)}. \tag{4.2}$$

If $\lambda_b = o(\log b)$, then $M_b = \Theta(h(b))$ w.h.p.

Proof:

1. For notational simplicity, for any given b, denote the sequence of random variables $\{X_{b,1}, X_{b,2}, \cdots, X_{b,b}\}$, by $\{X_1, X_2, \cdots, X_b\}$. For any $i =\in \{1, 2, \cdots, b\}$, X_i is a Poisson random variable with mean λ_b. Then, using a Chernoff bound argument, for any constants $c > 0$, $s > 0$,

$$
\begin{aligned}
P(X_i > c\lambda_b) &= P\left(\exp(sX_i) > \exp(sc\lambda_b)\right) \\
&\leq \frac{E\left(\exp(sX_i)\right)}{\exp(sc\lambda_b)} \\
&= \frac{\exp\left(\lambda_b(e^s-1)\right)}{\exp(sc\lambda_b)} \\
&= \exp\left(\lambda_b\left((e^s-1)-sc\right)\right).
\end{aligned}
$$

Using $s = 1$,

$$
P(X_i > c\lambda_b) \leq \frac{1}{\exp((c+1-e)\lambda_b)}, \qquad 1 \leqslant i \leqslant b.
$$

Then,

$$
P(M_b \leq c\lambda_b) \geq \left(1 - \frac{1}{\exp((c+1-e)\lambda_b)}\right)^b. \tag{4.3}
$$

Given $\lambda_b = \Omega(\log b)$, i.e., $\log b = O(\lambda_b)$, by definition, there exists some $k > 0$ independent of b, such that for some $b_0 > 0$, $\log b \leq k\lambda_b$, for $b > b_0$. Hence, for b sufficiently large, $\lambda_b \geq \log b/k$. Choosing $c = k + 2$, for $b > b_0$,

$$
\begin{aligned}
P(M_b \leq cn/b) &\geq \left(1 - \frac{1}{\exp((c+1-e)\lambda_b)}\right)^b \\
&\geq \left(1 - \frac{1}{\exp((k+3-e)\log b/k)}\right)^b \\
&= \left(1 - \frac{1}{b^{(k+3-e)/k}}\right)^b \\
&\to 1, \qquad b \to \infty.
\end{aligned}
$$

2. For any $X_{b,i}$, $i \in \{1, 2, \cdots, b\}$, let $F_b(x) = P(X_{b,i} \leq x)$ be its distribution function. It is known that in the case where $\lambda_b = \lambda$ is constant, there is no limiting distribution and M_b converges to one of two consecutive integers [2]. On the other hand, when

λ_b grows with b, it is shown in [3] that the maximum M_b exhibits two different behaviors depending on the growth rate of λ_b. The proof in the first part shows that M_b is bounded by a constant factor of λ_b when $\lambda_b = \Omega(\log b)$, which is consistent with the result in [3]. In the case where $\lambda_b = o(\log b)$, [3] shows that M_b converges to one of two integers. In other words, when $\lambda_b = o(\log n)$, there is a sequence of integers I_b such that

$$P(M_b \in \{I_b, I_b + 1\}) \to 1, \text{ as } b \to \infty. \tag{4.4}$$

However, it is of interest here to consider a question left open in the literature on the maximum of Poisson random variables, which is how M_b, i.e., I_b, scales when $\lambda_b = o(\log b)$. Note that for the special case of constant mean, $\lambda_b = \lambda$, it is shown in [37] that $I_b \sim \log b / \log \log b$, which, interestingly, is independent of the value of λ.

First, define the tail function $\mathcal{F}_b = 1 - F_b$. As in [37], we associate the following continuous function to the exact function $\mathcal{F}_b$, which agrees with $\mathcal{F}_b$ at integer values.

$$\mathcal{F}_{c,b}(x) = e^{-\lambda_b} \lambda_b^x \sum_{j=1}^{\infty} \lambda_b^j / \Gamma(x + j + 1), \tag{4.5}$$

where Γ is the gamma function. Second, define the sequence of real numbers $\{\beta_b, b = 1, 2, \cdots\}$ by the following relation:

$$1/b = \mathcal{F}_{c,b}(\beta_b) \tag{4.6}$$

Note that the function $\mathcal{F}_{c,b}$ is strictly decreasing, hence β_b is a growing sequence. In [2], it is shown that the integer sequence I_b is given by $I_b = \lfloor \beta_b + 1/2 \rfloor$. Therefore, the asymptotic behavior of I_b can be found by finding the growth rate of β_b.

By taking logarithms of both sides in (4.6),

$$\log b = \lambda_b - \beta_b \log \lambda_b - \log \sum_{j=1}^{\infty} \lambda_b^j / \Gamma(\beta_b + j + 1) \tag{4.7}$$

We do an asymptotic analysis on the above equation to analyze the growth rate of β_b. We first make the observation that, as b grows, the first term in the summation in (4.7) dominates the sum of the rest of the terms. This can be found by using the fact that for any $y > 0$, $\mathcal{F}_{c,b}(x)/\mathcal{F}_{c,b}(x+y) \to \infty$, as $x \to \infty$ [3, page 970]. The dominance result then follows by using $y = 1, x = \beta_b$. Hence, we may keep only the first term in the summation above and get

$$\log b \sim \lambda_b - \beta_b \log \lambda_b - \log \lambda_b + \log \Gamma(\beta_b + 2). \tag{4.8}$$

Then we proceed similarly. First, keeping the most dominant term in Stirling's approximation to the gamma function,

$$\log b \sim \lambda_b - \beta_b \log \lambda_b - \log \lambda_b + \beta_b \log \beta_b. \tag{4.9}$$

For the terms on the right hand side above, we look for the most dominant term(s). It is shown in [3] that β_b is asymptotically dominant to λ_b. (Note that $\log \beta_b$ does not necessarily dominate $\log \lambda_b$). Hence we are left with

$$\log b \sim \beta_b \log \beta_b - \beta_b \log \lambda_b. \tag{4.10}$$

From above, finally it can be shown that β_b satisfies

$$\beta_b \sim \frac{\log b}{\log(\frac{\log b}{\lambda_b})}.$$

□

4.5 One-dimensional Network

Theorem 4.1 is our main result for the one-dimensional hybrid network. We present its proof in the following. The proof is divided into two parts. The first part shows the achievability result by presenting a construction. The second part shows the upper bound by cutset arguments.

4.5.1 Achievability

We present a construction that describes how information is carried between source-destination pairs, and then calculate the throughput achieved by this construction, which gives a lower bound. Note that this construction is similar to the one presented in [46].

The interval $[0, n]$ is divided into small "segments" of length $\log n$, the first segment being $[0, \log n]$ (see Figure 4.8). It can be shown that each segment contains at least one node w.h.p. (see Appendix B.1). For ad hoc communication, data is carried through multihop where each time data is delivered to a node inside the next segment on the route. Note that segments are different from "cells", the subintervals of length n/b. Data is delivered from a source node to a destination node in three steps.

1. *Upload Phase*: The source sends the packet to the closest base station through multihop, where the packet is delivered to the next segment at each hop until it reaches the base station (see Figure 4.8). Note that the size of a cell becomes smaller than the size of a segment in the case $n/b \leq \log n$, and nodes reach the base station in one hop.

2. *Wired Phase*: The packet is carried through the wired network until it reaches the base station that is closest to the destination node.

3. *Download Phase*: The base station closest to the destination node delivers the packet to the destination node using multihop transmission by nodes in each segment. Note that if the base stations have enough power to reach the whole cell, this phase can be done with broadcast instead. However, this does not change the scaling result.

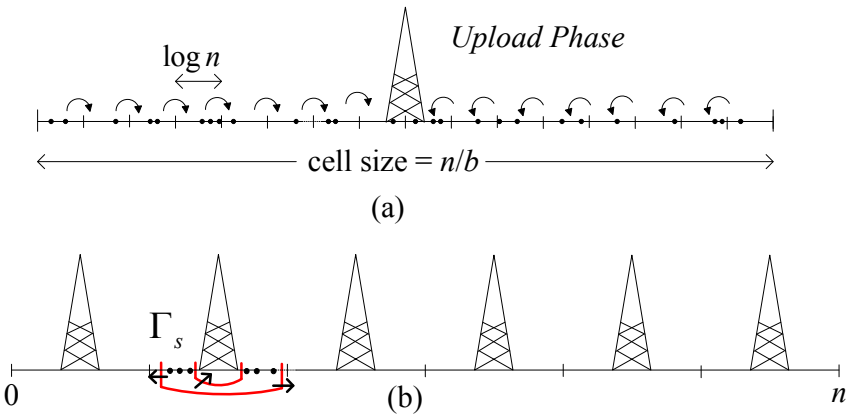

Figure 4.8: The 1-D network consists of b cells of length n/b. In the upload phase, the packet is delivered to the closest base station through multihop communication (a). After the wired phase, the destination base station delivers the packet to the destination node following the reverse of the operation in the upload phase (not shown). The cut Γ_s used to prove the upper bound is shown in (b). The cut is drawn around the ad hoc nodes in a cell and can be crossed in three places. All these crossings have constant capacity, bringing the overall cutset bound to a constant.

We next describe how to schedule transmissions for each phase using time division multiplexing. In the upload and download phases, nodes relay information for other nodes. Due to interference, nodes inside adjacent segments cannot transmit simultaneously. However, a standard spatial reuse scheme can be used where time is divided into slots and segments sufficiently far apart can be active in the same time slot. In particular, it can be shown that there exists a constant (independent of n) integer d, such that segments with d segments in between can transmit at the same time while satisfying the SINR requirement (see details in Appendix B.1) which includes exact values for the parameters for time division and transmit powers). Therefore, each segment can transmit at least once every $d+1$ time slots. The upload phase is completed once the segments finish relaying all the packets. A segment needs to relay information for at most all the nodes inside the cell. Hence, the number of nodes in a cell determines the number of time slots needed to finish its upload phase. Therefore, the upload phase can be finished in $(d+1)M_b$ time slots, where M_b is the number of nodes in the busiest cell. Hence, the throughput achievable in the upload phase

is $\Theta(1/M_b)$. As shown in Lemma 4.3, $1/M_b$ scales as b/n when $b \log b = O(n)$, and scales with $1/h(b)$ otherwise, where $h(b)$ is defined in (4.2). Note that the download phase brings the same throughput constraint and the wired phase brings no constraint.

Finally, the throughput achieved by the construction is given by considering the throughput constraint coming from all three phases, giving a lower bound of $\Omega(1/M_b)$ w.h.p.

4.5.2 Upper Bound

The construction presented above shows a way to share information between nodes, where the nodes inside the busiest cell become the bottleneck and determine the achievable throughput. A natural question of interest is whether this value can be further improved; in particular, whether these nodes can achieve better throughput by some other scheme. In this section, we answer this question by showing that, under the Physical Model, the nodes inside a cell cannot achieve a rate that scales better than the rates shown above regardless of the construction they use.

Let $s_i = [(i-1)n/b, in/b]$ be the ith cell $1 \leqslant i \leqslant b$. For any cell s, consider the cut Γ_s that divides the network into two regions (see Figure 4.8): Γ_s^i, which includes the ad hoc nodes inside s, and Γ_s^o which includes the rest of the nodes and all base stations. The cut capacity of Γ_s in the direction from Γ_s^i to Γ_s^o upper bounds the rate of information that can be carried away from the nodes inside s. This cut can be crossed in the direction to the base station or by ad hoc transmission to neighboring cells. The base station can receive W bps and is the only receiver for that crossing. For the crossings to the neighboring cells, the question is whether the nodes can achieve a rate that grows with n to ad hoc nodes outside the cell by some scheme. Lemma 4.1 shows that the total rate that can be achieved from inside of an arbitrary 1-D interval to the outside is upper bounded by a constant, namely $2W(1/\gamma + 1)$ bps, regardless of the number or placement of nodes inside or outside the interval, as long as communication is subject to the model presented in Section 4.2.2. Therefore, the nodes in any cell are bounded to have constant total rate

to the neighboring cells. Hence, the busiest cell determines the upper bound on the overall per-node throughput. Let s^* denote the busiest cell. Then the cut capacity of the cut Γ_{s^*} upper bounds the overall per-node throughput by $\Theta(1/M_b)$, which matches the per-node throughput achieved by our construction.

4.6 Two-dimensional Network

Our main result for the two-dimensional hybrid network is given in Theorem 4.2 in Section 4.2.3. The upper bounds and the achievability construction for the 2-D network are very similar to the 1-D case. Note that Lemma 4.3, which states how the maximum number of nodes in any cell scales, also applies to the 2-D case.

4.6.1 Achievability

As in the 1-D case, each source node delivers its packet to its destination in three phases. The only difference in the 2-D case is that the network is divided into "squarelets" of size $\sqrt{\log n} \times \sqrt{\log n}$. In the upload phase, the source delivers the packet to the closest base station by multihop communication, where at each hop the packet is delivered to a node in the next squarelet on the path following straight lines to the base station (see Figure 4.9). Full details of the 2-D construction are omitted here, but the arguments made in Appendix B.1 for the 1-D case can be very easily extended to 2-D. As in the 1-D case, the upload phase can be finished in a number of time slots proportional to M_b. Hence, the throughput achievable in the upload phase is $\Theta(1/M_b)$, which is the same as the download phase.

Note that nodes can achieve a per-node throughput on the order of $1/\sqrt{n \log n}$ bps by pure ad hoc communication using the construction shown in Section 2.4.3. Hence, for cases $b(n) = O(\sqrt{n}/\sqrt{\log n})$, nodes use pure ad hoc communication; otherwise they use the above three-step construction and achieve per-node throughput on the order of $1/M_b$ bps.

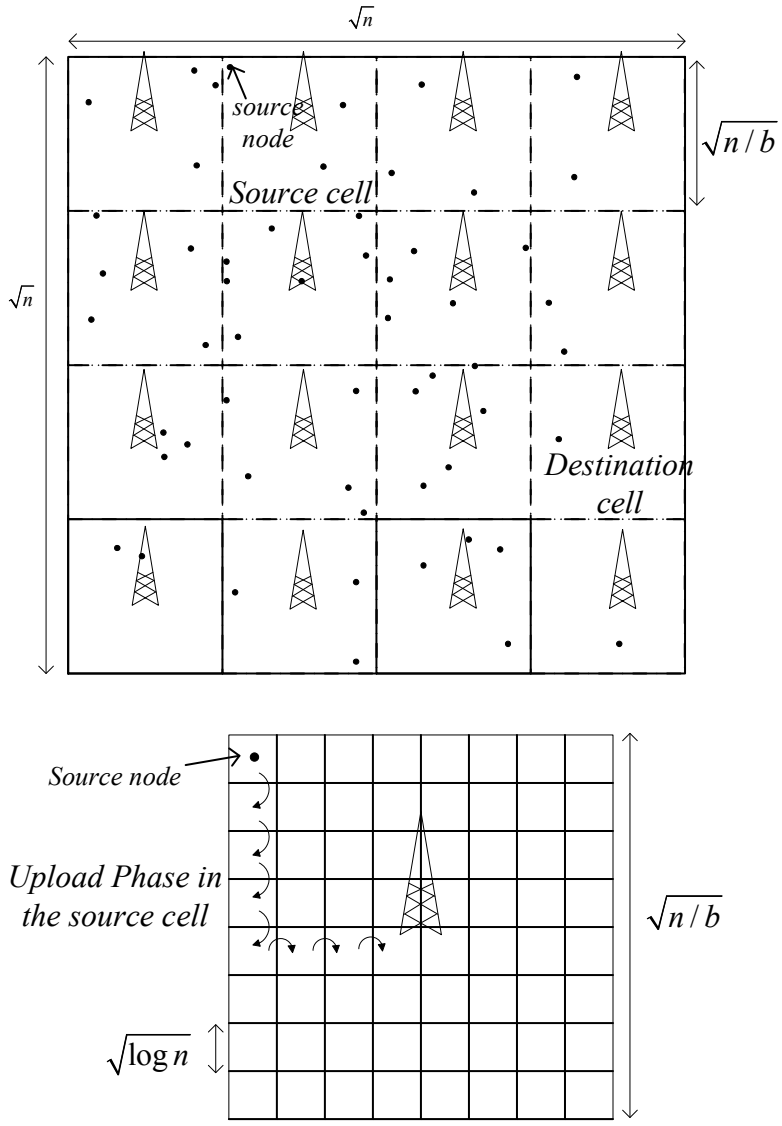

Figure 4.9: The region is divided into b cells, each of size $\sqrt{n/b} \times \sqrt{n/b}$ (top figure). A source node sends its packet to the destination in three steps. In the upload phase, the source node delivers the packet to the closest base station through multihop communication (bottom figure). In the wired phase, the packet is delivered from the source base station to the destination base station. The download phase follows the reverse operation of the upload phase (not shown).

4.6.2 Upper Bound

In the 2-D case, we use two cuts. Consider the first cut Γ shown in Figure 4.10. On one side of the cut, we have the set Γ^l containing the ad hoc nodes in the left half of the network. On the other side, the set Γ^r consists of *all* base stations and the remaining ad

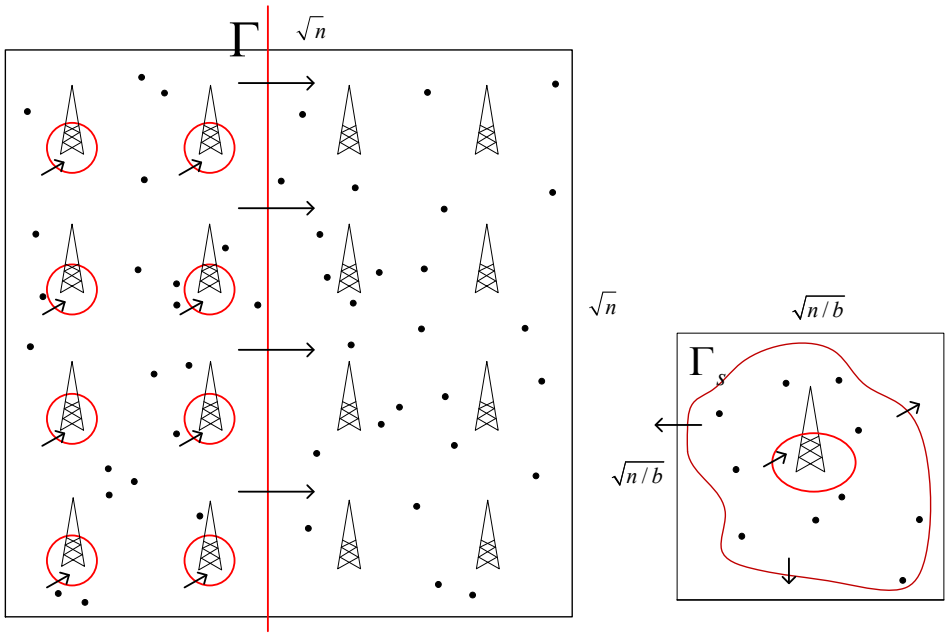

Figure 4.10: Cut Γ has half of the ad hoc nodes on one side and the rest of the ad hoc nodes and all base stations on the other side. Γ can be crossed into the $b/2$ base stations in addition to communication to other nodes through the middle line. Γ_s is drawn outside the nodes in a cell. This cut can be crossed to the base station and to nodes in other cells through ad hoc communication. Crossings to each base station has constant capacity, while crossings through ad hoc have capacity proportional to the corresponding edge length of the cut.

hoc nodes. The cut capacity in the direction from Γ^l to Γ^r consists of connections to the $b/2$ base stations, each with a capacity of W bps, and the crossing through the middle line which has capacity $\Theta(\sqrt{n})$ bps which can be seen by considering Lemma 4.2. Hence, the cut capacity of Γ is $\Theta(b+\sqrt{n})$ which serves a constant fraction of all nodes w.h.p., resulting in a per-node capacity of $\Theta(b/n + \sqrt{n}/n)$. The second cut Γ_s is defined similar to the 1-D case around the nodes inside the cell s. This cut has one crossing of capacity W bps to the base station, and other crossings through ad hoc connection to nodes outside the cell. Due to Lemma 4.2, the ad hoc crossing has capacity proportional to the edge length of the cell, i.e., $\sqrt{n/b}$. Hence, the cut for the busiest cell, Γ_{s^*} brings an overall per-node throughput upper bound of $\Theta(\sqrt{n/b}/M_b)$ bps. Finally, due to cuts Γ, Γ_s, we have an overall upper bound of $\Theta(\min\{b/n + \sqrt{n}/n, \sqrt{n/b}/M_b\})$ which gives the values listed in Theorem 4.2.

4.7 Discussion

Capacity scaling laws strongly depend on the communication and network model chosen. Achievability results presented in this chapter can be easily generalized to other models. For example, in contrast to the model assumed here, if nodes can perform power control, per-node throughput on the order of $1/\sqrt{n}$ bps can be achieved by pure ad hoc communication using the construction in [16]. However, we hasten to note that some of the cutset bounds we prove in this chapter may not apply under other models. For example, in contrast to the case shown in Lemma 4.1, under a model where the rate is a function of the SINR (and without any constraint on minimum inter-node distance, as assumed here), it is in fact possible for n nodes on a line to achieve a total rate that grows with n across a single point. This is shown in Appendix B.2.

Note that some previous work on hybrid networks explored the possibility of providing constant throughput to nodes [1, 40]. Our upper bounds show that (see Lemma 4.2), for regularly placed base stations, even under the case $b = n$, a constant rate is not possible for those nodes that occupy the busiest cell.

4.8 Acknowledgment

The work in this chapter was sponsored by the National Science Foundation under grant CNS-1018464 and by the U.S. Army Research Laboratory and the U.K. Ministry of Defence and was accomplished under Agreement Number W911NF-06-3-0001.

CHAPTER 5

SECRET COMMUNICATION IN WIRELESS NETWORKS

5.1 Introduction

Consider the transmission of a message from one party (Alice) to another (Bob), such that it is kept secret from an eavesdropping adversary (Eve). Cryptographic solutions assume that Eve will intercept the transmitted signal cleanly but impose a hard mathematical problem on Eve that is beyond her computational power to solve. Information-theoretic solutions do not rely on computational assumptions, but exploit the relative signal quality achieved at Bob compared to Eve. Specifically, if the signal quality is better at Bob than it is at Eve, a number of secret bits can be delivered to Bob [75] that is a function of the difference in signal qualities. Whether information-theoretic or cryptographic secrecy is employed in a system, there is utility in enhancing reception by the desired party while inhibiting reception by eavesdroppers. For information-theoretic security, the need is apparent, since a positive secrecy capacity relies on such. From the viewpoint of cryptographic security, inhibiting Eve's reception of the encrypted signal can be used to hide its existence or characteristics, or may be part of a defense-in-depth approach to information security. Hence, here we consider constructions that achieve a high signal quality at system nodes while providing a low signal quality to potential eavesdroppers. If a given high signal-to-interference-plus-noise ratio (SINR) threshold is exceeded at the system nodes while the eavesdroppers are unable to achieve a given (lower) SINR threshold, the communication will be deemed secret.

Here, we consider the secrecy problem in large wireless networks, both in the one-dimensional and the two-dimensional cases. In particular, we are interested in the amount

of information that can be carried by n (legitimate) nodes in a network while being kept secret from m eavesdroppers also present in the network. This problem can be seen as a security extension of the original problem of capacity scaling in large wireless networks [29], where an achievable per-node throughput that scales as $O(1/\sqrt{n \log n})$ is shown for a 2-D random network of n nodes. Since then, different strategies for achieving similar scaling results and also upper bounds on the capacity have been shown [16, 43]. When considering secrecy in large networks, the ability of network nodes to be securely *connected* (i.e., without any constraint on the throughput value) is studied in [30, 61]. Secrecy throughput scaling in a network with mobile nodes is studied in [44] using a one-hop transmission scheme [26]. The secrecy capacity scaling with static nodes, as assumed in our work, is studied in [39], where it is shown that if the eavesdropper locations are known, the eavesdroppers can be effectively routed around, and a secure per-node throughput of order $1/\sqrt{n}$ is feasible as long as the number of eavesdroppers in the network is $o(n/(\log n)^2)$. The case of eavesdroppers of unknown location is addressed in [73]. The trade-off between the per-node throughput that can be achieved and the number of eavesdroppers that can be tolerated is explicitly given in [73], where it is shown that a secure throughput on the order of $1/\sqrt{n \log n}$ is achieved if the number of eavesdroppers is on the order of $(\log n)^c$, for some $0 < c < 1$. The construction that achieves this trade-off uses artificial noise generation by legitimate nodes to degrade the signal quality at the potential eavesdropper locations, and uses a multi-user diversity effect exploiting the fading characteristics of the wireless channel.

A common assumption in most previous work in secrecy scaling is that the locations of the eavesdroppers are known. However, this assumption is highly undesirable especially for passive eavesdroppers [21]. In this chapter, we address the issue of unknown eavesdropper locations by requiring each source node to generate multiple "packets" for a single message such that the message can only be decoded if all packets are received, and no information about the message can be gained if even only one of the packets is

missing [63, 66]. These packets are sent in separate transmissions such that each packet is delivered to the destination but kept secure from potential eavesdroppers in a certain region of the network. Therefore, an eavesdropper anywhere in the network is guaranteed to miss some non-empty subset of the packets, and hence will not be able to decode the message. In the two-dimensional case, this is done by sending each packet on a different path, and maintaining sufficient separation between paths. In other words, the "path diversity" available in the network is utilized [48] to provide resilience against the lack of knowledge of the eavesdropper locations. From a graphical view, the eavesdropper has access to only a subset of the edges connecting the source-destination pair, hence it is possible to deliver secret bits by secret sharing at the source node and sending the pieces over the edges [6]. In the one-dimensional case, there exists only a single path connecting a source-destination pair, hence the one-dimensional network itself is partitioned into segments, where each packet is kept secure from eavesdroppers located in its corresponding segment.

We assume only path loss for the wireless channel, which means when a message is transmitted, it cannot be securely received by another legitimate node if an eavesdropper is closer to the transmitter compared to the receiver, since in that case, the SINR condition for secrecy cannot be satisfied. This makes achieving secret communication in the one-dimensional case especially challenging, since an eavesdropper located on a point on the line blocks any communication that has to be securely routed through this point. This makes secret communication between all legitimate nodes impossible even with a single eavesdropper in the network. In our work, we make use of the fact that enabling *cooperative jamming* makes secret communication possible in the one-dimensional network [8]. In cooperative jamming [22, 60], a legitimate node transmits artificial noise to degrade the signal quality at the potential nearby eavesdroppers. However, a legitimate node located far away from the jammer node can still achieve the required SINR, hence the transmission can "jump over" the eavesdroppers near the jammer to reach its destination. We present a construction that utilizes cooperative jamming to keep packets secure

from eavesdroppers located in the corresponding segment. If the number of eavesdroppers satisfies $m(n) = o(n/\log n)$, with this construction, almost all source-destination pairs achieve secure throughput of order $1/n$ with high probability, i.e., with probability one as the number of nodes n goes to infinity.

In the two-dimensional case, a fundamental advantage is the availability of many paths connecting a single source-destination pair. We present a construction that utilizes this path diversity and the fact that an eavesdropper cannot decode the packets that are transmitted over far-away paths. Using our construction, we show that in a two-dimensional network of n nodes, source-destination pairs can achieve a secure throughput on the order of $1/\sqrt{n \log n}$ if the number of eavesdroppers satisfies $m(n) = o(n/\log n)$. Furthermore, the throughput remains secure up to any constant number of eavesdroppers collaborating by combining their received packets. Note that cooperative jamming is not used in the construction in the two-dimensional case since the eavesdroppers with some minimum distance to a path cannot achieve the SINR threshold. However, this assumes a certain minimum noise level in the eavesdropper receivers, which may not be a desirable assumption in all cases. This can be avoided by using cooperative jamming for the transmissions on the paths, so that a noise floor is established at the potential eavesdroppers regardless of the quality of their receivers.

Inspired by the extensive improvements enabled by network coding, we explore whether additional coding techniques can provide further gains in secrecy in large wireless networks. The utility of network coding for secrecy has been recognized in previous work [6, 31], where it was studied in a more abstract setting. This motivates a more careful study of the application of general principles from the area of "secure network coding" to the wireless security problem. While the field of secure network coding is relatively well understood, the mapping of the wireless security problem to its framework is not clear. Secure network coding is a graph-based approach in which eavesdroppers tap edges (or not), which does not map well to the wireless environment where there are no edges but rather

there is a continuum of SNRs. Nevertheless, the coding methods proven to be useful to secrecy can easily be replicated for the wireless case. We show that by employing additional coding, in the non-collaborating eavesdropper case, our secrecy capacity results can be further improved by achieving a secure throughput on the order of $1/\sqrt{n \log n}$ for any number of eavesdroppers that may be arbitrarily located inside the network.

The rest of the chapter is organized as follows. We describe the network and channel models in the next section, which are used in our secrecy capacity results presented in Section 5.3 for the one-dimensional networks, and in Section 5.4 for the two-dimensional case. Our focused study in the utility of network coding ideas to wireless secrecy is presented in detail in Section 5.5, where we also present our improved results in the two-dimensional case. Section 5.6 is the conclusion.

5.2 Model

5.2.1 Network and Channel Model

The wireless network is composed of legitimate nodes and eavesdroppers inside the interval $[0, n]$ in the one-dimensional case, and inside the square region $[0, \sqrt{n}] \times [0, \sqrt{n}]$ in the two-dimensional case. Legitimate nodes are distributed according to a homogeneous Poisson point process with intensity $\lambda = 1$. All nodes are assumed to be static. Legitimate nodes are matched into source-destination pairs uniformly at random, such that each node is the destination of exactly one source node, and the source for exactly one destination node. For each pair, we associate a *stream* of information that needs to flow from the source to the destination. Eavesdroppers are assumed to be passive, and in the one-dimensional case, operating independently of each other, i.e., they do not collaborate by sharing their observations.

Only path loss is assumed for the wireless channels between transmitter and receiver nodes. Hence, whenever a node A transmits with some transmit power P, the received power at node B is modeled as

$$P_{\text{rcv},B} = P/d_{AB}^{\alpha},$$

where d_{AB} is the distance between nodes A, B, and $\alpha > 1$ in 1-D, $\alpha > 2$ in 2-D, is the path loss exponent. This model may be appropriate for a wideband system where fading is averaged out due to frequency diversity, or an environment without significant multipath effects.

We adopt a threshold model here, as motivated for both practical and information-theoretic security in [20]. Thus, we assume a message is successfully decoded if the received signal-to-interference-plus-noise ratio (SINR) exceeds a certain threshold $\gamma > 0$. In other words, node B successfully decodes node A's message if

$$\text{SINR}_B \triangleq \frac{P_{\text{rcv},B}}{N_0 + I_B} > \gamma, \tag{5.1}$$

where N_0 is the power in the additive white Gaussian noise (AWGN) at the receiver, and I_B is the interference received at node B due to other transmissions in the network. In our case, this interference may be due to other legitimate signal transmissions and/or artificial noise generated by legitimate nodes.

As mentioned above, for a message to be *securely* received at B in the presence of an eavesdropper E, we require the SINR at the eavesdropper SINR_E to be smaller than SINR_B. Furthermore, it may be desirable to have some positive *SINR gap* between nodes B and E. Hence, for some γ_e such that $0 < \gamma_e < \gamma$, in our model, we require $\text{SINR}_E < \gamma_e$, where γ_e can be selected to be arbitrarily small. Note that, from an information-theoretic secrecy perspective, this allows choosing some positive secrecy rate R_s given as [42]

$$R_s = \frac{1}{2}\big(\log(1 + \text{SINR}_B) - \log(1 + \text{SINR}_E)\big).$$

Therefore, for some region $\mathcal{R}$ in the network, a message is decoded by B while being secret from eavesdroppers inside $\mathcal{R}$ if (1) $\text{SINR}_B > \gamma$, and (2) any eavesdropper E inside

$\mathcal{R}$ has $\text{SINR}_E < \gamma_e$. For multihop transmission from a source node to a destination node, if this SINR condition is satisfied at every hop, we refer to the rate of information as the *secure throughput* achieved by this pair. Note that secrecy at each hop over a multihop path is shown to be sufficient for end-to-end secrecy in [39].

5.2.2 Performance Metrics

The network carries information streams to be delivered from the source nodes to their respective destinations. We consider the network's ability to carry these streams at a certain per-node throughput in the presence of eavesdroppers. Our performance metric is the number of eavesdroppers that can be tolerated while legitimate nodes maintain some *secure* throughput with high probability (w.h.p.).

5.3 One-dimensional Networks

The following theorem establishes security in the absence of eavesdroppers near the source-destination nodes, which is then used in Theorem 5.2 to establish the number of eavesdroppers that can be tolerated.

Theorem 5.1. *Consider the one-dimensional network inside the interval* $[0, n]$*, where eavesdroppers are arbitrarily distributed. The locations of the eavesdroppers are unknown, and they are assumed not to collaborate. Legitimate nodes can maintain a throughput of* $\Theta\big(1/n\big)$ *w.h.p. for all source-destination pairs, for any number of eavesdroppers. For some fixed positive constant* r*, the throughput achieved is secure for the source-destination pairs that satisfy the condition that no eavesdropper is placed within a distance* $r \log n$ *to the source and to the destination node.*

Overview of the Proof

We prove Theorem 5.1 by providing a construction summarized by the following steps:

1. In order to handle unknown eavesdropper locations, we partition the network into a finite number t of interlaced regions (also referred in the following as "coloring" the network), and treat each region (color) one by one, assuming each time that eavesdroppers are all confined to that particular region.

2. For each message to be delivered to the destination node, the source node generates t "packets", with each packet corresponding to one of the regions. These packets are generated in a way that ensures the message cannot be decoded by a node unless all packets are successfully received. These packets are delivered in separate transmissions such that each packet is protected from potential eavesdroppers in its corresponding region, thus guaranteeing that an eavesdropper located anywhere in the network misses at least one of the packets.

3. We provide an algorithm that routes packets from source to destination in such a way to ensure the secure transfer of the packet from potential eavesdroppers inside the region corresponding to it. This is achieved by legitimate nodes inside the region acting as "jammers" by transmitting random noise to prevent eavesdroppers in that region from decoding the packet.

4. We use time division multiplexing, where time is considered as a sequence of "periods". Each period consists of t "frames", and packets corresponding to color $i, i \in \{1, 2, \cdots, t\}$, are transmitted in the ith frame. Each frame is further divided into slots, where a standard spatial reuse scheme (as in [29]) is employed.

The proof is completed by showing that this construction achieves the stated throughput properties with probability one as the size of the network, n, goes to infinity.

Proof. Our construction consists of (1) partitioning of the network into regions (also referred to below as "coloring" the network), (2) a routing algorithm, and (3) a time-division multiplexing scheme, which are given in detail in the following. The proof is completed

by showing that this construction achieves a per-node secure throughput of $\Theta(1/n)$ w.h.p. regardless of the number of eavesdroppers, and that this throughput is securely achieved for the source-destination pairs with no very nearby eavesdroppers.

5.3.1 Coloring the Network

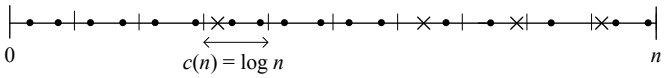

Figure 5.1: The one-dimensional network consists of legitimate nodes (represented by dots) and eavesdroppers (represented by crosses) placed in the interval $[0, n]$, divided into cells of length $c(n) = \log n$, as part of the signaling construction.

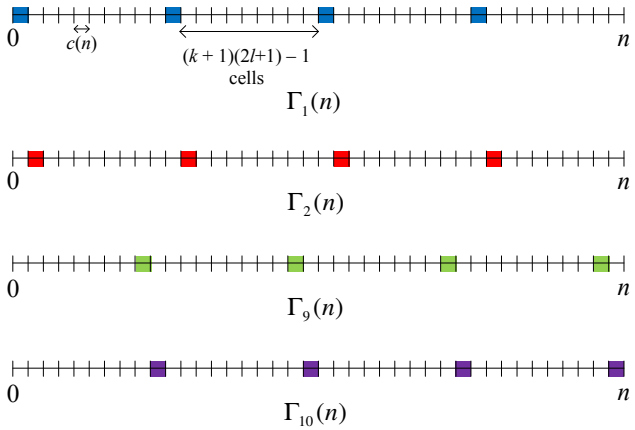

Figure 5.2: The network is partitioned into regions (colors), where each region is a collection of cells regularly sampled in the linear grid. Cells in a region are spaced $(k+1)(2l+1)-1$ cells apart ($k = 1$, $l = 2$ in the figure). Hence, the network consists of $t = (k+1)(2l+1)$ regions ($t = 10$ in the figure). The network is shown here with four of those 10 different regions highlighted.

We divide $[0, n]$ into sub-intervals referred to as "cells", each of length $c(n) = \log n$ (Fig. 5.1). Let $s_i(n)$ denote the ith cell, $i = 1, \cdots, n/\log n$, with $s_1(n) = [0, \log n]$.

We partition these cells into non-overlapping subsets, which we refer to as "coloring" the network. Specifically, we divide the network into $t = (k+1)(2l+1)$ regions (colors), where $k \geqslant 1$ and $l \geqslant 2$ are integers to be defined later. Denote the collection of regions as:

$$\{\Gamma_i(n), i = 1, 2, \cdots, t\}$$

Each region is a collection of non-contiguous cells regularly sampled in the grid as shown in Figure 5.2. Specifically, cells in $\Gamma_i(n)$ are spaced $t-1$ cells apart. In other words,

$$\Gamma_i(n) \triangleq \bigcup_{j=1}^{\frac{n/\log n}{t}} s_{i+(j-1)t}(n). \tag{5.2}$$

For convenience, we denote the j-th cell of region $\Gamma_i(n)$ as $\mathcal{C}_i^j(n)$. In other words,

$$\mathcal{C}_i^j(n) \triangleq s_{i+(j-1)t}(n).$$

The whole network is the union of the t regions:

$$[0, n] = \bigcup_{i=1}^{t} \Gamma_i(n)$$

Note that the number of regions t is independent of the size of the network n.

We refer to $\Gamma_i(n)$ and each of its cells $\mathcal{C}_i^j(n)$ as belonging to the i-th color. Also, we use the notation Γ_i, $\mathcal{C}_i^j$ in what follows, keeping in mind that the number of cells in a region, and the cell sizes depend on n. As will be clear in the description of the routing algorithm, the cells in a region can be thought of as potential locations of eavesdroppers corresponding to that region. For each cell $\mathcal{C}_i^j$, we define an interval called the "neighborhood" of this cell, and denote it by $N(\mathcal{C}_i^j)$. This neighborhood consists of $(2l+1)$ cells, with $\mathcal{C}_i^j$ being the middle cell (Figure 5.3). These neighborhoods are separated by $k(2l+1)$ cells.

It is also useful to define the "periphery" and the "interior" of a neighborhood. We define the *periphery* of $N(\mathcal{C}_i^j)$ as the two cells at the ends of the neighborhood, and the *interior* of $N(\mathcal{C}_i^j)$ as the smaller interval that consists of $(2l-1)$ cells centered at $\mathcal{C}_i^j$. Note that any given cell falls inside the interior of a neighborhood for $(2l-1)$ different colors (except the cells close to the two ends of the network).

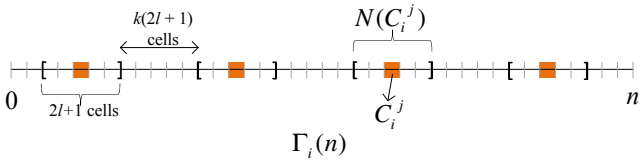

Figure 5.3: The network is shown with one region $\Gamma_i(n)$ highlighted as done in Figure 5.2. $\mathcal{C}_i^j$ denotes the jth cell in region $\Gamma_i(n)$. Around each cell, the "neighborhood" of that cell $N(\mathcal{C}_i^j)$ is defined as the interval consisting of $(2l+1)$ cells ($l = 2$ above). So, neighborhoods are separated by $k(2l+1)$ cells ($k = 1$ above).

For any source-destination pair $S - D$, a single message is delivered by sending t "packets" in separate transmissions, each corresponding to one of the t regions. Let w be the b-bit message to be delivered from S to D. S generates $(t-1)$ random b-bit packets $w_1, \cdots, w_{t-1}$ and then sets w_t such that the message w satisfies

$$w = w_1 \oplus w_2 \oplus \cdots \oplus w_t, \tag{5.3}$$

where $\oplus$ denotes bit-wise XOR operation. We refer to packet w_i as belonging to the ith color. The basic idea is that w_i is transmitted such that it is *protected* from potential eavesdroppers located in Γ_i. Note that any node that receives all t packets can compute w, while any node that misses one or more packets acquires no information about w.

5.3.2 Routing Algorithm

For the transmission of a packet of any color i from a source node S to its destination node D, S transmits the packet to a relay in the next cell on the route (Figure 5.4 (a)). Each relay that receives the packet does the same until the packet reaches the first neighborhood $N(\mathcal{C}_i^j)$ on the route. Inside $N(\mathcal{C}_i^j)$, we assign two nodes to act as relays, and one node to act as a jammer: A relay node A is selected from the cell where the route enters $N(\mathcal{C}_i^j)$, a jammer node J is selected from $\mathcal{C}_i^j$, and a relay node B is selected from the cell at the end of neighborhood (Figure 5.4 (b)). A receives the message from outside the neighborhood, and then transmits to B while J transmits random noise. Therefore, inside a neighborhood,

the message is transmitted across a number of cells in one slot. A jammer is only active when there is a transmission inside its corresponding neighborhood. When D receives all t packets, it decodes the message by performing the operation in (5.3).

Note that packets of color i are routed in a way that prevents them from entering the interiors of neighborhoods $N(\mathcal{C}_i^j)$, except possibly at the start or the end of the route. To see this, consider a source node S inside $\mathcal{C}_i^j$. S will generate a packet w_i of color i. This packet is first routed in single-cell hops as described above, and then follows the above scheme after it leaves outside $N(\mathcal{C}_i^j)$. Similarly, deliveries to destination nodes inside neighborhoods are also done in a sequence of single-cell hops (see Figure 5.4 (a)).

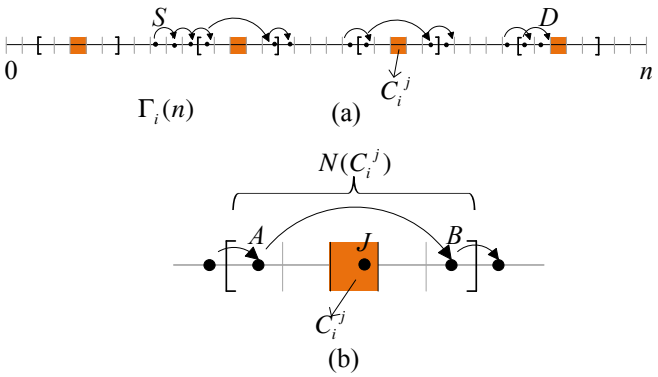

Figure 5.4: (a) The route connecting a source node S to a destination node D is shown. At each hop, the packet is delivered to the next cell on the route. (b) Whenever the route intersects a neighborhood $N(\mathcal{C}_i^j)$, the packet is transmitted such that it reaches over multiple cells at once. A transmitting relay A inside the cell where the route enters $N(\mathcal{C}_i^j)$ transmits to a receiving relay B inside the cell where the route exits $N(\mathcal{C}_i^j)$, while a jammer node J inside $\mathcal{C}_i^j$ transmits artificial noise. Hence, packets of color i are routed in a way that avoids entering the interiors of neighborhoods $N(\mathcal{C}_i^j)$. The only exception is possibly at the start or the end of the route, as the source or the destination node may be located inside the interior of a neighborhood (destination node D is inside the interior of a neighborhood in (a)).

5.3.3 Time Division Multiplexing Scheme

Time is divided into a sequence of "periods", where each period consists of t "frames" corresponding to the t colors. In the i-th frame, only packets belonging to the i-th color are

transmitted. In each frame, a spatial reuse scheme is employed such that in the i-th frame, every cell in the network transmits one packet of color i. This is done by further dividing each frame into t time slots. In each slot, transmitting cells are $t-1$ cells apart (see Figure 5.5). During the i-th frame, jammer nodes inside Γ_i may be active only during the two time slots where relays in the periphery of neighborhoods transmit.

The streams arriving to a cell take turns being relayed. A node in a given cell has to relay information for at most a constant factor of n streams w.h.p., hence a throughput of $\Theta\big(1/n\big)$ per stream is achieved w.h.p.

The route a packet takes contains the following types of hops: (1) single-cell hop outside neighborhoods, (2) multiple-cell hop inside a neighborhood, (3) single-cell hop inside a neighborhood if it contains either the source or destination (see Figure 5.4). In Appendix A.1, we show that the first two types of hops are achieved securely. We show that there exist constants k, l for coloring the network, and transmit power values for relays and jammer nodes, such that for any stream of color i, the destination node and the eavesdroppers inside Γ_i satisfy the SINR requirement for secure transmission. Hence, the only possible insecure transmissions are in the close proximity of the source and destination nodes (i.e., the third type above). For a source-destination pair, if no eavesdropper is within a distance $rc(n)$, $r = l$, to the source and the destination, then these hops will also be secure, hence the result follows. □

Theorem 5.2. *Consider the one-dimensional network inside the interval $[0, n]$, where the eavesdroppers are placed according to a Poisson point process with some density $\lambda_e > 0$, independent of the placement of the legitimate nodes. The locations of the eavesdroppers are unknown, and they are assumed not to collaborate. Then, the fraction of source-destination pairs that can maintain a per-node secure throughput of $\Theta\big(1/n\big)$ is arbitrarily close to one w.h.p, if $\lambda_e = o(1/\log(n))$.*

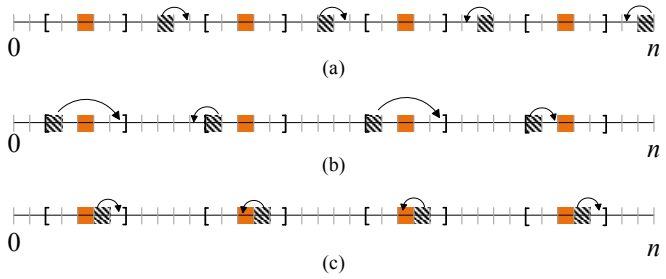

Figure 5.5: One period is divided into t frames. In the i-th frame, cells take turn in relaying packets of color i. Relaying is done according to the routing protocol corresponding to Γ_i (see Figure 5.4). Each frame consists of t time slots ($t = 10$ in the figure). Cells transmitting simultaneously (dashed cells) in one slot are $t - 1$ cells apart. For the i-th frame, three time slots are shown above: (a) shows a time slot with single-cell transmissions outside neighborhoods, (b) shows a time slot with transmissions in the periphery of neighborhoods (which may include multi-cell hops with jammers active), (c) shows a time slot with transmissions in the interiors of neighborhoods.

Proof. We use the same construction as that used to prove Theorem 5.1, which is shown to achieve w.h.p. the stated secure throughput for source-destination pairs free from any nearby eavesdroppers. The proof follows by showing that for $\lambda_e = o(1/\log n)$, the fraction of source-destination pairs that do not have any nearby eavesdroppers is arbitrarily close to one w.h.p.

Let the random variable $m(n)$ be the number of eavesdroppers in the network, which has an expected value of $\lambda_e n$. Let $y_i \in [0, n]$ be the location of the i-th eavesdropper, and define $A_i(n) = [y_i - l \log n, y_i + l \log n]$, with length $\ell(n) \triangleq |A_i(n)| = 2l \log n, \forall i$. Let $A(n)$ be the total region covered by the eavesdroppers, i.e., any source or destination node inside $A(n)$ will not be able to communicate secretly.

$$A(n) \triangleq \bigcup_{i=1}^{m(n)} A_i(n) \tag{5.4}$$

Let $N_i(n), N_o(n)$ be the random variables denoting the number of legitimate nodes inside and outside $A(n)$, respectively. For some $\varepsilon > 0$, define the event $C^{\varepsilon}(n)$ as

$$C^{\varepsilon}(n) \triangleq \left\{ \frac{N_i(n)}{N_i(n) + N_o(n)} < \varepsilon \right\}. \tag{5.5}$$

We can write $P(C^{\varepsilon}(n))$ as

$$P(C^{\varepsilon}(n)) = P(C^{\varepsilon}(n) \,|\, \{|A(n)| \leq 2\lambda_e n\ell(n)\})P(\{|A(n)| \leq 2\lambda_e n\ell(n)\}) \\ + P(C^{\varepsilon}(n) \,|\, \{|A(n)| > 2\lambda_e n\ell(n)\})P(\{|A(n)| > 2\lambda_e n\ell(n)\})$$

Define the random variable $X(n)$ as

$$X(n) \triangleq \frac{N_i(n)/n}{N_o(n)/n}.$$

Given $\lambda_e = o(1/\log n)$, and $|A(n)| \leq 2\lambda_e n\ell(n)$,

$$N_i(n)/n \to 0, N_o(n)/n \to 1, \text{ and } X(n) \to 0, \text{ a.s.}$$

Then,

$$P\big(C^{\varepsilon}(n) \,|\, \{|A(n)| \leq 2\lambda_e n\ell(n)\}\big) = \\ P\left(\frac{X(n)}{1 + X(n)} < \varepsilon \,|\, \{|A(n)| \leq 2\lambda_e n\ell(n)\}\right) \to 1, n \to \infty \tag{5.6}$$

Since, by a Chernoff bound,

$$P(|A(n)| \leq 2\lambda_e n\ell(n)) \geq P(m \leq 2\lambda_e n) \to 1, n \to \infty,$$

$P(C^{\varepsilon}(n)) \to 1$, as $n \to \infty$, for any $\varepsilon > 0$. Hence, with high probability, the fraction of nodes inside $A(n)$ is arbitrarily close to zero, which readily implies that the fraction of source-destination pairs inside $A(n)$ is arbitrarily close to zero w.h.p. □

5.4 Two-dimensional Networks

Similar to the one-dimensional case, we first establish security in the absence of eavesdroppers near the source-destination nodes in the following theorem by presenting a construction, which is then used in Theorem 5.4 to establish the number of eavesdroppers that can be tolerated.

Theorem 5.3. *Consider the two-dimensional network inside the square* $[0, \sqrt{n}] \times [0, \sqrt{n}]$*, where the eavesdroppers are arbitrarily distributed, and the locations of the eavesdroppers are unknown. Legitimate nodes can maintain a throughput of* $\Theta\big(1/\sqrt{n \log n}\big)$ *w.h.p. for all source-destination pairs, for any number of eavesdroppers. For some fixed positive constant* r*, the throughput achieved is secure for the source-destination pairs that satisfy the condition that no eavesdropper is placed within a distance* $r\sqrt{\log n}$ *to the source and to the destination node. For any given integer* $t < \infty$*, the throughput remains secure for any number* $g < t$ *of collaborating eavesdroppers arbitrarily chosen from the network.*

Overview of the proof:

Similar to the one-dimensional case, the key technique adopted in the construction to prove Theorem 5.3 is to require each source node to generate multiple packets to be sent in separate transmissions. However, a fundamental advantage in the two-dimensional case is that there exist many paths connecting each source-destination pair. By carefully selecting paths, and sending each packet on a different path, it can be ensured that an eavesdropper anywhere in the network cannot decode at least some of the packets since it is far from some of the paths. Therefore, unlike the one-dimensional case, "coloring" is done across different paths, rather than across different segments of a single path. By choosing the number of paths accordingly, it is further ensured that for any number of collaborating eavesdroppers up to some constant, the eavesdroppers cannot decode messages by combining their received packets.

Proof. In the following, we present the construction and prove that the construction achieves the stated properties.

5.4.1 Routing Algorithm

We divide $[0, \sqrt{n}] \times [0, \sqrt{n}]$ into a square lattice of cells, each with a side of length $c(n) = \sqrt{\log n}$ (Figure 5.6); hence, each cell contains a legitimate node w.h.p. (see Appendix A.1). For each source-destination pair $S - D$, S generates t packets $\{w_1, \cdots, w_t\}$ for each message w to be sent. The packets are generated in the same way as done in the one-dimensional case (see Section 5.3.1).

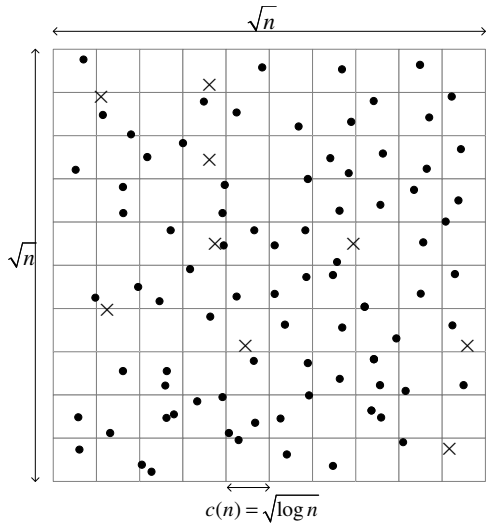

Figure 5.6: The two-dimensional network consists of legitimate nodes (represented by dots) and eavesdroppers (represented by crosses) placed in the square $[0, \sqrt{n}] \times [0, \sqrt{n}]$, divided into square cells of size $c(n) \times c(n)$, with $c(n) = \sqrt{\log n}$, as part of the signaling construction.

Consider square regions with $(t-1)(2l-1)+1$ cells on each side with S, and D in the center cells. We refer to these as S and D's "bases" (Figure 5.7). We define t "paths" connecting S to D, and packets of color i are sent on the i-th path. As shown in Figure 5.7, each path exits the source base on a horizontal line, then follows a vertical line entering the destination base. The first path exits the edge of the source base from the top cell on the edge. Outside the bases, the paths have a minimum spacing of $(2l-2)$ cells. Inside the

source base, a packet is delivered from S to a path following a vertical route. Similarly, when inside the destination base, a packet is delivered to D following a horizontal line. At each hop, the packet is delivered to a relay inside the next cell on the path. When D receives all t packets, it decodes the message by performing the operation in (5.3).

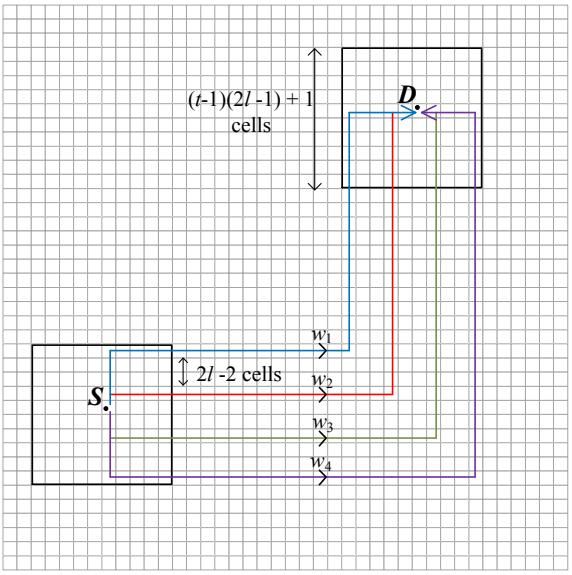

Figure 5.7: Around each source and destination node S, D, a square region is defined as the "base" of that node, and consists of $[(t-1)(2l-1)+1]^2$ cells ($t = 4, l = 2$ in the figure). Each source and destination pair $S-D$ is connected by t paths. Outside the source and the destination base, the paths consist of a horizontal line followed by a vertical line, and have a minimum spacing of $(2l-2)$ cells. The t packets generated by S for a single message are carried on these t paths.

Note that this routing algorithm (including the definition of source and destination base) is slightly modified for source or destination nodes close to the edges of the network, or when the bases are roughly aligned horizontally or vertically.

5.4.2 Time Division Multiplexing Scheme

Time is divided into a sequence of periods, where each period consists of t frames. Only packets of color i are transmitted in the i-th frame. Each frame is further divided into $(h+1)^2$ time slots for some constant h, where nodes with a distance of h cells transmit simultaneously in each time slot (Figure 5.8).

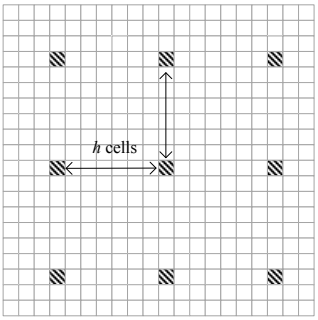

Figure 5.8: One period is divided into t frames, where only packets of color i are transmitted in the ith frame. Each frame is further divided into time $(h+1)^2$ slots. Nodes transmitting simultaneously (shaded cells) in a given time slot are h cells apart. In each time slot, relays in the active cells transmit a packet to a relay inside the next cell on the path.

In each cell, streams that have arrived to that cell take turns being relayed. As proved in Appendix A.3, the number of streams arriving to each cell is at most a constant times $\sqrt{n \log n}$ w.h.p. Hence, a throughput value of $\Theta\big(1/\sqrt{n \log n}\big)$ is achieved for each source-destination pair w.h.p.

For the secrecy of the achieved throughput, consider the transfer of a message w to be carried from node S to D, and focus on the transmission of a packet w_i on its corresponding path. Consider a hop where w_i is transmitted from node A to B. It is shown that (Appendix A.2), the receiving node B, and any eavesdropper E located at least a distance of $(l-1)$ cells from the transmitting cell satisfy the SINR condition for secrecy. This shows that a packet of color i is protected from all the eavesdroppers located outside a strip of width $(2l-1)$ cells surrounding the path carrying that packet. Note that, outside the bases, an eavesdropper can be located less than $(l-1)$ cells to at most one path due to the spacing of the paths. If the source and the destination are free from eavesdroppers inside a radius of $r \log n$, for any $r \geqslant 2tl$, then the source and destination bases do not contain any eavesdroppers. Hence, an eavesdropper in the network can decode at most one packet out of the t packets. Therefore, any number $g < t$ of collaborating eavesdroppers are not able to decode the message by combining their received packets. □

Theorem 5.4. *Consider the two-dimensional network inside* $[0, \sqrt{n}] \times [0, \sqrt{n}]$*, where the eavesdroppers are placed according to a Poisson point process with some density* $\lambda_e > 0$*, independent of the placement of the legitimate nodes. Then, almost all source-destination pairs can maintain a per-node secure throughput of* $\Theta\big(1/\sqrt{n \log n}\big)$ *w.h.p, if* $\lambda_e = o(1/\log(n))$*, and the throughput achieved remains secure for any number* $g < t$ *of collaborating eavesdroppers arbitrarily chosen from the network.*

The proof is very similar to the proof of Theorem 5.2, and is omitted.

5.5 Network Coding for Secrecy

In this section, motivated by the results in Sections 5.3 and 5.4, we take a more general view and study the utility of network coding approaches to help guarantee information-theoretic secrecy in the wireless environment. We present "toy" examples in Section 5.5.2 to demonstrate the salient aspects, and then show in Section 5.5.4 how the insight gained allows us to improve secrecy scaling results presented in Section 5.4.

5.5.1 Model

Here we describe the main tools used in the section. The first is the wiretap network model [6], which is an abstract graph-based tool that allows a formal way to check whether secure communication is possible using network coding [31]. The second is a very useful tool called the secrecy graph [30] which allows one to map a given physical wireless network topology (including eavesdroppers) to a graph which we study using the wiretap network model.

5.5.1.1 Wiretap Network

Let $G = (V, E)$ be a directed graph, where V is the set of legitimate wireless nodes including one source node s, and one destination node d. E is the set of edges representing the connections between the nodes. Assume that all nodes in V have a path to d. There is a

wiretapper who has access to what is transmitted on some of the edges. More specifically, let $\mathcal{A} = \{A_1, A_2, \cdots, A_m\}$, where $A_i \subseteq E, i \in \{1, 2, \cdots, m\}$, be the (known) collection of subsets of edges that can be wiretapped. The wiretapper has access to any member of the set $\mathcal{A}$, but no more than one member. Here, for the described wiretap network, the question of interest is whether it is possible to send a secret message from s to d, i.e., such that the wiretapper has no information about the message delivered to d. In [31], the sufficient and necessary condition for securely connecting s to d is given. Let $\mathcal{S} = \{S_1, S_2, \cdots, S_\ell\}$ be the collection of all subsets $S_i \subseteq V$ which contain the source node s. For any $S_i \in \mathcal{S}$, let $\delta(S_i)$ be the collection of incoming and outgoing edges connecting S_i to the rest of the nodes. Then, a message can be securely sent from s to d if and only if $\delta(S_i) \not\subseteq A_j$ for any i, j [31]. The necessity of this condition is clear: if some A_i contains all the edges between a source cut and the rest of the network, then the wiretapper can read whatever is coming in and out of the source and secrecy cannot be possible. On the other hand, if at least one edge is not wiretapped, this result says secret communication is indeed possible.

5.5.1.2 Secrecy Graph

The secrecy graph is introduced in [30] to study the secrecy capability of a wireless network. Here, we start with the topology (e.g., on $\mathbb{R}^2$) of the network with given locations of the legitimate nodes $\phi = \{x_i\}$, and the eavesdroppers $\psi = \{y_i\}$. Next each legitimate node x_i is connected to another node x_j with a directed edge if x_j is within x_i's transmit range, hence forming a graph. Then we turn this "baseline graph" into a directed "secrecy graph" by deleting unsecure edges. In particular, we delete the edge from x_i to x_j if there is an eavesdropper y_k which is closer to x_i compared to x_j, i.e., if $d(x_i, y_k) \leqslant d(x_i, x_j)$ for some $y_k \in \psi$, where d is the Euclidean distance. We call the edge (x_i, x_j) *wiretapped* by y_k. Note that the directed edge (x_j, x_i) may still be secure. Finally, we turn all directed edges in the secrecy graph to undirected edges, and the resulting graph is called the *enhanced* secrecy graph [30].

5.5.2 Network Coding Techniques to Aid Secrecy

In this section, we first show three examples of small networks where we demonstrate how network coding helps wireless secrecy. In all of these examples, the topology is a small square grid and the legitimate nodes are positioned on the corners with connections only to their nearest neighbors. These examples provide the insight to how network coding helps secrecy and serve as the basis for the secrecy result for the infinite square grid network given as the last example.

5.5.2.1 A simple two-way scheme

We start with a very simple example given in Figure 5.9. The wireless network consists of one source-destination pair $V = \{s, d\}$ and one eavesdropper e (the wiretapper). The nodes s, d are at the two ends of an edge of a square; hence, in the baseline graph, s and d are connected in both directions. The eavesdropper e is located on the same line with s, d, positioned close to s but on the side opposite to d. For the node s, e is the closest node, so the edge (s, d) is wiretapped and hence deleted in the directed secrecy graph; however, the edge (d, s) remains. Therefore, the enhanced secrecy graph has the undirected edge between s, d, suggesting that s and d are *securely connected*.

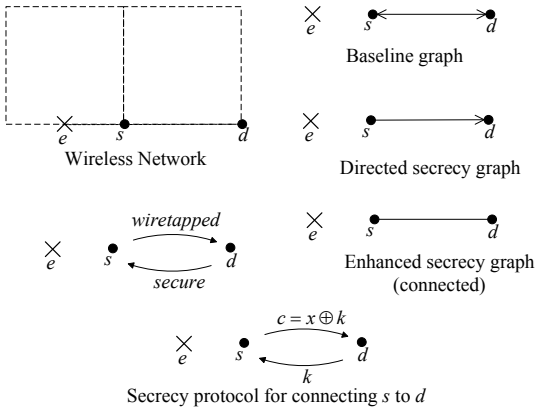

Figure 5.9: An example showing that a secure incoming connection to a source may be enough to deliver a secret message from the source to the destination, although the connection from the source to the destination is wiretapped.

Now consider this example with the wiretap network model. For the wiretapper, we have the set $\mathcal{A} = \{A_1\}$, where $A_1 = \{(s, d)\}$. There is a single source cut $S_1 = \{s\}$, and $\delta(S_1) = \{(s, d), (d, s)\}$. Hence, $\delta(S_1) \not\subseteq A_1$, and the secrecy condition is satisfied, which means there is a way to send a secret message from s to d. A secret message x is sent from s to d in two steps. In the first step, d generates a random string k and sends it to s. In the second step, s uses k as a one-time pad, and sends the string $c = x \oplus k$, where $\oplus$ is the XOR operation. In the end, d has the strings k, c and extracts x; however, e only has the string c and can obtain no information about x. This example illustrates the powerful idea that an incoming connection to the source can be very valuable for secrecy, and this will be exploited in the examples below. The fact that two nodes can be securely connected as long as one of the edges is secure was recognized in [30], and is the reason for the introduction of the enhanced secrecy graph to check secure connectivity.

5.5.2.2 Non-collaborating eavesdroppers of known location

Here, we have four legitimate nodes $V = \{s, a, b, d\}$ on the four corners of a square, and two eavesdroppers e_1, e_2 located in the middle of the edges between the pairs s, a, and s, b (Figure 5.10). The edges in both directions between s, a and s, b are wiretapped, hence the resulting secrecy graph is *disconnected*. Although the source is disconnected from both of its neighbors in both directions, we show that with the help of network coding, delivering a secure message from s to d is possible.

We first check whether the secrecy condition is satisfied. Assuming the two eavesdroppers do not collaborate, we have the following sets of wiretapped edges. $\mathcal{A} = \{A_1, A_2\}$, where

$$A_1 = \{(s, a), (s, b), (a, s), (a, d)\},$$
$$A_2 = \{(s, a), (s, b), (b, s), (b, d)\}.$$

Now consider the cuts $\mathcal{S} = \{S_1, S_2, S_3, S_4\}$, where

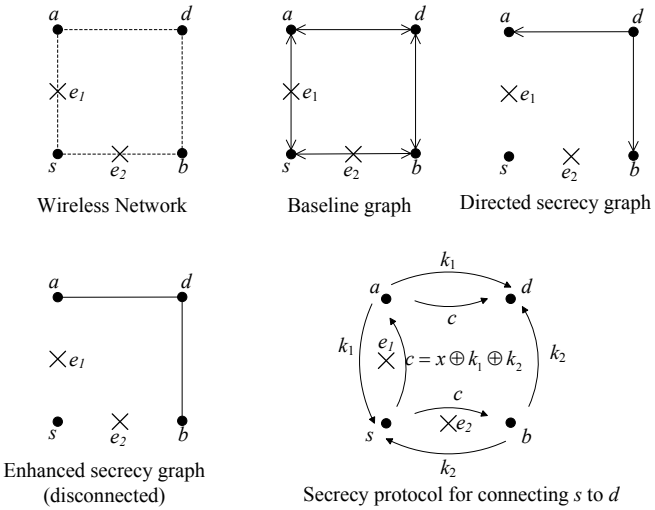

Figure 5.10: An example which shows that even though the source is disconnected from its neighbors in both directions, secure communication may still be possible if these blockages are due to separate non-collaborating wiretappers.

$$S_1 = \{s\}, \qquad \delta(S_1) = \{(s,a),(s,b),(a,s),(b,s)\},$$
$$S_2 = \{s,a\}, \qquad \delta(S_2) = \{(s,b),(a,d),(b,s),(d,a)\},$$
$$S_3 = \{s,b\}, \qquad \delta(S_3) = \{(s,a),(b,d),(a,s),(d,b)\},$$
$$S_4 = \{s,a,b\}, \qquad \delta(S_4) = \{(a,d),(b,d),(d,a),(d,b)\}.$$

Notice that $\delta(S_i) \not\subseteq A_j$, for any i, j. Hence, the condition for secrecy is satisfied and it is possible to securely connect s to d. In Figure 5.10, we describe a protocol that achieves such. First, nodes a, b generate random strings k_1, k_2, respectively and send them over their outgoing edges successively. Next, s calculates $c = x \oplus k_1 \oplus k_2$, and sends it. Finally, a forwards the string c to d. The receiver d now has the strings c, k_1, k_2 and can extract the secret message x. At the end of the protocol, the eavesdropper e_1 has the strings k_1, c, but misses k_2. Similarly, e_2 has c, k_2 but not k_1. Therefore, the eavesdroppers do not have any information about the message x. Also, note that the message is not revealed to the nodes a, b.

5.5.2.3 Eavesdroppers of Unknown Location

For our third example, consider the square grid given in Figure 5.11 with the two squares labeled B_1, B_2 as shown. There are six legitimate nodes $V = \{s, d, r_1, r_2, r_3, r_4\}$. A very important difference in this example is that the location of the eavesdroppers are unknown. There may an arbitrary number of (non-collaborating) eavesdroppers located anywhere inside the square grid except at the exact same locations with the legitimate nodes. Here, to check the secrecy condition, for each of the squares, we consider an optimally located eavesdropper.

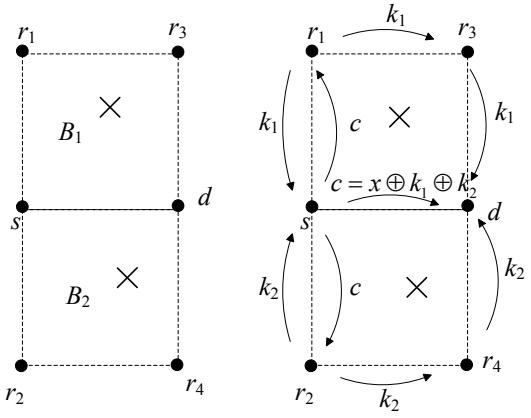

Figure 5.11: An example which shows how network coding also helps against eavesdroppers of unknown location. The idea is to partition the network into regions and consider the worst-case wiretapper in each region.

Let A_1 be the worst-case set of edges that can be wiretapped by an eavesdropper located inside B_1. A_1 contains all the outgoing edges of the nodes s, r_1, r_3, d. Similarly A_2 contains all the outgoing edges of the nodes s, r_2, r_4, d. For this graph, there are many source cuts. As an example, consider the smallest cut $S_1 = \{s\}$. For S_1, we have $\delta(S_1) = \{(s, r_1), (r_1, s), (s, d), (d, s), (s, r_2), (r_2, s)\}$. Note that, when checked against S_1, the set A_1 misses the edge (r_2, s), and A_2 misses (r_1, s), i.e., $\delta(S_1) \not\subseteq A_1$ and $\delta(S_1) \not\subseteq A_2$. It can be easily verified that for no $S_i \in \mathcal{S}$, $\delta(S_i)$ is fully contained in A_1 or A_2. Hence, it is possible to connect s to d securely.

We next describe a protocol that securely connects s to d as shown in Figure 5.11. In the first step, nodes r_1, r_2 generate the random strings k_1, k_2, respectively, and send them on their outgoing edges. Then, the source replies with the string $c = x \oplus k_1 \oplus k_2$. The protocol completes by delivering the strings k_1, k_2 to the destination d as shown in Figure 5.11. In the end, d extracts the message x from the received strings. An eavesdropper located inside B_1 is guaranteed to miss the string k_2, while an eavesdropper inside B_2 misses k_1. Hence, regardless of their location, no eavesdropper in the network has any information about x. In addition, the message is not revealed to any legitimate node except d.

5.5.3 Scaling Results

The benefits of network coding as illustrated in the previous section has very important implications for secrecy in large wireless networks. Here, we consider two important cases: 1) secure connectivity on a square lattice network, 2) secrecy capacity of a random extended network.

5.5.3.1 Secrecy in a Square Lattice

Here, we consider the square lattice network on $\mathbb{Z}^2$ where the legitimate nodes are located on the lattice points. Secure connectivity of this network was previously studied in [21, 30] and percolation thresholds were calculated. Here, we show how the network coding techniques presented in the previous section immediately improves these results. The following theorem states our result:

Theorem 5.5. *Consider a square lattice network, where the legitimate nodes are located on $\mathbb{Z}^2$ and the eavesdroppers are arbitrarily distributed with their locations unknown. The eavesdroppers are assumed not to collaborate. Then, the node at the origin is securely connected to any legitimate node on the lattice for any number of eavesdroppers.*

Proof. The examples in the previous section provide the basic steps in the proof of this result. In particular, we prove the theorem by showing how the node s at the origin $(0, 0)$

can be connected to some selected lattice points in the first quadrant. Secure connectivity to other points can be similarly shown.

Let d be located at $(1, 0)$. s can send a secret message to d by simply using the protocol given in Figure 5.11, by employing the nodes at $(0, 1), (0, –1), (1, 1), (1, –1)$ as relays. Similarly s can send a secret message to a node located at $(0, 1)$ by employing the four nodes located at points $(–1, 0), (–1, 1), (1, 0), (1, 1)$ and executing the same protocol. The secrecy protocol to go from s at the origin to a node d at $(1, 1)$ is given in Figure 5.12. Again, roughly, the idea is that the source receives two keys k_1, k_2 from the relays on two opposite directions, and these keys also arrive to d from two opposite directions. Connection to other points can be shown in a similar manner and therefore, the source is connected to any node on the lattice. □

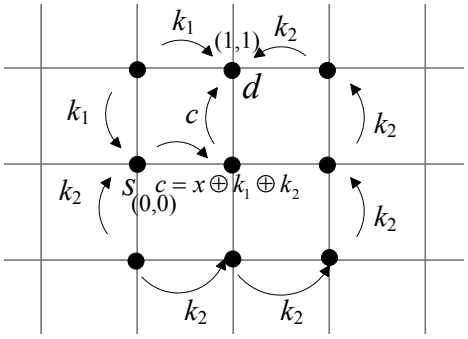

Figure 5.12: Secrecy protocol connecting a source node at the origin $(0, 0)$ to a node at $(1, 1)$.

Note that in the percolation results stated in [21, 30], the origin being connected to another node refers to the existence of a "path" starting at the origin and ending at the destination node. However, in our case, the connection to each node potentially requires a different subset of nodes forming a network and employing network coding to reach that node, which we refer to as the origin being "connected" to the destination node.

5.5.4 Secrecy Capacity Scaling

In our result given in Theorem 5.4, the requirement is that the number of eavesdroppers (with unknown location) should grow more slowly than $n/\log n$ for the achieved throughput to remain secure. In this and other similar secrecy scaling results [39], the main feature constraining the number of eavesdroppers that can be tolerated is the requirement that *legitimate nodes should be free from very nearby eavesdroppers*, and this requirement still applies even when the location of the eavesdroppers are assumed known [39].

The reason behind this major restriction is that whenever a node initiates the flow of a secret message, a very nearby eavesdropper has a significant SNR advantage over any receiver for any signal transmitted by this node. However, as shown in the previous section, one major advantage of network coding techniques is that an incoming connection to a source can be used to enable secrecy. For an incoming signal, the SNR values at a source and a very nearby eavesdropper are almost the same, i.e., the use of network coding *evens out* the SNR gap. Hence, a physical-layer secrecy scheme that achieves secrecy at equal SNRs can be used to initiate the secure transmission.

The following theorem states our main result in this section which improves on the result in Theorem 5.4 significantly in terms of the number of eavesdroppers tolerated. In the construction used to prove this result, we assume a slightly modified secrecy scheme than given in 5.2.1. Here we assume that, for all transmissions in the wireless network, the sender node a employs a physical-layer secrecy scheme to deliver the message to the receiver node b at some fixed rate, which is designed to guarantee secrecy from any eavesdropper e that has roughly the same signal quality with b (or worse). More precisely, for some decoding threshold γ for the signal-to-interference-and-noise ratio (SINR), and some (small) δ such that $0 < \delta < 1$, a sends bits to b at some fixed rate R bits per second, which is kept secret from any eavesdropper e if 1) $\text{SINR}_b \geqslant \gamma$, 2) $\text{SINR}_e \leqslant (1+\delta)\text{SINR}_b$. One example of such a secrecy scheme is the low-complexity on-off method in [24], which utilizes fading by sending only at instants when the main channel gain is larger than a certain

threshold in a given transmission period, and is shown to achieve a positive secrecy rate even when the eavesdropper channel is more capable than the main channel. Many other methods are available (e.g., see [76]).

Theorem 5.6. *Consider an extended two-dimensional network, where legitimate nodes are placed according to a Poisson point process with density 1 over a torus formed by wrapping around a square region of size* $[0, \sqrt{n}] \times [0, \sqrt{n}]$ *at the edges. Legitimate nodes are matched into* n *source-destination pairs uniformly at random. In addition to the legitimate nodes, eavesdroppers are arbitrarily distributed with their location unknown. Eavesdroppers are assumed not to collaborate. Each source-destination pair can achieve a throughput that scales as* $1/\sqrt{n \log n}$ *with probability one as* $n \to \infty$*. The throughput achieved is secure for any number of eavesdroppers.*

Proof. We present a construction that achieves the stated secrecy property. The construction consists of a routing algorithm and a time division multiplexing scheme. For this construction, the square region is divided into square cells of side length $c(n) = \sqrt{\log n}$. For each source-destination pair s–d, s generates four "packets" for each secret message x to be conveyed from s to d. First three packets w_1, w_2, w_3 are generated randomly, and the last packet w_4 is set such that $x = w_1 \oplus w_2 \oplus w_3 \oplus w_4$. For convenience, we consider these packets as belonging to four different colors, i.e., we refer to w_i as belonging to the ith color. Note that no information about x can be obtained unless all four packets are decoded.

5.5.4.1 Routing Algorithm

For each source-destination pair, we define four paths connecting the source to the destination. The basic idea is that these packets are sent on separate distant paths and since an eavesdropper in the network cannot be close to many paths at once, it is guaranteed to miss at least one packet. This argument is true except for eavesdroppers very close to s or d, which is addressed by a careful handling of the initiation of the packet transmissions at

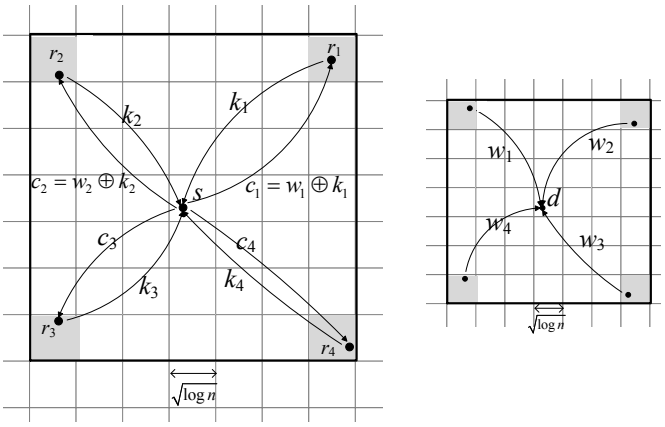

Figure 5.13: (Left) Around each source s, a "source base" is defined, which is a square region of size 7×7 cells. The four (shaded) corner cells are the relay cells, where nodes are selected to help initiate the transmission. The four relays do two-way exchanges with the source to receive four packets that form the secret message. The locations of the relays ensure that (compared to the source) no eavesdropper can be located closer to all relays at once, i.e., for any given eavesdropper e, $d(s, r_i) \leqslant d(e, r_i)$ for some $i \in \{1, 2, 3, 4\}$. (Right) The delivery of the four packets to the destination is shown. As is the case for the draining phase, due to the location of the relays, no eavesdropper can be close enough to all relays at once to collect all four packets.

the source, and the delivery of the packets to the destination. Hence, our routing algorithm consists of three stages: draining, routing, and delivery.

• **Draining:**

For each source node s, we define a square region of size 7×7 cells with the source cell at its center as the "source base" (see Figure 5.13). The four corner cells of the source base are designated as the "relay cells". Four legitimate nodes r_1, r_2, r_3, r_4 are selected from these four relay regions, and the packets w_i are conveyed to the relays using the two-way scheme described in Section 5.5.2. For example, the node r_1 generates a random key k_1 and sends it to s, and s replies with $c_1 = w_1 \oplus k_1$, and r_1 extracts the packet w_1 (Figure 5.13).

• **Routing:**

We define four paths between the source and the destination bases (Figure 5.14). Each packet w_i is carried on a different path. The paths consist of vertical or horizontal lines, which are traversed by the packets in single-cell hops, where the packet is delivered to a node in the next cell on the path. Two paths leave the top two relay cells on a vertical line, and arrive to the correponding relay cells in the destination base on a vertical line while keeping the same spacing (Figure 5.14). The same is true for the paths leaving the bottom relay cells.

• **Delivery:**

For each destination node d, a "destination base" is defined in the same way as the source base (see Figure 5.13). Again, the four corners are labeled as relay cells. After a packet reaches a relay cell in the destination base, the packet is delivered from the relay directly to d by reaching over multiple cells as done for the draining case. Once all four packets arrive to d, it decodes the secret message x by XORing the packets.

Remark 5.1. *: Some special cases need to be considered: (i) Source and destination bases which are roughly vertically aligned: the paths leave the source base and arrive at the destination base on horizontal lines. (ii) The source and the destination bases overlap: the secret message is delivered via a helper node. In particular, a helper node is selected from the network, and the secret message is delivered first to this helper node, and then from the helper node to the destination node using the routing algorithm described above for both stages. The helper node is selected from a cell that is far enough away from the source and the destination bases to allow employing the routing algorithm as described above. Details are omitted.*

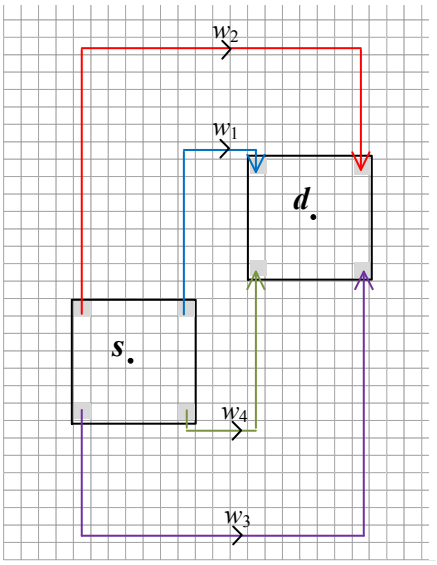

Figure 5.14: The source and the destination bases are connected with four paths, each carrying one of the packets. The paths have the same minimum spacing throughout the route; hence, no eavesdropper can be close enough to all four paths at once.

5.5.4.2 Time Division Multiplexing Scheme

Time is divided into three phases corresponding to the draining, routing, and delivery stages.

• **Draining:**

The draining phase is divided into eight frames. The first four frames are for transmissions of the keys from the relays to the sources, and the last four frames are for the responses of the sources. Each frame consists of a constant number of time slots, where cells take turns for signal transmissions employing a standard spatial reuse scheme as assumed in the similar construction in Section 5.4.1. Hence, at the end of each frame, it is ensured that each cell has transmitted once.

• **Routing:**

The routing phase is divided into four frames for each type of packet. In the ith frame, packets of color i are routed. Each frame is further divided into time slots again employing

a spatial reuse scheme. In each time slot, relaying nodes from the active cells deliver their packets to the next cell on the path.

• **Delivery:**

The delivery phase consists of four frames for the transmission of the packets of four colors. Again, each frame is divided into time slots, and transmissions are done as in the draining phase.

The proof completes by showing that: (i) this construction is feasible, (ii) it achieves a per-node throughput on the order of $1/\sqrt{n \log n}$, and (iii) the achieved throughput is secure.

The first two statements can be shown by standard arguments as used in Sections 5.3 and 5.4 and similar works (see e.g., [16, 73]), and we omit the detailed proof here. The throughput achieved by the construction is found by considering the throughput constraint imposed by each phase. For the draining and delivery phases, the difference in our construction compared to a standard construction is that transmissions require multi-cell hops, and that these phases complete in more than one transmissions. However, these both bring only a constant factor to the throughput achieved and do not affect the scaling. The difference in the routing phase is that each message requires four packets to be carried, which again does not affect the order. It can be shown that the performance bottleneck is due to the routing phase, and since the relaying load in each cell grows with $\sqrt{n \log n}$ (see Appendix A.3), the overall per-node throughput scales as $1/\sqrt{n \log n}$. Finally, note that the construction requires nodes to transmit with power that is proportonal to $(\log n)^{\alpha/2}$, where $\alpha > 2$ is the path loss exponent of the medium.

Next we show that for each source-destination pair s–d, each message x is delivered from s to d securely. For secrecy, we show that an eavesdropper located anywhere in the network is guaranteed to miss at least one packet out of the four packets after listening to all the transmissions required for the delivery of x. First consider the draining phase. Due to the relative locations of the relays with respect to the source, any given eavesdropper e

satisfies $d(e, r_i) \geqslant d(s, r_i)$ for some $i \in \{1, 2, 3, 4\}$ (Figure 5.13). Hence, for the transmission of k_i from r_i to s, the received signal power at s is larger than the received signal power at e. In addition, even with the interference at e ignored, the spatial reuse scheme can be designed such that the interference at s is low enough to allow $\text{SINR}_e \leqslant (1+\delta)\text{SINR}_b$. Therefore, k_i is delivered to s but not to e; hence, e misses the packet w_i. Therefore, any eavesdropper is guaranteed to miss at least one packet, and the message x is not leaked during the draining phase. A similar argument can be made for the delivery phase. The four packets arrive to d from four directions and any eavesdropper e satisfies $d(e, r_i) \geqslant d(d, r_i)$ for some i. Outside the bases, the packets are carried on paths with some minimum spacing; hence, no eavesdropper can be close enough to many paths at once, thus establishing secrecy during the routing phase. Also note that it can be ensured that an eavesdropper cannot decode a packet by combining observations from all hops on the packet's path as proved in [39]. Finally, it can be easily verified that no eavesdropper can collect the four packets by listening to all three phases.

Therefore, using this construction, as n grows, each source-destination pair can share on the order of $1/\sqrt{n \log n}$ secret bits per second for any number of independent eavesdroppers arbitrarily distributed to the network. □

5.6 Conclusion

We address the important problem of secure communication in a wireless network in the presence of eavesdroppers. We present achievable scaling results on the rate of information that can be securely carried in a network, when the size of the network becomes large. In contrast to most of the previous work in this area, we assume the locations of the eavesdroppers are unknown. Compared to previous works that consider unknown eavesdropper locations, our construction can achieve the same secure throughput scaling while tolerating a significantly higher number of eavesdroppers. Our work shows the big potential network coding techniques have to improve information-theoretic secrecy in wireless

networks, most notably by enabling the secure connection of one node to another in the presence of very nearby eavesdroppers.

This work partially completes a line of research that originated with the secrecy-capacity tradeoffs in asymptotically large networks of [73]. In [73], even when multi-user diversity and cooperative jamming were employed, the near eavesdropper problem severely limited the number of uniformly distributed eavesdroppers that could be tolerated in the network. In [8] and [9] (presented in previous sections), we began to realize the utility of modifications at higher layers in resolving difficult secrecy problems caused by certain geometries of the system nodes and eavesdroppers, but we still were not able to address eavesdroppers very near the nodes originating messages. The work presented in Section 5.5 (published in [7]) addresses this last problem and thus allows for a secure per-session throughput of $O(1/\sqrt{n \log n})$ in the presence of an arbitrarily located set of non-collaborating eavesdroppers.

5.7 Acknowledgment

The work in this chapter was supported by the National Science Foundation under grants CNS-0721626, CNS-0721861, CNS-0905349, CNS-0953620, and CNS- 1018464, and by the U.S. Army Research Laboratory and the U.K. Ministry of Defence under Agreement Number W911NF-06-3-0001.

CHAPTER 6

PERCOLATION IN MULTILAYER GRAPHS

6.1 Introduction

Previous chapters are concerned with large wireless ad hoc networks. The network model we use in those chapters contains an asymptotically large number of nodes, as we are interested in the network's limiting behavior. As discussed in Chapter 2, a network can be studied by mapping it to a graph, and important asymptotic properties of a network can be deduced by studying the corresponding infinite graph. In particular, some of the important results in wireless ad hoc networks discussed in previous chapters make use of *percolation theory*, which studies the connectivity behavior of infinite random graphs. Central to percolation theory is the study of the "phase transition" that infinite random graphs demonstrate. Phase transition here refers to the sudden change of the connectivity properties of the network as a local parameter is varied. This behavior of the random infinite graph is used to explain and model many real-life phase transition phenomena in diverse fields such as soil physics, polymer science, and epidemiology [64].

In addition to the random geometric graphs used to model wireless ad hoc networks, phase transition behavior can be observed on many other types of random graphs where vertices may have fixed locations or, as studied in this chapter, there is no geometric (location) notion to the graph. For example, consider a square lattice graph. Here, each vertex has four edges connecting it to its four neighbors. One can run a random process on this graph by independently and randomly deleting edges. Suppose deletion happens with some probability $1 - p$, so each edge survives with probability p. When p is large, the resulting graph (subgraph of the original square lattice) will still be well-connected.

As p decreases, the square lattice will transition from a well-connected graph to one that consists of many small connected islands. Here, the surprising result is that this transition happens very *abruptly*. When the square lattice is very large, at a certain critical p value, the graph suddenly changes state from having one big spanning cluster to having many small clusters. Consider this lattice as modeling a physical structure; here, this sudden transition corresponds to the structure "breaking down". The critical value of p, called p_c, where this phase transition happens is of interest. In general, this critical value is very difficult to calculate analytically, and, except for a few types of regular graphs, it has only been numerically estimated. For the square lattice, calculating p_c analytically was an open problem for many years, and the result that p_c is exactly 0.5 for the square lattice is one of the famous results of percolation theory [36].

In percolation theory, the random process of deleting edges from a graph is referred to as "bond percolation". Another option is to delete vertices (or mark them as "unoccupied") randomly. The idea is that when a vertex is unoccupied, the edges arriving to it are blocked. An equivalent way to consider this process is to assume all edges from an unoccupied vertex are deleted. This process is called "site percolation" (see Figure 6.1). Suppose each vertex remains occupied with probability q. Again, there is a critical value q_c, called the "site percolation threshold", where the phase transition is observed. For the square lattice, q_c is numerically estimated to be around 0.59275 [54] (see Figure 6.2). In this chapter, we extensively study site percolation.

In our work, we consider site percolation on "multilayer graphs". Multilayer graphs are formed by combining different graphs that share the same vertex set. An example of a multilayer graph is one representing a social network of a set of people, where each vertex represents a person, and an edge between two people represents a social relationship. In a multilayer social network, each layer may represent a different type of relationship such as "work" or "family". The overall multilayer graph is formed by combining these layers. Another example is a wireless network where nodes may be equipped with more than

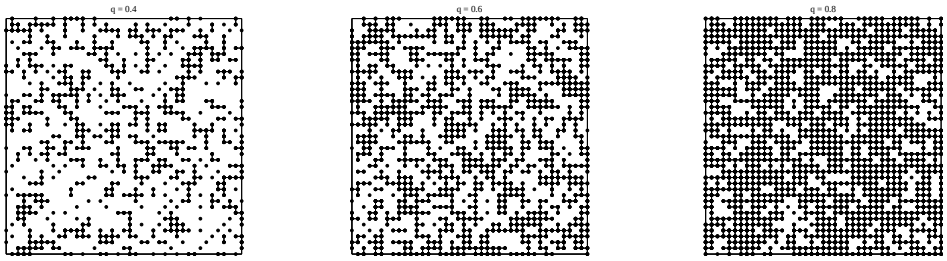

(a) (b) (c)

Figure 6.1: Three instances of site percolation on a square lattice of size 41×41 is shown. For ease of exposition, the sites labeled as unoccupied are not shown. The site occupation probabilities used for generating the graphs in (a), (b), (c) are $0.4, 0.6, 0.8$, respectively. As q increases, the graph transitions from many small clusters to one giant cluster.

one type of radio, e.g., WiFi and cellular. Again, the multilayer wireless network is the combination of the individual layers formed for the respective wireless technology. Note that, in general, the multilayer network has the potential to be better connected than the individual layers it contains. For example, in the social network case, two people who are connected neither on the work nor the family layer may still be connected in the overall multilayer network through a chain of connections traversing across layers.

In the multilayer case studied in this chapter, site percolation process is applied on each layer with the same occupation probability q. We study the critical (single-layer) q value that enables the multilayer graph to transition to a well-connected state, i.e., "to percolate". Clearly, the critical value for the multilayer case is smaller than the original site percolation threshold. For example, a two-layer square lattice will have a critical site occupation probability that is less than 0.59275. As the number of layers increases, the critical threshold should decrease. In this work, by numerical simulations, we show how this value changes as a function of the number of layers. We observe that, for a general graph, the critical occupation probability scales with the inverse square root of the number of layers. Furthermore, we analytically study the observed behavior and conjecture the exact asymptotic behavior as the number of layers gets large. Our findings in this chapter are reported in [27].

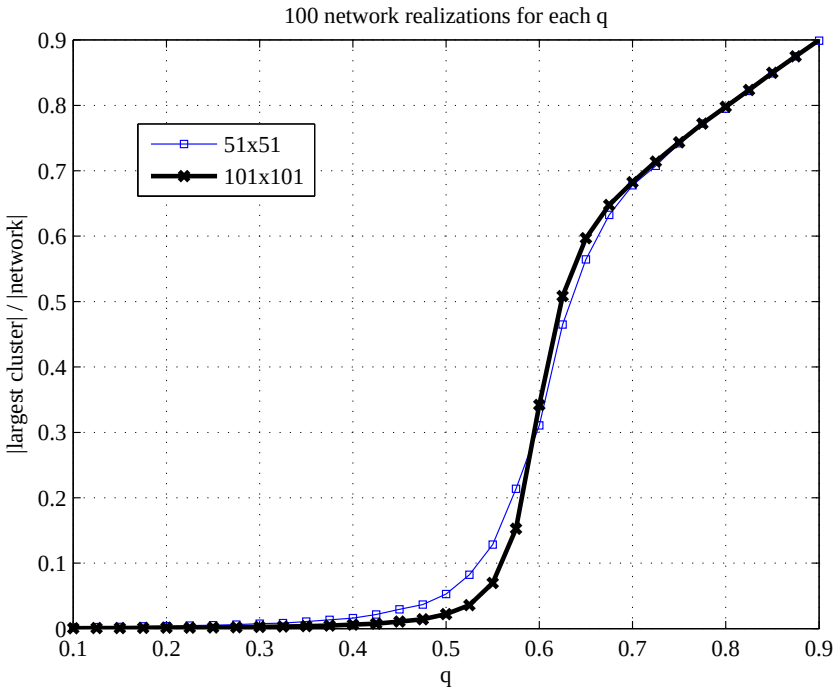

Figure 6.2: The number of nodes in the largest cluster divided by the size of the network averaged over 100 runs for a square lattice graph plotted for different values of site occupation probability q. As q gets larger, the value approaches one, showing that the network goes from many small clusters to one single big cluster. Two plots are shown for lattices of size 51×51 and 101×101. As the simulated graph gets larger, the plots get steeper. For the infinite square lattice, this transition is sharp around a critical q value numerically estimated to be around $q_c = 0.59275$ [54].

6.2 Multilayer Percolation

Consider a graph $G(V, E)$, where V is the set of vertices (sites), and E is the set of edges. A site percolation process is applied on G, and we refer to G as the "base graph", or the "underlying graph". In the site percolation process, each site $v \in V$ is independently labeled as "occupied" with some probability q, and "unoccupied" with probability $1 - q$, and all edges incident on unoccupied sites are removed. The remaining subgraph is called a "site percolation instance" of the underlying graph G with site occupation probability q.

Suppose the multilayer graph is composed of $M \geqslant 1$ layers. Then, M site percolation instances of G are created, each with the same site occupation probability q, with the ith

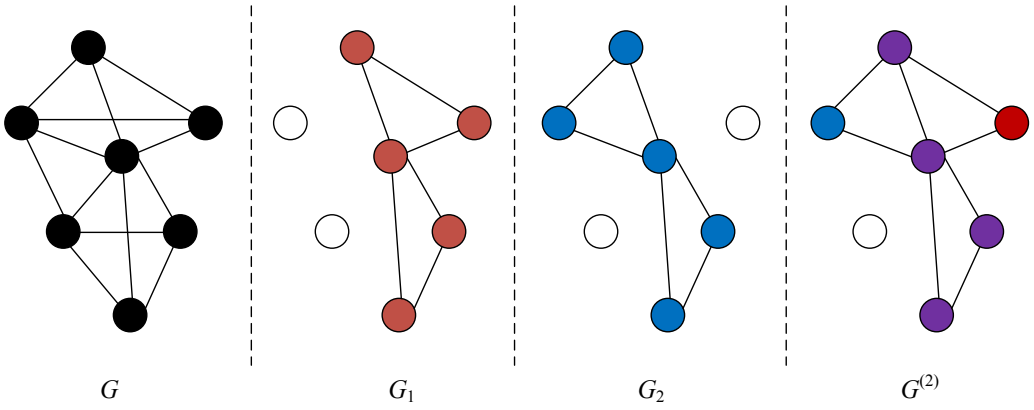

Figure 6.3: The multilayer graph is formed by combining subgraphs of the same underlying graph G. A two-layer graph $G^{(2)}$ is shown, which is the union of the two layers G_1 and G_2.

layer denoted as G_i, $i = 1, 2, \cdots, M$. Each G_i is a subgraph of the underlying graph G, with vertex set V and edge set E_i. Finally, we denote the multilayer graph $G^{(M)}$, defined as

$$G^{(M)} = \bigcup_{i=1}^{M} G_i(V, E_i). \tag{6.1}$$

An example for a small graph is shown in Figure 6.3. We study the critical value of q at which $G^{(M)}$ percolates. We denote this value as $q_c(M)$, with $q_c(1)$ corresponding to the classical site percolation threshold for the graph G.

6.3 Numerical Results

In order to study the value of the critical site occupation probability for the M-layer graph, $q_c(M)$, we ran computer simulations on large graphs and numerically determined the values. Our simulations are based on the algorithm introduced in [54], which runs in time linear with the number of sites in the lattice. Figure 6.4 shows an example with multilayer square lattices for different values of M.

In Figure 6.5, we plot $q_c(M)$ as a function M for the square and triangular lattices. As expected, the critical site occupation probability decreases with increased number of layers.

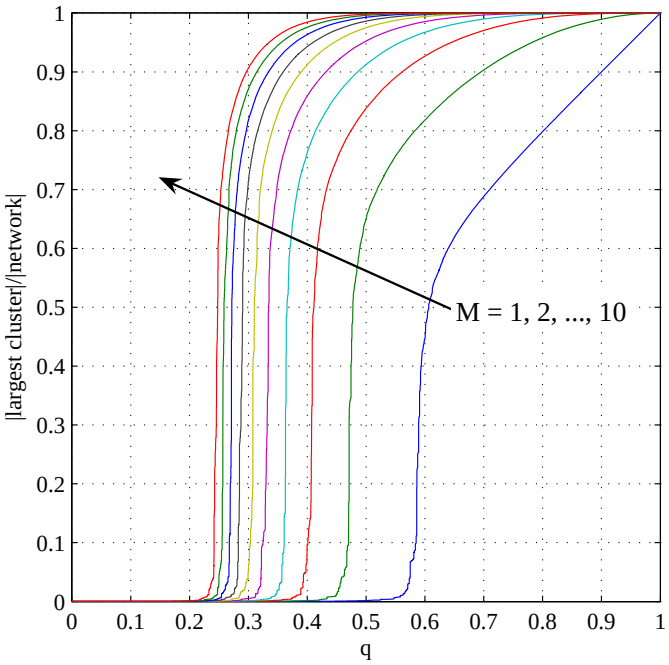

Figure 6.4: The size of the largest cluster divided by the network size is plotted for an M-layer square lattice of size 512×512 for different values of single-layer site occupation probability q. The critical threshold $q_c(M)$ is estimated using the algorithm presented in [54] which is roughly the value where the curve makes a steep climb. The plots are drawn for values of $M = 1, 2, \cdots, 10$. Percolation happens at smaller q values as M increases.

Note that calculation of the exact value of $q_c(M)$, even for the classical case of $M = 1$, is in general very difficult. Our focus here is on the asymptotic behavior of $q_c(M)$, as M gets large. With numerous simulations on many different types of graphs, we have observed that $q_c(M)$ decreases with the reciprocal of the square root of the number of layers, i.e., $q_c(M)$ seems to scale with $1/\sqrt{M}$, and this scaling relation was observed to be consistent across all types of graphs simulated. Hence, the exact asymptotic expression for $q_c(M)$ is of interest. In the next section, we derive an expression for the asymptotic behavior, which agrees with the simulated values, and we elaborate on our reasoning for this conjectured function.

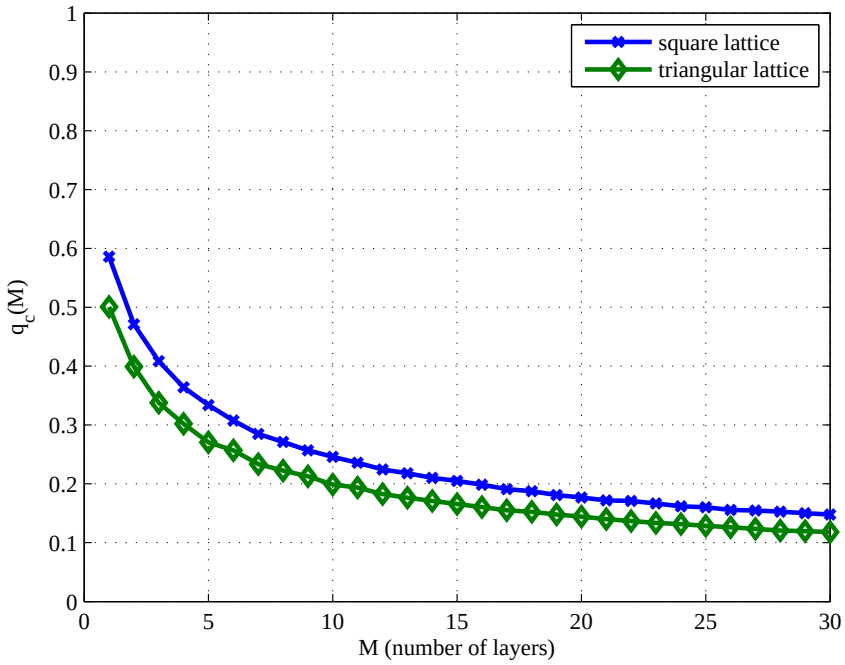

Figure 6.5: Critical site-occupation probability $q_c(M)$ for the M-layer graph plotted against the number of layers, M. As M increases, the multilayer graph percolates for a smaller value of single-layer site occupation probability q, hence $q_c(M)$ decreases. The values are numerically estimated using an algorithm based on [54], on a square lattice and a triangular lattice of size both 512×512.

6.4 Asymptotic behavior of $q_c(M)$

The site percolation process can be thought of as a random process of deleting edges from the graph G, as is done in the classical bond percolation process. However, a major difference is that, under site percolation, edge deletion events are not *independent*. When a site is labeled as unoccupied, all edges incident on this site are removed. Hence, edges are removed randomly, but according to a *spatially-correlated* random process. This is also true in the multilayer case, as each individual layer carries this spatial correlation property despite independence across layers.

In order to study this correlation property in more detail, consider a simple one-dimensional multilayer graph of $n + 1$ sites and n edges. A two-layer example is given in Figure 6.6.

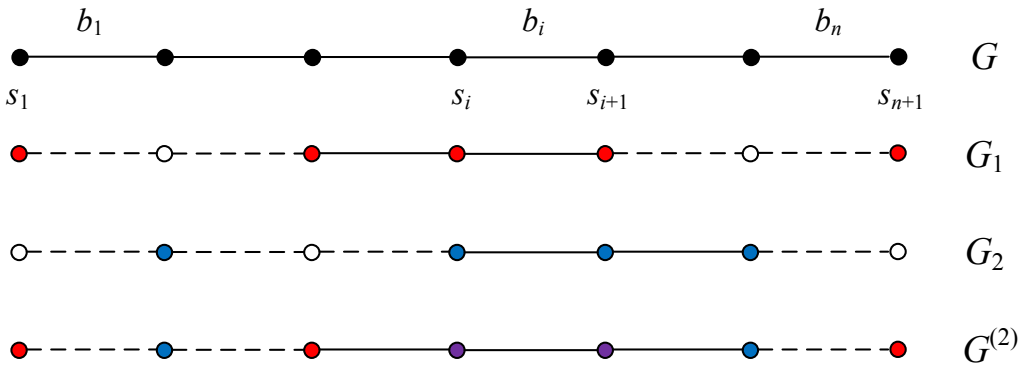

Figure 6.6: The multilayer graph is formed by combining subgraphs of the same underlying graph G. A two-layer graph $G^{(2)}$ is shown, which is the union of the two layers G_1 and G_2.

The base graph G consists of $n+1$ sites, with the vertex set $V = \{s_1, \cdots, s_n\}$, and n edges (bonds) $E = \{b_1, \cdots, b_n\}$. Each bond b_i connects the sites s_i and s_{i+1}. A site percolation process is applied on G with site occupation probability q, with edges on unoccupied sites removed. M independent instances of the site percolation process are the graphs $G_1, G_2, \cdots, G_M$ with their edge sets, $E_1, E_2, \cdots, E_M$, respectively. We refer to an edge that is in E_i as a bond that is "open" in the ith layer. Similarly, if an edge exists in E but not E_i, we call it a bond that is "closed" in the ith layer. Finally, $G^{(M)}$ is formed by taking the union $\bigcup_{i=1}^{n} E_i$.

We call an edge b_i "open in $G^{(M)}$", if it is open in at least one layer, and call it "closed in $G^{(M)}$" otherwise. Furthermore, we define the event B_i, as $B_i =$ "b_i is open in $G^{(M)}$". Note that for a given layer, a bond b_i is open in that layer only if both sites on each end, s_i, s_{i+1}, are occupied, which happens with probability q^2. Because the layers are generated independently, for the multilayer graph $G^{(M)}$,

$$P(B_i) = 1 - (1 - q^2)^M. \tag{6.2}$$

As mentioned above, the state of neighboring bonds are dependent at a given layer. Now, consider the event that two neighboring bonds b_i, b_{i+1}, $i = 1, 2, \cdots, n$, are both open

in $G^{(M)}$, i.e., $B_i \cap B_{i+1}$). The probability of this event can be written as

$$\begin{aligned} P(B_i \cap B_{i+1}) &= 1 - P(\overline{B_i} \cup \overline{B_{i+1}}) \\ &= 1 - \left(P(\overline{B_i}) + P(\overline{B_{i+1}}) - P(\overline{B_i} \cap \overline{B_{i+1}})\right). \end{aligned} \tag{6.3}$$

The event $\overline{B_i} \cap \overline{B_{i+1}}$ corresponds to the event that b_i and b_{i+1} are both closed in $G^{(M)}$, which means b_i, b_{i+1} are closed in all M layers. For any given layer $j \in \{1, 2, \cdots, M\}$,

$$P(\text{“}b_i \text{ and } b_{i+1} \text{ closed in the } j\text{th layer”}) = 1 - 2q^2 + q^3. \tag{6.4}$$

The above value can be easily found by enumerating all possible states of the sites $\{s_i, s_{i+1}, s_{i+2}\}$ and summing up the probabilities of states that correspond to both bonds being closed. Therefore, for all $i \in \{1, 2, \cdots, n\}$,

$$P(\overline{B_i} \cap \overline{B_{i+1}}) = (1 - 2q^2 + q^3)^M. \tag{6.5}$$

Finally, replacing the above value in (6.3),

$$P(B_i \cap B_{i+1}) = 1 - 2(1 - q^2)^M + (1 - 2q^2 + q^3)^M. \tag{6.6}$$

Also note that,

$$P(B_1)P(B_2) = \left(1 - (1 - q^2)^M\right)^2 = 1 - 2(1 - q^2)^M + (1 - 2q^2 + q^4)^M. \tag{6.7}$$

Therefore, for any finite M,

$$P(B_i \cap B_{i+1}) \geq P(B_i)P(B_{i+1}). \tag{6.8}$$

Hence, as expected, events B_i and B_{i+1} are *positively correlated*. Therefore, compared to classical bond percolation where states of all edges are determined independently, we ex-

pect percolation to occur "sooner", i.e., with a smaller marginal bond occupation probability $P(B_i)$. In addition, note that, for a given q value, $P(B_i \cap B_{i+1})$ approaches $P(B_i)P(B_{i+1})$ as M increases. In other words, correlation between neighboring bonds *dies out* with an increasing number of layers. *Hence, in the limit as $M \to \infty$, the M-layer graph can be thought of as a graph generated by a single-layer independent bond percolation process with bond occupation probability $P(B_i)$, which percolates at $P(B_i) = p_c$.* On the other hand, for any finite M, the multilayer graph has a smaller critical threshold than a graph generated with a bond percolation process of the same marginal bond occupation probability. Therefore, we have the following conjecture:

Conjecture 6.1. *Consider a graph $G(V, E)$ with critical bond percolation threshold p_c, and the multilayer graph $G^{(M)}$ generated by combining M random site percolation instances of G, each with site occupation probability q. Suppose $G^{(M)}$ percolates at some critical value $q = q_c(M)$. Then the critical site percolation threshold $q_c(M)$ is upper bounded as*

$$q_c(M) \leq \sqrt{1 - (1 - p_c)^{1/M}}. \tag{6.9}$$

Further, this upper bound is asymptotically tight as $M \to \infty$.

Note that the upper bound above satisfies

$$\sqrt{1 - (1 - p_c)^{1/M}} \sim \frac{\sqrt{\log(1 - p_c)}}{\sqrt{M}}, \tag{6.10}$$

which makes the inverse square root scaling explicit and shows that the scaling coefficient is $\sqrt{\log(1 - p_c)}$.

We compared the $q_c(M)$ values numerically estimated for many types of graphs (see Figure 6.5) with the conjectured upper bound. All these simulations show perfect agreement. Figure 6.7 shows the case of the square lattice graph.

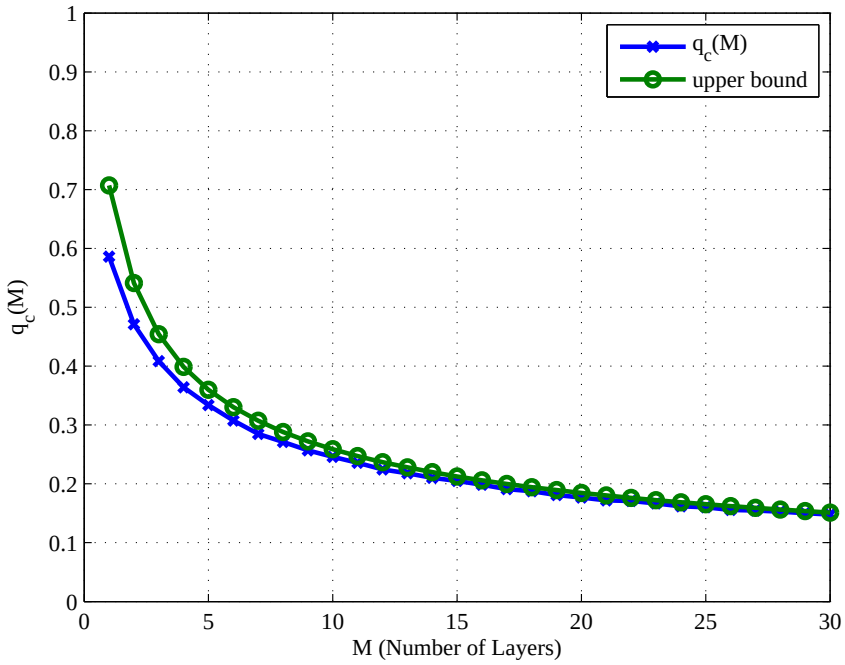

Figure 6.7: Critical site-occupation probability $q_c(M)$ for the M-layer square lattice graph plotted against the number of layers, M, along with the conjectured upper bound. The plotted upper bound is given by $\sqrt{1-(1-p_c)^{1/M}}$, where p_c is the critical bond percolation threshold. $p_c = 0.5$ for the square lattice. The upper bound gets tight as M increases.

6.5 Conclusions

Recently, there has been a surge of research activity in network science in the area of multilayer networks. In general, these works consider extensions of graph properties studied for classical networks to the case of multilayer networks such as random walks [13], time evolution of graphs [56], and, as studied in this work, percolation [18] (see [38] for an extensive review).

This chapter is confined to a general discussion of site percolation in arbitrary graphs, and our presented results are on regular graphs such as lattices. However, the ideas in this chapter can be also used to study important special cases. An example is percolation in multilayer graphs formed by merging random graphs with arbitrary degree distributions

[53]. In fact, contrary to the case of regular graphs discussed here, exact expressions for the critical site occupation probability are found in this case [27].

One important insight gained in studying percolation in multilayer graphs is that important properties can be deduced by considering the problem as a spatially-correlated bond percolation process that converges to an independent bond percolation process as the number of layers increases. This also naturally ties the multilayer percolation problem to the case of mixed "site-bond percolation" considered in the literature [71]. In site-bond percolation, each site *and* bond in the graph is labeled as occupied or unoccupied independently, with probabilities q and p, respectively, and only occupied bonds with occupied sites on its both ends are declared open. Clearly, the special cases of $q = 1$ and $p = 1$ correspond to site and bond percolation, respectively. Hence, the transition from site to bond percolation for the multilayer graph as the number of layers increases is also observed in the site-bond percolation problem as values of p, q are varied. This similarity allows us to adapt bounds established for site-bond percolation to the multilayer percolation problem. In fact, these adapted bounds show perfect agreement with the multilayer case as presented in [27].

For future work, we plan to rigorously prove Conjecture 6.1. This requires us to prove the argument that under two probability measures with the same marginal bond occupation probabilities on the same infinite graph, the percolation probability is greater under the measure which implies correlation between neighboring bonds than the one where the states of all bonds are independent.

6.6 Acknowledgment

The work in this chapter was supported in part by the National Science Foundation under grant CNS-1018464, and in part by the U.S. Army Research Laboratory and the U.K. Ministry of Defence, and was accomplished under Cooperative Agreement Number W911NF-09-2-0053 (the ARL Network Science CTA).

CHAPTER 7

CONCLUSION

This thesis work consists of four projects concerned with asymptotic analysis of large random networks. In the first three projects, we focus on the asymptotic properties of wireless ad hoc networks. In the last project, we study percolation properties of arbitrary large random networks.

In the first project, we study broadcast in a large wireless ad hoc network. We model the network as consisting of nodes randomly placed on the infinite real-line or, in the two-dimensional case, on the infinite $\mathbb{R}^2$ plane. Because the locations of the nodes are random, broadcasting a message to the entire infinite network is difficult. We explore how cooperation between nodes can improve this situation. In particular, we study a special case of cooperation where nodes that have decoded the broadcast message coordinate and transmit the message at the same time so that their signal power is added at a receiver node. This helps the broadcast message reach farther distances. We analytically calculate the probability that a node can broadcast its message to the entire infinite network when this type of cooperation is enabled. We show that although cooperation helps increase the broadcast range, for a wide range of cases, the probability that the message reaches every node in the infinite region is zero. However, for mediums with low attenuation, cooperation indeed makes broadcast possible.

In the second project we are interested in the rate data can be exchanged by nodes in a large wireless ad hoc network. Wireless ad hoc networks are known to not scale well in terms of capacity, meaning that the number of bits each node can share goes down to zero as the network gets larger. Supporting the wireless network with a high-capacity

wired network through placement of base stations, thereby creating a hybrid network, is a method to improve this situation. Previous work has shown capacity scaling results for hybrid networks. These works show what capacity benefit is obtained through the use of base stations; however, it is of interest whether even better capacity is possible. We show upper bounds on hybrid network capacity, hence showing the limits on the capacity benefit that can be provided.

The third project is also concerned with sharing of data in a large wireless ad hoc network; however, this time our focus is on secret communication. We assume the network contains eavesdropping nodes, and we explore whether nodes can share information while keeping their messages secret from these eavesdroppers. Previous work has shown that this is possible without any compromise on the achieved throughput. However, it is assumed that the locations of the eavesdroppers are known. In our work, we show that it is possible to achieve the same amount of secret information exchange without having to know the locations of the eavesdroppers. Central to our solution is the use of coding techniques for wireless secrecy. Our results highlight how upper layer solutions can address difficult physical layer problems.

In the final project, we study percolation properties of large random multilayer networks. Members of a given network may have more than one type of relationship, and each type of relationship can be represented by a separate network. Multilayer networks are formed by combining these individual networks, called layers. We study the connectivity of the corresponding multilayer graph as a function of the connectivity of individual layers. Because the multilayer graph is the combination of the layers, many poorly-connected layers can form a well-connected union. We study the critical connectivity threshold for the individual layers that enable the multilayer graph to percolate. In addition to showing the behavior of the critical threshold numerically, we study analytically why this behavior is observed.

Each project in this thesis involves theoretical analysis of the behavior of a large random network. The main goal of such theoretical analysis is to gain insight into the network's real-life performance. Especially in the first three projects, where we study wireless networks, the network needs to be mathematically modeled before such analysis can be carried out. Modeling the network inevitably involves making simplifying assumptions to yield theoretical study. In a complicated operation such as wireless networking, modeling requires assumptions on many different aspects such as how each physical device is modeled, how communication takes place, how interference affects communication, etc. An important fact that has repeatedly demonstrated itself in these projects is that each detail of this model has the potential to dramatically affect the conclusions one can draw from analysis. One example of this is discussed in Chapter 4, where we show how two different assumptions on the rate of information carried on a wireless link can lead to two different conclusions on the total rate that can be achieved by nodes confined in a region. Therefore, conclusions drawn from such theoretical analysis should always be carefully considered with attention given to how they are tied to the underlying model.

In our project on secret communication presented in Chapter 5, the main tool behind the solution that enabled secrecy in the presence of eavesdroppers is the coding techniques employed. Simple coding techniques for enabling secrecy in a wiretapped network were already considered in previous work; however, their application to wireless information-theoretic secrecy has proved to be particularly useful as illustrated by our results. The main reason behind that is, in wireless secrecy, uncertainty about the eavesdropper is of particular concern. For example, the state of the channel to an eavesdropper, although central to the secrecy performance, is very difficult to model and make assumptions on in the wireless case. As demonstrated in our work, coding techniques help relax the assumptions that have to be made about the eavesdropper, and help address very difficult questions such as unknown eavesdropper location or the near-eavesdropper problem. Our results show the usefulness of these techniques to enable secrecy in a large wireless network; however,

the coding techniques employed in fact do not require a large number of nodes for their benefit to be realized. The techniques used in our work, such as secret sharing or two-way communications, can be very easily employed in a small network scenario. Overall, secrecy obtained through the use of coding techniques illustrate how upper layer solutions can be useful to address difficult physical layer problems.

APPENDIX A

SECRECY

A.1 One-dimensional Networks

The routing algorithm given in Section 5.3.2 can be applied if there exists a legitimate node in each cell. The probability of this event is given by:

$$\left(1-e^{-c(n)}\right)^{n/c(n)} = \left(1-\frac{1}{n}\right)^{n/\log n} \to 1,\ n\to\infty.$$

Hence, as the network grows, a relay (or a jammer) node can be found for each hop. For the two-dimensional case, replacing $c(n)$ by $c^2(n)$ above, with $c(n) = \sqrt{\log n}$, it can be shown that all cells are occupied w.h.p.

Using the routing algorithm in Section 5.3.2 (see Fig. 5.4) under the time division multiplexing scheme in Section 5.3.3, consider the transmission of a packet for any color i. We show that this packet is securely delivered during (1) single-cell hops outside neighborhoods, (2) multi-cell hops inside the neighborhoods. We show that during these hops, the relays and the eavesdroppers inside Γ_i satisfy the SINR condition for secrecy given in Section 5.2.1 for given SINR thresholds $0 < \gamma_e < \gamma$.

Assume relays for single-cell hops transmit with some power P (Fig. 5.4 (a)), the relays for multi-cell hops inside the neighborhoods (node A in Fig. 5.4 (b)) transmit with power P_A, and jammers transmit with power P_J. We have three transmit power values, P, P_A, P_J,

and two constants, k, l to set to satisfy the SINR requirements. We select the following values for P, P_A, P_J, l:

$$P = 4^\alpha c^\alpha \gamma N_0 \qquad l = 1 + 12(\gamma/\gamma_e)^{1/\alpha} \tag{A.1}$$

$$P_A = 2^\alpha (2l+1)^\alpha c^\alpha \gamma N_0 \qquad P_J = (l-1)^\alpha c^\alpha N_0 \tag{A.2}$$

In order to determine k, we bound the SINR values achieved during the transmissions.

Consider the first type of hop, where a packet of color i is transmitted outside the neighborhoods of Γ_i, where a relay R receives the signal from an adjacent cell.

$$\text{SINR}_R = \frac{P_{\text{rcv},R}}{N_0 + I_R},$$

where $P_{\text{rcv},R}$ is the received signal power at R, and I_R is the interference due to other transmissions.

$P_{\text{rcv},R}$ can be lower bounded by noting that the distance between the transmitting and receiving relay cannot exceed $2c$:

$$P_{\text{rcv},R} > \frac{P}{2^\alpha c^\alpha} = \frac{4^\alpha c^\alpha \gamma N_0}{2^\alpha c^\alpha} = 2^\alpha \gamma N_0$$

Considering the interference power I_R, note that jammers are silent, and other transmitting nodes in both directions are located in cells spaced with larger than $2kl$ cells in between (see Fig. 5.5). Hence, the two closest interferers are both at a distance larger than $2kl$ to R, the second two closest interferers are more than $4kl$ cells away, and so on. Thus,

$$\begin{aligned} I_R &< \sum_{i=1}^{\infty} 2\frac{P}{(2iklc)^\alpha} = \frac{P}{k^\alpha l^\alpha c^\alpha}\beta \\ &= \frac{4^\alpha c^\alpha \gamma N_0}{k^\alpha l^\alpha c^\alpha}\beta < \frac{1}{k^\alpha}\beta\frac{\gamma_e N_0}{3^\alpha}, \end{aligned}$$

where we define

$$\beta = \frac{2}{2^\alpha} \sum_{i=1}^{\infty} \frac{1}{i^\alpha}.$$

Note that $\beta < \infty$ for $\alpha > 1$. Hence,

$$\text{SINR}_R > \frac{2^\alpha \gamma N_0}{N_0 + \frac{1}{k^\alpha} \beta \frac{\gamma_e N_0}{3^\alpha}} > \gamma,$$

provided

$$k^\alpha > \frac{\beta \gamma_e}{3^\alpha \left(2^\alpha - 1\right)}. \tag{A.3}$$

During this single-cell hop for packet i, the SINR value at the closest eavesdropper E inside Γ_i can be bounded as

$$\text{SINR}_E < \frac{P/(l-1)^\alpha c^\alpha}{N_0} = \frac{4^\alpha c^\alpha \gamma N_0}{12^\alpha (\gamma/\gamma_e) c^\alpha N_0} = \frac{\gamma_e}{3^\alpha} < \gamma_e.$$

Therefore, single-cell hops outside the neighborhoods satisfy the SINR requirements (with k satisfying (A.3)).

Second, consider any multi-cell hop inside a neighborhood $N(\mathcal{C}_i^j)$ (see Fig. 5.4 (b)), where the transmitting relay A sends the packet to the receiving relay B.

$$\text{SINR}_B = \frac{P_{\text{rcv},B}}{N_0 + I_B + \tilde{I_B}}$$

Here, I_B is the interference due to other relay transmissions, $\tilde{I_B}$ is the jamming noise suffered due to all the active jammer nodes in the network. $P_{\text{rcv},B}$ can be bounded by noting the maximum distance between A and B.

$$P_{\text{rcv},B} \geq \frac{P_A}{(2l+1)^\alpha c^\alpha} = 2^\alpha \gamma N_0$$

The interfering relays and jammers (with power P_A, P_J, respectively) are located in the network as in the single-cell hop case. Hence,

$$I_B < \sum_{i=1}^{\infty} 2\frac{P_A}{(2iklc)^\alpha} = \frac{P_A}{k^\alpha l^\alpha c^\alpha}\beta < \frac{1}{k^\alpha}\beta\gamma N_0 6^\alpha,$$

and

$$\begin{aligned} \tilde{I_B} &< \frac{P_J}{(l-1)^\alpha c^\alpha} + \sum_{i=1}^{\infty} 2\frac{P_J}{(2iklc)^\alpha} \\ &= \frac{P_J}{(l-1)^\alpha c^\alpha} + \frac{P_J}{k^\alpha l^\alpha c^\alpha}\beta \\ &\leq N_0 + \frac{1}{k^\alpha}\beta N_0, \end{aligned}$$

where the first term in the upper bound for $\tilde{I_B}$ is due to the jammer node inside $\mathcal{C}_i^j$. Hence,

$$\text{SINR}_B > \frac{2^\alpha \gamma N_0}{N_0 + \frac{1}{k^\alpha}\beta\gamma N_0 6^\alpha + N_0 + \frac{1}{k^\alpha}\beta N_0} > \gamma,$$

provided

$$k^\alpha > \frac{\beta(6^\alpha\gamma + 1)}{2^\alpha - 2}. \tag{A.4}$$

The bound in (A.4) is stricter than the bound in (A.3).

The SINR value at an eavesdropper E inside $\mathcal{C}_i^j$ can be bounded as

$$\begin{aligned} \text{SINR}_E &\leq \frac{P_A/(l-1)^\alpha c^\alpha}{P_J/c^\alpha} = \gamma 2^\alpha \left(\frac{2l+1}{l-1}\right)^\alpha \frac{1}{(l-1)^\alpha} \\ &< \frac{6^\alpha}{12^\alpha}\frac{\gamma}{\gamma/\gamma_e} < \gamma_e. \end{aligned}$$

The next closest eavesdropper $\tilde{E}$ inside Γ_i has

$$\text{SINR}_{\tilde{E}} < \frac{P_A/(2klc)^\alpha}{N_0} = \frac{1}{k^\alpha}\left(\frac{2l+1}{l}\right)^\alpha \gamma < \gamma_e,$$

provided

$$k^\alpha > 3^\alpha \big(\gamma/\gamma_e\big)^\alpha. \tag{A.5}$$

Thus, any value of k satisfying below can be used.

$$k^\alpha > \max\left\{\frac{\beta(6^\alpha\gamma+1)}{2^\alpha-2}, 3^\alpha\big(\gamma/\gamma_e\big)^\alpha\right\} \tag{A.6}$$

A.2 Two-dimensional Networks

Similar to the one-dimensional case, we show that the SINR condition is achieved in the two-dimensional case for each hop. Consider the transmission of a packet under the routing protocol (Fig. 5.7), where the signal is transmitted to a relay R from an adjacent cell using a transmit power P with the value given in (A.1).

$$\text{SINR}_R = \frac{P_{\text{rcv},R}}{N_0 + I_R}$$

The maximum distance between the relays is $2\sqrt{2}c$, hence

$$P_{\text{rcv},R} > \frac{P}{(2\sqrt{2})^\alpha c^\alpha} = \frac{4^\alpha c^\alpha \gamma N_0}{(2\sqrt{2})^\alpha c^\alpha} = (\sqrt{2})^\alpha \gamma N_0.$$

Considering the interference power I_R, note that other transmitting nodes are placed on the edges of concentric squares due to the time division multiplexing scheme. The first such square contains 8 transmitting nodes (see Fig. 5.8), each with a distance larger than $(h-1)$ cells to R, the next square contains 16 transmitting nodes, and so on. Thus,

$$I_R < \sum_{i=1}^{\infty} 8i \frac{P}{(i(h-1)c)^\alpha} = \mu \frac{P}{(h-1)^\alpha c^\alpha} = \mu \frac{4^\alpha \gamma N_0}{(h-1)^\alpha},$$

where we define

$$\mu = 8 \sum_{i=1}^{\infty} \frac{1}{i^{\alpha-1}}.$$

Note that $\mu < \infty$ for $\alpha > 2$. Hence,

$$\text{SINR}_R > \frac{(\sqrt{2})^{\alpha} \gamma N_0}{N_0 + \mu \dfrac{4^{\alpha} \gamma N_0}{(h-1)^{\alpha}}} > \gamma,$$

provided

$$(h-1)^{\alpha} > \mu \frac{4^{\alpha} \gamma}{\left((\sqrt{2})^{\alpha} - 1\right)}. \tag{A.7}$$

During this transmission, consider any eavesdropper E that is located at a distance larger than $(l-1)$ cells to the transmitting relay with l having the value in (A.1).

$$\text{SINR}_E < \frac{P/(l-1)^{\alpha} c^{\alpha}}{N_0} = \frac{4^{\alpha} c^{\alpha} \gamma N_0}{N_0 (l-1)^{\alpha} c^{\alpha}} < \gamma_e \tag{A.8}$$

Hence, the transmission of a packet on a path remains secure from any eavesdropper that is located a distance of more than $(l-1)$ cells to any point on the path.

A.3 The Number of Streams Arriving to a Cell in 2-D

Consider any stream arriving at a cell $s_{ij}(n)$, which is located on the ith row and jth column in the square lattice, $1 \leqslant i, j \leqslant \sqrt{n/\log n}$ (see Fig. 5.6). The source node of this stream has a path passing through $s_{ij}(n)$, hence the source base should contain cells on the ith row. Therefore, the source node is located on a row i_s such that $(i-z) < i_s < (i+z)$, $z = 4tl$, so the sources of all the streams arriving to $s_{ij}(n)$ is contained in a rectangular region $\mathcal{R}_i$ of size $z\sqrt{\log n} \times \sqrt{n}$. Similarly, the destination base of any stream contains a cell

on column j, therefore the destination nodes of all streams are contained in a rectangular region $\mathcal{R}_j$ of size $\sqrt{n} \times z\sqrt{\log n}$. Hence, the number of streams N arriving at $s_{ij}(n)$ can be upper-bounded by the number of nodes inside $\mathcal{R}_i \cup \mathcal{R}_j$. Let the random variables N_i, N_j be the number of nodes located in $\mathcal{R}_i, \mathcal{R}_j$, respectively. N_i, N_j are Poisson random variables with parameter $z\sqrt{n \log n}$. Note that $N \leqslant N_i + N_j$. Hence,

$$\begin{aligned} P(N < 4z\sqrt{n\log n}) &\geq P(N_i + N_j < 4z\sqrt{n\log n}) \\ &\geq P\big(\{N_i < 2z\sqrt{n\log n}\} \\ &\qquad \cap\{N_j < 2z\sqrt{n\log n}\}\big) \\ &\geq 1 - \big[P(\{N_i \geq 2z\sqrt{n\log n}\}) \\ &\qquad + P(\{N_j \geq 2z\sqrt{n\log n}\})\big] \\ &\geq 1 - 2(e/4)^{z\sqrt{n\log n}} \to 1, n \to \infty, \end{aligned}$$

where the third inequality is due to a union bound, and the last inequality is due to a Chernoff bound. This shows $N < 4z\sqrt{n \log n}$ with high probability.

APPENDIX B

HYBRID NETWORKS

B.1 1-D Construction Details

Each segment has a Poisson number of nodes with mean $\log n$. Hence,

$$P(\text{"each segment has at least one node"}) = \left(1 - \frac{1}{n}\right)^{n/\log n} \to 1, n \to \infty$$

Each node (including base stations in the download phase) transmits with the same power P. For $b \log b = O(n)$, nodes need to reach a node in the next segment, whereas when $b \log b = w(n)$, nodes reach the closest base station in a single hop. The transmit power is given by

$$P = 4^{\alpha} c(n)^{\alpha} \gamma N_0, \tag{B.1}$$

where, $c(n) = \log n$ for the case $b \log b = O(n)$, and $c(n) = n/b$ otherwise.

Consider a transmission from node A to node B which is in the next segment. The SINR at node B is

$$\text{SINR}_B = \frac{P^{A \to B}}{N_0 + I_B},$$

where I_B is the interference due to transmissions that take place in other segments. These segments are regularly placed with d cells apart. Hence,

$$I_B \leq 2 \sum_{i=1}^{\infty} \frac{P}{(idc(n))^{\alpha}} = N_0 \frac{1}{d^{\alpha}} \eta, \tag{B.2}$$

where, for convenience, we define $\eta < \infty$ as in the following:

$$\eta = 4^{\alpha}\gamma 2 \sum_{i=1}^{\infty} \frac{1}{i^{\alpha}} \tag{B.3}$$

Hence, by choosing the value of d such that $d^{\alpha} \geqslant \eta/(2^{\alpha} - 1)$,

$$\text{SINR}_B = \frac{P^{A \to B}}{N_0 + I_B} \geq \frac{2^{\alpha}\gamma N_0}{N_0 + N_0 \frac{\eta}{d^{\alpha}}} \geq \gamma, \tag{B.4}$$

where we use the fact that $d_{AB} \leqslant 2c(n)$.

B.2 1-D Cutset example with total unbounded throughput

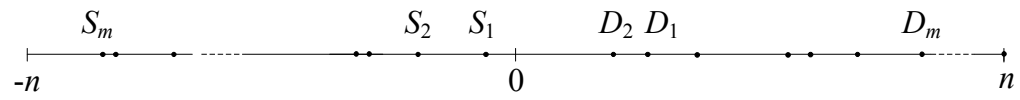

Figure B.1: Source-destination pairs are placed inside the interval $[-n, n]$, where source nodes are on one side of the point 0 and the destination nodes are on the other side.

Consider a one-dimensional wireless network, where nodes lie in $[-n, n]$. Suppose m source-destination pairs are placed in this network such that all source nodes are located in $[-n, 0]$ and all destination nodes are in $[0, n]$ (see Fig. B.1). We are interested in the total throughput that can be achieved between the source-destination pairs with simultaneous single-hop transmissions. In this example, we use a communication model where the rate that can be achieved between a source-destination pair is a function of the SINR achieved at the receiving node [1]. In particular, node A can transmit R_B bps to node B, given by

$$R_B = \log_2 (1 + \text{SINR}_B),$$

where SINR_B is calculated as in (4.1). Note that this model is different than the threshold model presented in Section 4.2.2, where a transmission is successful only if $\text{SINR}_B \geqslant \gamma$.

Under this communication model, consider the following placement of nodes (see Fig. B.2): We define the point $+i$ as the "ith destination bin" for $i = 1, 2, \cdots, f(n)$, where $f(n) \leqslant n$ is the number of bins. At each destination bin, we place $g(n)$ nodes. We denote D_i^k as the kth destination node located at the ith bin, where $i \in \{1, 2, \cdots, f(n)\}$ and $k \in \{1, 2, \cdots, g(n)\}$. The corresponding source node, S_i^k, is located at $-i$, which we define as the "ith source bin". Note that there are a total of $m(n) = f(n)g(n)$ source-destination pairs. Let $P^{A \to B}$ be the power received at node B due to node A. Then, the SINR achieved at D_i^k is:

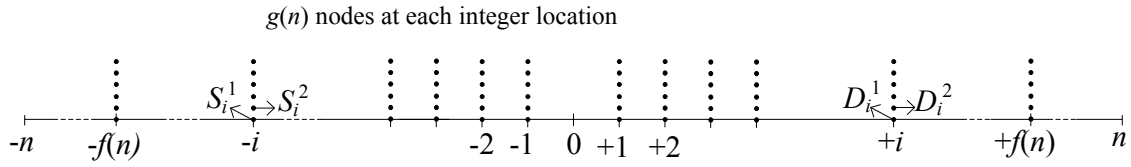

Figure B.2: Placement of source-destination pairs that lead to unbounded total rate through a single point as the network size increases.

$$\text{SINR}_i^k = \frac{P^{S_i^k \to D_i^k}}{N_0 + \left(\sum_{j=1}^{f(n)} \sum_{\ell=1}^{g(n)} P^{S_j^\ell \to D_i^k} \right) - P^{S_i^k \to D_i^k}}$$

The total rate achieved by these source-destination pairs is:

$$R(n) = \sum_{i=1}^{f(n)} \sum_{k=1}^{g(n)} \log_2 \left(1 + \text{SINR}_i^k\right)$$

In the following, we consider the total SINR instead of the total rate, and show that the total SINR goes to infinity as n grows, which we later show that implies the total rate also goes to infinity.

Let the distance between nodes A, B denoted as $|A-B|$. Then, SINR_i^k can be bounded as:

$$\begin{aligned}
\text{SINR}_i^k &= \frac{P|S_i^k - D_i^k|^{-\alpha}}{N_0 + \left(\sum_{j=1}^{f(n)}\sum_{\ell=1}^{g(n)} P|S_j^\ell - D_i^k|^{-\alpha}\right) - P^{S_i^k \to D_i^k}} \\
&\geq \frac{P|S_i^k - D_i^k|^{-\alpha}}{N_0 + \sum_{j=1}^{f(n)}\sum_{\ell=1}^{g(n)} P|S_j^\ell - D_i^k|^{-\alpha}} \\
&= \frac{|S_i^k - D_i^k|^{-\alpha}}{N_r + \sum_{j=1}^{f(n)}\sum_{\ell=1}^{g(n)} |S_j^\ell - D_i^k|^{-\alpha}} \\
&= \frac{1}{|S_i^k - D_i^k|^{\alpha}\left(N_r + \sum_{j=1}^{f(n)}\sum_{\ell=1}^{g(n)} |S_j^\ell - D_i^k|^{-\alpha}\right)},
\end{aligned}$$

where we define $N_r = N_0/P$ for convenience. For the placement described above:

$$\begin{aligned}
\text{SINR}_i^k &\geq \frac{1}{(2i)^{\alpha}\left(N_r + \sum_{j=1}^{f(n)}\sum_{\ell=1}^{g(n)} (j+i)^{-\alpha}\right)} \\
&= \frac{1}{(2i)^{\alpha}\left(N_r + g(n)\sum_{j=1}^{f(n)} (j+i)^{-\alpha}\right)} \\
&\geq \frac{1}{(2i)^{\alpha}\left(N_r + g(n)\int_{t=0}^{n} (t+i)^{-\alpha} dt\right)} \\
&\geq \frac{1}{(2i)^{\alpha}\left(N_r + \frac{g(n)}{\alpha-1}\frac{1}{i^{\alpha-1}}\right)}
\end{aligned}$$

Let $Y(n)$ be the total SINR. Then,

$$
\begin{aligned}
Y(n) &= \sum_{i=1}^{f(n)} \sum_{k=1}^{g(n)} \text{SINR}_i^k \\
&\geq \sum_{i=1}^{f(n)} \frac{g(n)}{(2i)^\alpha \left(N_r + \dfrac{g(n)}{\alpha - 1} \dfrac{1}{i^{\alpha-1}} \right)} \\
&= \frac{1}{2^\alpha} \sum_{i=1}^{f(n)} \frac{1}{\dfrac{i^\alpha N_r}{g(n)} + \dfrac{i}{\alpha - 1}}
\end{aligned}
$$

For the case where $f(n)^{\alpha-1} \leqslant g(n)$, and $f(n) \to \infty$, as $n \to \infty$,

$$
\begin{aligned}
Y(n) &\geq \frac{1}{2^\alpha} \sum_{i=1}^{f(n)} \frac{1}{\dfrac{i^\alpha N_r}{i^{\alpha-1}} + \dfrac{i}{\alpha - 1}} \\
&= \frac{1}{2^\alpha \left(N_r + 1/(\alpha - 1) \right)} \sum_{i=1}^{f(n)} \frac{1}{i} \\
&\to \infty, \quad \text{as } n \to \infty.
\end{aligned}
$$

Therefore, it is possible to choose appropriate values for $f(n), g(n)$, e.g., for $\alpha = 3$, $f(n) = n^{1/3}, g(n) = n^{2/3}$, so that the corresponding placement of $m(n) = f(n)g(n)$ nodes enable the total SINR grow to infinity with increasing network size. Finally, it can be shown that the total rate also grows to infinity. For convenience, let us relabel the SINR values in an arbitrary way as $\{a_i, i = 1, 2, \cdots, n\}$. Now consider the total rate:

$$
\begin{aligned}
R(n) &= \sum_{i=1}^{n} \log_2 (1 + a_i) \\
&= \log_2 \left(\prod_{i=1}^{n} (1 + a_i) \right) \\
&\to \infty, \quad \text{as } n \to \infty,
\end{aligned}
$$

where the divergence follows from the fact that $\prod_{i=1}^{n} (1 + a_i)$ diverges if the sum $\sum_{i=1}^{n} (1 + a_i)$ diverges [32].

Hence, the total rate through a single point can grow with the number of nodes. Contrasting this result with Lemma 4.1, we see that the cutset bounds can vary under different communication models.

BIBLIOGRAPHY

[1] Agarwal, A., and Kumar, P. R. Capacity bounds for ad hoc and hybrid wireless networks. *ACM SIGCOMM Computer Communication Review* (2004), 71–81.

[2] Anderson, C. W. Extreme value theory for a class of discrete distributions with applications to some stochastic processes. *Journal of Applied Probability* (1970), 99–113.

[3] Anderson, C. W., Coles, S. G., and Husler, J. Maxima of Poisson-like variables and related triangular arrays. *The Annals of Applied Probability* (1997), 953–971.

[4] Blair, A., Brown, T., Chugg, K. M., Halford, T. R., and Johnson, M. Barrage relay networks for cooperative transport in tactical MANETs. In *Proc. MILCOM 2008*.

[5] Blair, A., Brown, T., Chugg, K. M., and Johnson, M. Tactical mobile mesh network system design. In *Proc. MILCOM 2007*.

[6] Cai, N., and Yeung, R.W. Secure network coding. In *Proc. ISIT 2002*.

[7] Capar, C., and Goeckel, D. Network coding for facilitating secrecy in large wireless networks. In *Proc. CISS 2012*.

[8] Capar, C., Goeckel, D., Liu, B., and Towsley, D. Cooperative jamming to improve the connectivity of the 1-D secrecy graph. In *Proc. CISS 2011*.

[9] Capar, C., Goeckel, D., Liu, B., and Towsley, D. Secret communication in large wireless networks without eavesdropper location information. In *Proc. IEEE INFOCOM 2012*.

[10] Capar, C., Goeckel, D., and Towsley, D. Broadcast analysis for extended cooperative wireless networks. *IEEE Transactions on Information Theory* (2013), 5805–5810.

[11] Chang, Y. J., Jung, H., and Ingram, M. A. Demonstration of a new degree of freedom in wireless routing: Concurrent cooperative transmission. In *Proc. HotEMNETS 2010*.

[12] Chen, X., Huang, W., Wang, X., and Lin, X. Multicast capacity in mobile wireless ad hoc network with infrastructure support. In *Proc. IEEE INFOCOM 2012*.

[13] De Domenico, M., Sole, A., Gomez, S., and Arenas, A. Random Walks on Multiplex Networks. arXiv:1306.0519.

[14] Dousse, O. *Asymptotic properties of wireless multi-hop networks*. PhD dissertation, EPFL, 2005.

[15] Dousse, O., Thiran, P., and Hasler, M. Connectivity in ad-hoc and hybrid networks. In *Proc. IEEE INFOCOM 2002*.

[16] Franceschetti, M., Dousse, O., Tse, D. N. C., and Thiran, P. Closing the gap in the capacity of wireless networks via percolation theory. *IEEE Transactions on Information Theory* (2007), 1009–1018.

[17] Franceschetti, M., and Meester, R. *Random networks for communication: from statistical physics to information systems*. Cambridge University Press, 2007.

[18] Gao, J., Buldyrev, S. V., Stanley, H. E., Xu, X., and Havlin, S. Percolation of a general network of networks. *Physical Review E* (2013), 062816.

[19] Goeckel, D., Liu, B., Towsley, D., Wang, L., and Westphal, C. Asymptotic connectivity properties of cooperative wireless ad hoc networks. *IEEE Journal on Selected Areas in Communications* (2009), 1226–1237.

[20] Goeckel, D., Vasudevan, S., Towsley, D., Adams, S., Ding, Z., and Leung, K. Artificial noise generation from cooperative relays for everlasting secrecy in two-hop wireless networks. *IEEE Journal on Selected Areas in Communications* (2011), 2067–2076.

[21] Goel, S., Aggarwal, V., Yener, A., and Calderbank, A. R. Modeling location uncertainty for eavesdroppers: A secrecy graph approach. In *Proc. ISIT 2010*.

[22] Goel, S., and Negi, R. Guaranteeing secrecy using artificial noise. *IEEE Transactions on Wireless Communications* (2008), 2180–2189.

[23] Goldsmith, A. *Wireless Communications*. Cambridge University Press, 2005.

[24] Gopala, P. K., Lai, L., and El Gamal, H. On the secrecy capacity of fading channels. *IEEE Transactions on Information Theory* (2008), 4687–4698.

[25] Grimmett, G. *Percolation*. Springer Verlag, 1999.

[26] Grossglauser, M., and Tse, D. N. C. Mobility increases the capacity of ad hoc wireless networks. *IEEE/ACM Transactions on Networking* (2002), 477–486.

[27] Guha, S., Towsley, D., Capar, C., Swami, A., and Basu, P. Layered percolation. arXiv:1402.7057.

[28] Gupta, P., and Kumar, P. R. Critical power for asymptotic connectivity. In *Proc. IEEE Conference on Decision and Control* (1998).

[29] Gupta, P., and Kumar, P. R. The capacity of wireless networks. *IEEE Transactions on Information Theory* (2000), 388–404.

[30] Haenggi, M. The secrecy graph and some of its properties. In *Proc. ISIT 2008*.

[31] Jain, K. Security based on network topology against the wiretapping attack. *IEEE Wireless Communications* (2004), 68–71.

[32] Jeffrey, A., and Dai, H. H. *Handbook of Mathematical Formulas and Integrals*. Academic Press, 2008.

[33] Jung, H., Chang, Y. J., and Ingram, M. A. Experimental range extension of concurrent cooperative transmission in indoor environments at 2.4GHz. In *Proc. MILCOM 2010*.

[34] Kailas, A., and Ingram, M. A. Analysis of a simple recruiting method for cooperative routes and strip networks. *IEEE Transactions on Wireless Communications* (2010), 2415–2419.

[35] Kailas, A., Thanayankizil, L., and Ingram, M. A. A simple cooperative transmission protocol for energy-efficient broadcasting over multi-hop wireless networks. *KICS/IEEE Journal of Communication and Networks* (2008), 213–220.

[36] Kesten, H. The critical probability of bond percolation on the square lattice equals 1/2. *Communications in Mathematical Physics* (1980), 41–59.

[37] Kimber, A. C. A note on Poisson maxima. *Probability Theory and Related Fields* (1983), 551–552.

[38] Kivela, M., Arenas, A., Barthelemy, M., Gleeson, J. P., Moreno, Y., and Porter, M. A. Multilayer networks. arXiv:1309.7233.

[39] Koyluoglu, O. O., Koksal, C. E., and Gamal, H. E. On secrecy capacity scaling in wireless networks. *IEEE Transactions on Information Theory* (2012), 3000–3015.

[40] Kozat, U. C., and Tassiulas, L. Throughput capacity of random ad hoc networks with infrastructure support. In *Proc. MobiCom 2003*.

[41] Laneman, J. N., Tse, D. N. C., and Wornell, G. W. Cooperative diversity in wireless networks: Efficient protocols and outage behavior. *IEEE Transactions on Information Theory* (2004), 3062–3080.

[42] Leung-Yan-Cheong, S. K., and Hellman, M. E. The gaussian wire-tap channel. *IEEE Transactions on Information Theory* (1978), 451–456.

[43] Leveque, O., and Telatar, I. E. Information-theoretic upper bounds on the capacity of large extended ad hoc wireless networks. *IEEE Transactions on Information Theory* (2005), 858–865.

[44] Liang, Y., Poor, H. V., and Ying, L. Secrecy throughput of MANETs with malicious nodes. In *Proc. ISIT 2009*.

[45] Liu, B., Liu, Z., and Towsley, D. On the capacity of hybrid wireless networks. In *Proc. IEEE INFOCOM 2003*.

[46] Liu, B., Thiran, P., and Towsley, D. Capacity of a wireless ad hoc network with infrastructure. In *Proc. MobiHoc 2007*.

[47] Liu, J., Goeckel, D., and Towsley, D. Bounds on the throughput gain of network coding in unicast and multicast wireless networks. *IEEE Journal on Selected Areas in Communications* (2009), 582–592.

[48] Lou, W., Liu, W., and Fang, Y. SPREAD: enhancing data confidentiality in mobile ad hoc networks. In *Proc. IEEE INFOCOM 2004*.

[49] Lu, N., and Shen, X. S. Scaling laws for throughput capacity and delay in wireless networks - a survey. *IEEE Communications Surveys Tutorials* (2014), 642–657.

[50] Mao, X. F., Li, X. Y., and Tang, S. J. Multicast capacity for hybrid wireless networks. In *Proc. MobiHoc 2008*.

[51] Meester, R., and Roy, R. *Continuum Percolation*. Cambridge University Press, 1996.

[52] Miorandi, D., Sicari, S., Pellegrini, F. D., and Chlamtac, I. Internet of things: Vision, applications and research challenges. *Ad Hoc Networks* (2012), 1497–1516.

[53] Newman, M. E. J., Strogatz, S. H., and Watts, D. J. Random graphs with arbitrary degree distributions and their applications. *Physical Review E* (2001), 026118.

[54] Newman, M. E. J., and Ziff, R. M. Efficient monte carlo algorithm and high-precision results for percolation. *Physical Review Letters* (2000), 4104–4107.

[55] Ni, S.-Y., Tseng, Y.-C., Chen, Y.-S., and Sheu, J.-P. The broadcast storm problem in a mobile ad hoc network. In *Proc. MobiCom 1999*.

[56] Nicosia, V., Bianconi, G., Latora, V., and Barthelemy, M. Growing multiplex networks. *Physical Review Letters* (2013), 058701.

[57] Nosratinia, A., Hunter, T. E., and Hedayat, A. Cooperative communication in wireless networks. *IEEE Communications Magazine* (2004), 74–80.

[58] Ozgur, A., Leveque, O., and Tse, D. Hierarchical cooperation achieves optimal capacity scaling in ad hoc networks. *IEEE Transactions on Information Theory* (2007), 3549–3572.

[59] Ozgur, A., Leveque, O., and Tse, D. Operating regimes of large wireless networks. *Foundations and Trends in Networking* (2011), 1–107.

[60] Perron, E., Diggavi, S., and Telatar, E. On noise insertion strategies for wireless network secrecy. In *Proc. ITA 2009*.

[61] Pinto, P. C., Barros, J., and Win, M. Z. Wireless secrecy in large-scale networks. In *Proc. ITA 2011*.

[62] Quintanilla, J. A., and Ziff, R. M. Asymmetry in the percolation thresholds of fully penetrable disks with two different radii. *Physical Review E* (2007), 051115.

[63] Rabin, M. O. Efficient dispersal of information for security, load balancing, and fault tolerance. *Journal of the ACM* (1989), 335–348.

[64] Sahimi, M. *Applications Of Percolation Theory*. Taylor & Francis, 1994.

[65] Scaglione, A., Goeckel, D. L., and Laneman, J. N. Cooperative communications in mobile ad hoc networks. *IEEE Signal Processing Magazine* (Sept. 2006), 18–29.

[66] Shamir, A. How to share a secret. *Communications of the ACM* (1979).

[67] Shin, W. Y., Jeon, S. W., Devroye, N., Vu, M. H., Chung, S. Y., Lee, Y. H., and Tarokh, V. Improved capacity scaling in wireless networks with infrastructure. *IEEE Transactions on Information Theory* (2011), 5088–5102.

[68] Sirkeci-Mergen, B., and Scaglione, A. A continuum approach to dense wireless networks with cooperation. In *Proc. IEEE INFOCOM 2005*.

[69] Sirkeci-Mergen, B., Scaglione, A., and Mergen, G. Asymptotic analysis of multistage cooperative broadcast in wireless networks. *IEEE Transactions on Information Theory* (2006), 2531–2550.

[70] Sozer, E. M., Stojanovic, M., and Proakis, J. G. Underwater acoustic networks. *IEEE Journal of Oceanic Engineering* (2000), 72–83.

[71] Tarasevich, Y. Y., and van der Marck, S. C. An investigation of site-bond percolation on many lattices. *International Journal of Modern Physics C* (1999), 1193–1204.

[72] Toumpis, S. Capacity bounds for three classes of wireless networks: asymmetric, cluster, and hybrid. In *Proc. MobiHoc 2004*.

[73] Vasudevan, S., Goeckel, D., and Towsley, D. F. Security-capacity trade-off in large wireless networks using keyless secrecy. In *Proc. MobiHoc 2010*.

[74] Williams, B., and Camp, T. Comparison of broadcasting techniques for mobile ad hoc networks. In *Proc. MobiHoc 2002*.

[75] Wyner, A. D. The wire-tap channel. *Bell Systems Technical Journal* (1975), 1355–1387.

[76] Xiao, S., Gong, W., and Towsley, D. Secure wireless communication with dynamic secrets. In *Proc. IEEE INFOCOM 2010*.

[77] Xie, L.-L., and Kumar, P. R. A network information theory for wireless communication: scaling laws and optimal operation. *IEEE Transactions on Information Theory* (2004), 748–767.

[78] Xie, L.-L., and Kumar, P. R. On the path-loss attenuation regime for positive cost and linear scaling of transport capacity in wireless networks. *IEEE Transactions on Information Theory* (2006), 2313–2328.

[79] Xue, F., and Kumar, P. R. Scaling laws for ad hoc wireless networks: An information theoretic approach. *Foundations and Trends in Networking* (2006), 145–270.

[80] Zemlianov, A., and de Veciana, G. Capacity of ad hoc wireless networks with infrastructure support. *IEEE Journal on Selected Areas in Communications* (2005), 657 –667.